788001

MICROFILMED

CRA EXPLORATION PTY.LTD.

Dept of Mines | A.O. | C.G. | E.O. | D.S.M.E.
Received 12 MAY 1982
Answered
DEPT. OF MINES
REF. No. 3548/82
E & T

GEOPHYSICAL SURVEYS ON THE

DALCOATH GRANITE GRID

SHEFFIELD EL 7/73

NORTH TASMANIA

OPEN FILE

Author : M.F.Flis

Date : 3rd May, 1982.

Submitted To : T.W.Dickson

Accepted By :

Copies To : Department of Mines
CRAE Hobart
CRAE Burnie
CRAE Melbourne
Carpentaria Exploration Co. (2)

The contents of this report remain the property of C.R.A. Exploration Pty. Limited and may not be published in whole or in part nor used in a company prospectus without the written consent of the Company.

CRAE Report No. 11268

CONTENTS

1. SUMMARY

Ground magnetics, V.L.F. - E.M. and U.T.E.M. geophysical surveys were conducted on the Dalcoath Granite Grid to evaluate two E.M. anomalies detected by an airborne E.M. survey.

The anomalies were found to be associated with lead-zinc mineralisation located in old adits on the grid. Extensions of this mineralisation are suggested by the two E.M. surveys, and drilling is recommended.

2. INTRODUCTION

The Dalcoath Granite Grid is located on the west bank of the River Forth, 21 kilometres south-west of Sheffield, North Tasmania.

The grid was established to investigate two Dighem Multicoil II E.M. anomalies associated with small old mine workings adjacent to the northern margin of the Dalcoath Granite. The grid has been covered by ground magnetics and V.L.F. E.M. surveys. Selected lines were surveyed using the U.T.E.M. transient E.M. system as a follow-up to identification of zones of interest from the geophysical and geochemical surveys. The target is silver-lead-zinc-gold mineralisation believed to be stratiform within metasediments proximal to, and possibly modified by, the granite.

3. CONCLUSIONS

The V.L.F. and U.T.E.M. surveys detected persistent, albeit weak, anomalous zones associated with two old workings known to contain disseminated (10-15%) lead-zinc mineralisation. Extensions of this mineralisation to the east and west of the workings are postulated on the basis of the surveys. The mineralisation appears to exist in an area of complex magnetic fields probably due to faulting and/or shearing. The mineralisation is not anomalously magnetic.

Small occurences of skarn are highly magnetic so it does not seem likely that there exist further skarn developments not already known on the grid.

The major single magnetic anomaly appears to be too deep for inclusion as a high priority target at this stage. A small bull's eye magnetic anomaly on line 6200mE gave no U.T.E.M. response and is therefore of little interest.

4. RECOMMENDATIONS

It is recommended that:

1) the observation that mineralisation at Higgs Mine is an I.P. target be tested by an orientation I.P. survey consisting of three seven-electrode spreads on lines 5900mE, 6000mE, and 6100mE; and that the survey be extended if results are encouraging;

2) shallow drilling of conductor targets be carried out on the following targets (in order of priority):

   a) line 5959mE, 4900mN at 35 metres depth
   b) line 6100mE, 4962mN at 30 metres depth
   c) line 5900mE, 5050mN at 35 metres depth

3) Zone 'C' of the U.T.E.M. survey must be further investigated. Two lines of I.P. on lines 5600mE and 5700mE, with extensions if results are encouraging, should adequately test it. Reference to the orientation survey over Higgs Mine to be made.

5. DISCUSSION

5.1 Geology

The grid is bounded to the south-east by the Dalcoath Granite. While outcrop of this granite is limited to an area some 1.5 kilometres in diameter, aeromagnetic data suggest it is far more extensive, plunging shallowly to the west.

The granite, of Devonian age, is "typically a medium to coarse-grained cream to pink biotite granite with common narrow aplite veins and dykes" (Jennings, 1979). It is responsible for the metamorphism and metasomatism of the Gordon Limestone to form the Moina skarn deposit, and possibly for the extensive mineralisation in the area.

Quartzites of the Moina Sandstone (Ordovician) occur to the north and northwest of the granite. This unit, covering most of the grid, is in places metasomatized and sericitic. Minor impure dolomites, rhyolites, hornfels, and skarns have been noted.

A water tunnel to the immediate north of the grid has established the presence of concealed carbonate rocks in the vicinity. These belong to the Gordon Limestone which outcrops at Moina and parts of which have been metamorphosed to a skarn.

5.1.1. Mineralisation

Mineralisation around the Granite is zoned. The area has a profusion of mines and workings. Three workings occur on the grid.
These are:

a) Higgs Mine - pyrite, galena, arsenopyrite, chalcopyrite and gold. There is some contention as to whether the mineralisation is stratiform, or even stratabound, or shear controlled.

b) Narrawa Reward - fine grained arsenopyrite, pyrite, chalcopyrite and galena disseminations in metaquartzites adjacent to a quartz - feldspar porphyry dyke.

c) Squib - wolframite, molybdenite, bismuthinite, cassiterite, gold, pyrite, chalcopyrite, sphalerite, arsenopyrite, topaz, fluorite, beryl and monazite in quartz veins continuous across the granite - quartzite contact.

Minor disseminated sulphide mineralisation within the host Moina Sandstone is evident.

A number of minor skarns, principly hedenbergite and diopside, occur towards the eastern end of the grid (lines 6100mE and 6200mE).

Greisen zones within the granite carry wolframite, molybdenite, bismuthinite and minor cassiterite.

5.2 Previous Geophysics

The area has been included in two regional aeromagnetic surveys. The first was flown by Adastra Hunting Geophysics Pty.Ltd. for Rio Tinto Australian Exploration in 1958.

The second was flown by Australasian Mining and Engineering Geophysics Pty.Ltd. for the Broken Hill Proprietory Company Ltd. in 1966. Flight line specifications were the same for both surveys: half mile line spacing, east-west flight lines and 500ft mean terrain clearance.

No previous ground geophysics has been recorded for the grid area.

5.3 Dighem Airborne E.M. and Magnetic Survey

An airborne E.M. and magnetic survey was conducted over the entire Sheffield E.L. by Dighem Ltd. in February 1981. The Multicoil II frequency domain E.M. system was used (Fraser, 1979).

Two related E.M. anomalies, designated 19I and 20xR were detected on the northern margin of the Dalcoath Granite. These were described as being due to "weak bedrock conductors of short strike length" (Dvorak and Vergos, 1981). Automated computer modelling by Dighem Ltd. ascribed a conductance of 1 Siemen at a depth of about five metres to the causative body (vertical dyke model).

The anomalies reside in an isolated area of depressed resistivities and along a moderately strong magnetic gradient (see plans TASh 730, 731 and 732). Anomaly 19I is attributable to the Higgs Mine.

5.4 Ground Magnetic Survey

A ground magnetic survey was conducted over the grid using a station spacing of 12.5 metres on lines 100 metres apart. The instrument was a Geometrics G816/826A proton magnetometer with a pole-mounted sensor (2.5 metres high). All lines were levelled to the baseline and data was drift corrected.

The total magnetic intensity contour map (TASh 237) is dominated by a large high on the western side of the grid and a band of very intense and disturbed magnetics striking diagonally across the grid in a north-easterly direction.

Whilst it is difficult to carry out modelling on the large anomaly due to a lack of data to the south of it, a simple dyke model at a depth of 165 metres and containing an equivalent 3% magnetite would explain it. As the anomaly has no associated elevated geochemistry it is, at this stage, a low priority target.

The central band of disturbed magnetics is interpreted as being attributable to a zone of complex faulting, or shearing, with associated near surface mineralisation. Both north-easterly and east-west structure are present.

On lines 6400mE and 6500mE small, but intense highs are associated with blebs of skarn containing concentrations of magnetite.

This zone may represent a belt of contact mineralisation and skarn development caused by metasomatism associated with the granite emplacement.

A small "bulls's eye" anomaly on line 6200mE at 4799mN was modelled. The causative body appears to be dipping moderately to the south and at a depth of 95 metres although, once again, the magnetic field is not well enough known to the south to give a reliable interpretation. The body's magnetic susceptibility is equivalent to about 5% magnetite.

Ore taken from Higgs Mine is not anomalously susceptible (0.002 S.I.) and is thus not expected to show up on the magnetic contour map.

5.5 V.L.F. - E.M. Survey

Due to the ease and cost-effectiveness of conducting a V.L.F. -E.M. survey the grid was covered by the method as a prelude to defining target areas for more quantitative E.M. methods. A Phoenix V.L.F.-2 instrument was used. The North West Cape transmitter (Aust.) operating at 22.3 KHz. lies at 295° MN which is within 10° of the general lithology strike direction. This transmitter was therefore ideal as the primary field source.

Stations were occupied at 25 metre intervals. Both dip angle and maximum horizontal field strength were recorded - although the field strength data is not presented here. The quadrature component was not recorded as the instrument used does not satisfactorily measure it. Dip data was "normalized" using Fraser's V.L.F. filter (Fraser, 1981) and contoured (TASh 536).

The V.L.F. dip contour map may be divided into three broad sections:

1) the north end of the grid which is dominated by a relatively strong response coincident with a topographic ridge. This is most probably a terrain induced anomaly,

2) a central zone of low-order difuse anomalies possibly associated with lithological contacts, and

3) a southern zone consisting of narrow well defined linear anomalies.

The main area of interest is around the old workings near the baseline and immediately south of the baseline. Here, three sub-parallel zones having a narrow linear character, two, which are quite intense, strike in an easterly direction.

The northernmost, and weakest, of these may be directly attributable to the Narrawa Reward Mine (lines 5600mE to 5900mE). The central anomaly, running just south of the baseline from 6000mE to 6300mE, is probably associated with Higgs Mine (at 5950mE) although the trend does not extend to 5900mE. Dighem anomaly 19I plots on this anomaly. The southernmost anomaly is much more extensive, running from line 5900mE to 6400mE. This response reflects Dighem anomaly 20xR. The northern and central anomalies may reflect the synclinal situation in which Higgs Mine resides (Jennings, 1979) although there is no real evidence for this.

Two of the major skarn shows on the grid are reflected in the V.L.F. data. They are the anomaly centred on line 6400mE at 5200mN and the narrow high centred on line 6400mE at 5400mN (this latter anomaly not being caused by the previously mentioned terrain effects which occur here).

An intense high centred on line 5700mE at 4612mN has, at this stage, no explanation. It has a very intense, but small, magnetic response associated with it and may thus also be due to skarn development.

Dip angle profiles suggest that all responses encountered are due to narrow (< 10 metres) conductive zones, or lithological contacts, usually at a shallow depth (within 25 metres of the surface). Quantitative depth estimations, dips, and conductivities cannot be confidently derived from dip angle data.

5.6 U.T.E.M. Survey

The U.T.E.M. transient E.M. system was used to survey selected lines on the basis of V.L.F. and geological data. Whilst a full copy of the contractor's report appears as Appendix I the interpretation section of that report is here reproduced:

"The UTEM survey in the area showed only short time constant anomalies that could be attributed to regional conductivity. As a result, it would appear that the country rock is reasonably resistive, and that near surface weathering, if present, has not lead to a significant conductivity increase. The response present is interpreted to be due to a near surface layer of conductance less than 0.2 Siemens. Its effect shows up as a migrating crossover at the earliest times, limiting amplitudes close to -200% for channel 9 (the earliest time channel plotted), and in a small positive rise in the intermediate time channels away from the loop.

No good conductors were detected within the survey area. However crossover anomalies with short time constant response are present on all lines, and have been grouped into zones as shown on the compilation map. Each zone will be individually discussed.

Zone A: The anomalies in this zone have the largest amplitudes of any of the localized anomalies detected. The source is interpreted to be fairly steeply dipping. However, as the response has a fairly short time constant of only 0.2 msec, and at the early delay times there is a fair response due to regional conductivity, a quantitative estimation of dip cannot be made as this requires a fix on zero levels.

It is also possible that the observed response is due to current channeling rather than direct toroidal induction in a localised conductor. A poorly conducting shear zone for example, in contact with the overburden conductivity could explain the response. However, the fact that the response changes character significantly from line to line argues against this. The zone appears shallowest on lines 5950 and 5900E with an interpreted depth to top of less than 25m, and appears to end at around line 6000E. The zone extends west off the grid, and is interpreted to be at somewhat greater depths of around 35 to 50m on the westernmost lines surveyed.

Assuming a 500m strike length and that pure toroidal induction is the cause of the anomaly, the conductance of the source would be about 1.3 Siemens.

This is quite low for the source to be massive sulphides, however as the expected conductors in the region are unlikely on geological grounds to be massive, the zone may be of geological interest.

Zone B: The zone B response is most prominent on lines 5950, 6000, and 6100E. Its source is interpreted to be at a shallower depth than that of zone A, with depth to top estimates less than 20m on all lines. Again, this is a very short time-constant response so that it is difficult to determine if toroidal induction or current channeling is the cause. If pure toroidal induction is the cause, then the source must have a large depth extent due to the size and shape of the negative lode of the anomaly. The conductance of the zone based on a time constant of 0.25 milliseconds and a strike length of 400m is 2 Siemens.

Zone C: Zone C shows up as prominent responses on two lines at the west end of the grid. Its source is near surface on line 5700E, and has an interpreted depth to top of 25m on line 5600E. A reasonably large depth extent and an extension of the zone further west are indicated by the large amplitude of the response. If toroidal induction is the cause, then the zone must have a conductance in the 2 to 3 Siemen range.

Zone D: Zone D is a small amplitude, limited strike length feature that is present on lines 5700E and 5800E. Its source has a top near surface, and based on the amplitude must also have a limited depth extent. The response has a very unusual shape, in that most of the anomaly seems to be a positive rather than negative deflection. An equally possible explanation for the source of this anomaly would be a depth limited body dipping towards the loop, with its location below the reverse rather than normal cross-over point. In this case it would lie at station 47+50N on line 5700E, and at station 47+75E on line 5800E rather than at the points plotted on the compilation map. Again this feature has a very short time constant of response, which makes geometrical interpretation difficult due to the presence of a large background response at delay times where the anomaly is present.

Zone E: The UTEM response over zone E is very small and sharp, and would likely have a poor depth, limited or discontinuous conductor as its source.

Zone F: This one line anomaly may well represent an extension of zone A. However, its smaller amplitude and shorter time constant could equally well indicate a separate, discontinuous small local conductor".

5.7 Discussion on U.T.E.M. Survey Results in Relation to Ground Magnetics and V.L.F. Surveys.

The U.T.E.M. survey was designed to test the mineralisation, and possible extensions of the area around the old workings. The existence of V.L.F. anomalies in the vicinity of the workings indicated E.M. targets were present although their quality was not known.

Some conclusions which may be drawn from the U.T.E.M. survey are:

1) there is good agreement between the U.T.E.M. and V.L.F. surveys, indicating that ground resistivities were locally high enough to allow detection of conductive zones by V.L.F.

   Reasons for any disagreements may be cited as:

   a) the conductor was possibly too deep to be detected by V.L.F. (e.g. 5800mE, 4875mN),

   b) the source was too minor (surficial, weak conductor) to be detected by U.T.E.M. (e.g. the V.L.F. trend running through 4762mN on lines 5900mE to 6200mE), or

   c) the line was not surveyed by V.L.F. (north end of line 6100mE and intermediate line 5950mE).

2) All U.T.E.M. anomalies indicated poor quality conductors. This may indicate that responses may be due to fault/shear zones, due to slightly more conductive horizons, or due to disseminated mineralisation.

The latter explanation may certainly be applied to the set of anomalies associated with Higgs Mine (zone'B' in section 5.7.5) where ore is definately disseminated and is an I.P. target rather than an E.M. target.

3) Responses associated with Higgs and Narrawa Reward Mines indicate that both have the potential of being more extensive. Higgs mine has a potential strike length of 400 metres whilst Narrawa Reward may have a strike length of up to 500 metres. The anomalies associated with Narrawa Reward Mine follow a mapped contact between orthoquartzites and metasomatized orthoquartzites along which a porphyry dyke associated with the mineralisation runs.

4) E.M. activity on lines 5600mE and 5700mE around 4612mN persists on the U.T.E.M. survey in association with the magnetic activity.

5) The magnetic anomaly on 6200mE at 4700mN has no E.M. response.

6. REFERENCES

Fraser, D.C.	1979	"The Multocoil II Airborne Electromagnetic System".
	1981	"A Review of Some Useful Algarithms in Geophysics".
Jennings, I.B.	1979	"Geological Atlas 1 Mile Series. Sheet 37 (8115S). Sheffield". Explan. Rep. Dep. Mines Tas.
Dvorak, Z. and Vergos, S.	1981	"Dighem II Surveys in Sheffield Area, Tasmania, for CRA Exploration Pty. Ltd. CRAE Report No. 11263.

7. KEYWORDS

Geophysics - E.M., magnetics, airborne, interpret. theory, sulphides, skarns.

8. LOCATION

Burnie 1:250 000 SK 55-3

9. LIST OF PLANS

Plan Number	Title	Scale
TASh 237	Dalcoath Granite Grid Ground Magnetic Survey	1:2500
TASh 536	Dalcoath Granite Grid Normalized VLF-EM Dips	1:2500
TASh 730	Portion of Dighem II Survey Sheffield, Tasmania - Resistivity	1:25 000
TASh 731	Portion of Dighem II Survey Sheffield, Tasmania - Electromagnetics	1:25 000
TASh 732	Portion of Dighem II Survey Sheffield, Tasmania - Magnetics	1:25 000
TASh 733	Dalcoath Granite Grid Location Diagram	1:100 000
TASh 734	Dalcoath Granite Grid Line 6200mE Magnetic Model	As shown
TASh 735	Dalcoath Granite Grid Line 5300mE Magnetic Model	As shown

10. LIST OF APPENDICES

Appendix I "Report on a UTEM Survey at Dalcoath Granite Area, Tas."

Appendix II "UTEM: A Wideband, Time Domain E.M. System Using a Fixed Transmitter and Mapping Receiver".

788016

APPENDIX I

REPORT ON A UTEM SURVEY

AT

DALCOATH GRANITE AREA, TASMANIA

788017

REPORT ON A UTEM SURVEY

AT

DOLCOATH GRANITE AREA, TASMANIA

FOR

CRA EXPLORATION (PTY) LTD.

BY

LAMONTAGNE GEOPHYSICS LTD.

MARCH 1982

J.C. MACNAE
F. GLASS

INTRODUCTION

During the latter part of December 1981 and the first half of January 1982, a UTEM survey was performed by Lamontagne Geophysics of Toronto, Canada on the Dolcoath Granite Area prospect, located south of Wilmot, Tasmania. The survey was performad on behalf of CRA Exploration Pty. Ltd. of Burnie, Tasmania, with the object of determining if any of the small mineralized showings present on the property might have extensions, with increased conductivity, at depth.

Because of a series of different but intermittent electro-mechanical malfunctions with the receiver, the survey took nearly two weeks longer to complete than what would normally have been the case.

FIELD SURVEY

Between 24 December 1981 and 14 January 1982, a UTEM time domain electromagnetic survey was carried out by F. Glass of Lamontagne Geophysics on the Dolcoath Granite area prospect. G. Weber, regional geologist and manager of the Burnie office represented CRA and assisted in the layout of the loop during the first day of work. The survey crew was based in Sheffield and drove to the Dolcoath prospect some 35km away and about a forty five minute drive to the transmitter setup.

The survey area is underlain by quartzites which show an increasing grade of metamorphism towards the northern part of the property. Near the centre of the property, numerous small adits and gloryholes are evident attesting to the past presence of mineralization. A disused compressor, a stamp mill and the remains of a primitive smelter may be seen, and illustrate the former interest once accor-

ded the property.

The object of the UTEM survey was to determine if any of the previous showings might have a conductive extension at depth. Judjing from the size of the holes, the pockets of mineralization that had been present were not much wider than a metre or so, and some of the larger pockets might have had a strike length of 30 metres. Based on the presence of several rock heaps at the surface, some shafts and underground workings were likely developed in the past but their extent is not known. Some of the mineralized rocks from the muck heaps had disseminated sulphides (pyrite, pyrrhotite) to a maximum of perhaps ten percent by volume in a quartz matrix.

The topography of the area was moderately hilly with a stream valley diagonally intersecting the survey area. The loop and the ends of the lines were situated near the top of two adjacent hills facing each other. The survey lines were well cut and the pickets were all in place and clearly marked. Travel along the lines or from the transmitter set-up to the lines was generally slow due to the steep gradients. An old mining road, recently upgraded by power company crews made access to the eastern part of the grid easier.

During the first half of the survey period, the weather was generally cool with frequent drizzle and light showers throughout the day. Towards the latter part of the survey, after equipment repair, the weather became quite hot and humid.

The equipment used on the survey was the UTEM 3 electromagnetic system which has a step function system response. The particular model used on this survey had been modified just prior to its shipment to Australia to acheive

two significant specification improvements. The received signal to noise ratio had been improved by a factor of 3.5 to 1 in the presence of spheric noise with an advanced signal processing technique, and the transmitter output power had been increased by reducing internal power dissipation and hence operating temperature. The UTEM method is described in greater detail in Appendix 1.

Because the mineralized targets being sought were likely both limited in dimensions and probably poorly conducting, longer than usual averaging times were used at all stations. On the first day of surveying, a 4k stack was used (about 150 secs) on line 5600E, and subsequently only 2k stacks were found to be adequate. Without the noise level due to the Wilmot dam generating station just to the east of the survey area, it would have been possible to cut this averaging time in half, and hence greatly increase production.

The equipment problems experienced throughout the survey were due to intermittent contact and variable contact resistance effects which influenced the quartz crystal clock stability. When the last of three independent problems had been isolated and cured on 8 January, the receiver became virtually drift free. All data previously collected that showed unacceptable drift characteristics was rejected and the lines resurveyed. In fact, only lines 5600E, 5900E and 5950E of those surveyed prior to the 8th January had calibration tests that showed acceptable drift.

LAYOUT AND SURVEY DESIGN

The coordinates of the loop and the lines surveyed are presented in table 1. The loop straddles the top of a prominent hill and, as such, three of the edges are all lower than the fourth (5500E). The back edge was placed alongside the Cradle mountain road, the only area where dense bush was not encountered. The emplacement of the loop on the northern side of the survey area was requested by CRA. It should be noted that the observed dip of the quartzites vary from 45^{o} to 70^{o} towards the transmitter loop.

The large loop size was used to adequately cover the proposed survey area and to ensure maximum signal at large distances from the loop front, so that early time channels would have sufficient precision for the detection of poorly conducting targets. The base frequency used was 26.2 Hz and the vertical component (H_z) of the magnetic field set up by the transmitter was measured. This base frequency was sufficiently low as the thickness of overburden was minimal and conductive weathering in the country rocks did not appear to be significant.

DATA PRESENTATION

Field plots os all lines are presented in Appendix 1. Data presentation and format for the UTEM system are a standard procedure explained in sections 2 and 4 of Appendix 2. Figures 1 and 2 of Appendix 1 show the standard legends used of plotted data and on the compilation map.

INTERPRETATION

The UTEM survey in the area showed only short time constant anomalies that could be attributed to regional conductivity. As a result, it would appear that the country rock is reasonably resistive, and that near surface weathering, if present, has not lead to a significant conductivity increase. The response present is interpreted to be due to a near surface layer of conductance less than 0.2 Siemens. Its effect shows up as a migrating crossover at the earliest times, limiting amplitudes close to -200% for channel 9 (the earliest time channel plotted), and in a small positive rise in the intermediate time channels away from the loop.

No good conductors were detected within the survey area. However crossover anomalies with short time constant response are present on all lines, and have been grouped into zones as shown on the compilation map. Each zone will be individually discussed. .

Zone A: The anomalies in this zone have the largest amplitudes of any of the localized anomalies detected. The source is interpreted to be fairly steeply dipping. However as the response has a fairly short time constant of only 0.2 msec, and at the early delay times there is a fair response due to regional conductivity, a quantitative estimation of dip cannot be made as this requires a fix on zero levels.

It is also possible that the observed response is due to current channeling rather than direct toroidal induction in a localized conductor. A poorly conducting shear zone for example, in contact with the overburden conductivity could explain the response. However, the fact that the response changes character significantly from line to line argues against this. The zone appears shallowest on lines 5950 and 5900E with an interpreted depth to top of less than 25m, and appears to end at around line 6000E. The zone extends west off the grid, and is interpreted to be at somewhat greater depths of around 35 to 50m on the westernmost lines surveyed.

Assuming a 500m strike length and that pure toroidal induction is the cause of the anomaly, the conductance of the source would be about 1.3 Siemens. This is quite low for the source to be massive sulphides, however as the expected conductors in the region are unlikely on geological grounds to be massive, the zone may be of geological interest.

Zone-B: The zone B response is most prominent on lines 5950, 6000, and 6100E. Its source is interpreted to be at a shallower depth than that of zone A, with depth to top estimates less than 20m on all lines. Again, this is a very short time-constant response so that it is difficult to determine if toroidal induction or current channeling is the cause. If pure toroidal induction is the cause, the the source must have a large depth extent due to the size and shape of the negative lode of the anomaly. The conductance of the zone based on a time constant of 0.25 milliseconds and a strike length of 400m is 2 Siemens.

Zone C: Zone C shows up as prominent responses on two lines at the west end of the grid. Its source is near surface on line 5700E, and has an interpreted depth to top of 25m on line 5600E. A reasonably large depth extent and an extension of the zone further west are indicated by the large amplitude

of the response. If toroidal induction is the cause, then the zone must have a conductance in the 2 to 3 Siemen range.

Zone D: Zone D is a small amplitude, limited strike length feature that is present on lines 5700E and 5800E. Its source has a top near surface, and based on the amplitude must also have a limited depth extent. The response has a very unusual shape, in that most of the anomaly seems to be a positive rather than negative deflection. An equally possible explanation for the source of this anomaly would be a depth limited body dipping towards the loop, with its location below the reverse rather than normal crossover point. In this case it would lie at station 47+50N on line 5700E, and at station 47+75E on line 5800E rather than at the points plotted on the compilation map. Again this feature has a very short time constant of response, which makes geometrical interpretation difficult due to the presence of a large background response at delay times where the anomaly is present.

Zone E: The UTEM response over zone E is very small and sharp, and would likely have a poor depth limited or discontinuous conductor as its source.

Zone F: This one line anomaly may well represent an extension of zone A. However, its smaller amplitude and shorter time constant could equally well indicate a separate, discontinuous small local conductor.

CONCLUSIONS

A number of short time-constant anomalies corresponding to poor conductors with conductances in the 1 to 2 Siemen range were detected by the UTEM survey over the Dolcoath Granite are grid. Due to the presence of a near surface conducting layer of poor conductivity, but similar short time constant response, it was not possible to say with certainty whether the cause of the anomalies was pure toroidal induction or current gathering effects. Of the conductors, two zones had strike lengths in the 400m range. All detailed zones were interpreted to lie fairly close to surface, with the deepest part of zone A lying at a maximum depth of 50m.

Interpretation of dip was not possible due to the presence of the large amplitude early time anomalies of the overburden. Had the conductors been more conductive, dip estimates could have been made using the anomalies at later times where the zero level to use could have been well established.

None of the detected zones stands out in a geophysical sense. Their potential of being of interest can only be established on geological or other grounds. Apart from the unresolved question of zone D, the location of the zones on the compilation map should be sufficient to locate the location of the top of conductive material, and the interpreted depths shown are maximum depth to source. Dip can best be geologically determined.

APPENDIX 1

DATA SECTIONS

LEGEND FOR UTEM PLOTS

Symbol	Channel number	Mean Delay Time (milliseconds) f=30Hz	f=26Hz	f=15Hz	f=13Hz
◇	10	0.025	0.029	0.05	0.058
△	9	0.05	0.058	0.1	0.115
⧗	8	0.1	0.115	0.2	0.231
⅂	7	0.2	0.231	0.4	0.462
⅄	6	0.4	0.462	0.8	0.923
⅀	5	0.8	0.923	1.6	1.85
⧈	4	1.6	1.85	3.2	3.69
\	3	3.2	3.69	6.4	7.38
/	2	6.4	7.38	12.8	14.77
|	1	12.8	14.77	25.6	29.54

All channels are plotted as:

$$\frac{\text{Channel - reference}}{\text{base}} \times 100\%$$

For total field normalization: reference = 0

secondary : reference = primary component or Channel 1.

If Ch 1 symbol appears on plot then:

reference = primary for Chan 1
reference = Chan 1 for all other channels.

If no Ch 1 symbol is present then:

reference = primary component for all channels.

Normally base = primary field (total) at reading station.

If symbol ***> appears then base = primary field at reference station marked with symbol.

LEGEND FOR UTEM COMPILATION MAPS

Axis of a crossover type anomaly. The number a indicates the estimated geometrical depth to top of the source. Text must always be consulted for discussion of validity of estimate

Axis of reversed crossover - can be produced when a small conductor dips towards the transmitter. The number b indicates latest anomalous time channel.

Indicates a negative anomaly of width shown by the dash. Can sometimes be confused with negative lobe of a crossover anomaly.

NOTE: SYMBOLS MAY HAVE VARYING SIZE ACCORDING TO IMPORTANCE

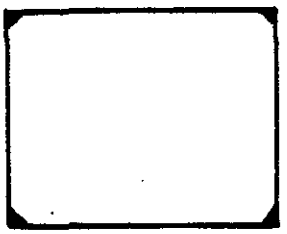

Outline of Transmitter Loop

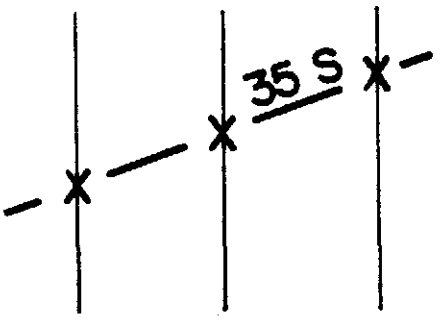

Conductor axis as shown by crossover anomalies. Conductance in Siemens (mhos) is interpreted value of zone as a whole.

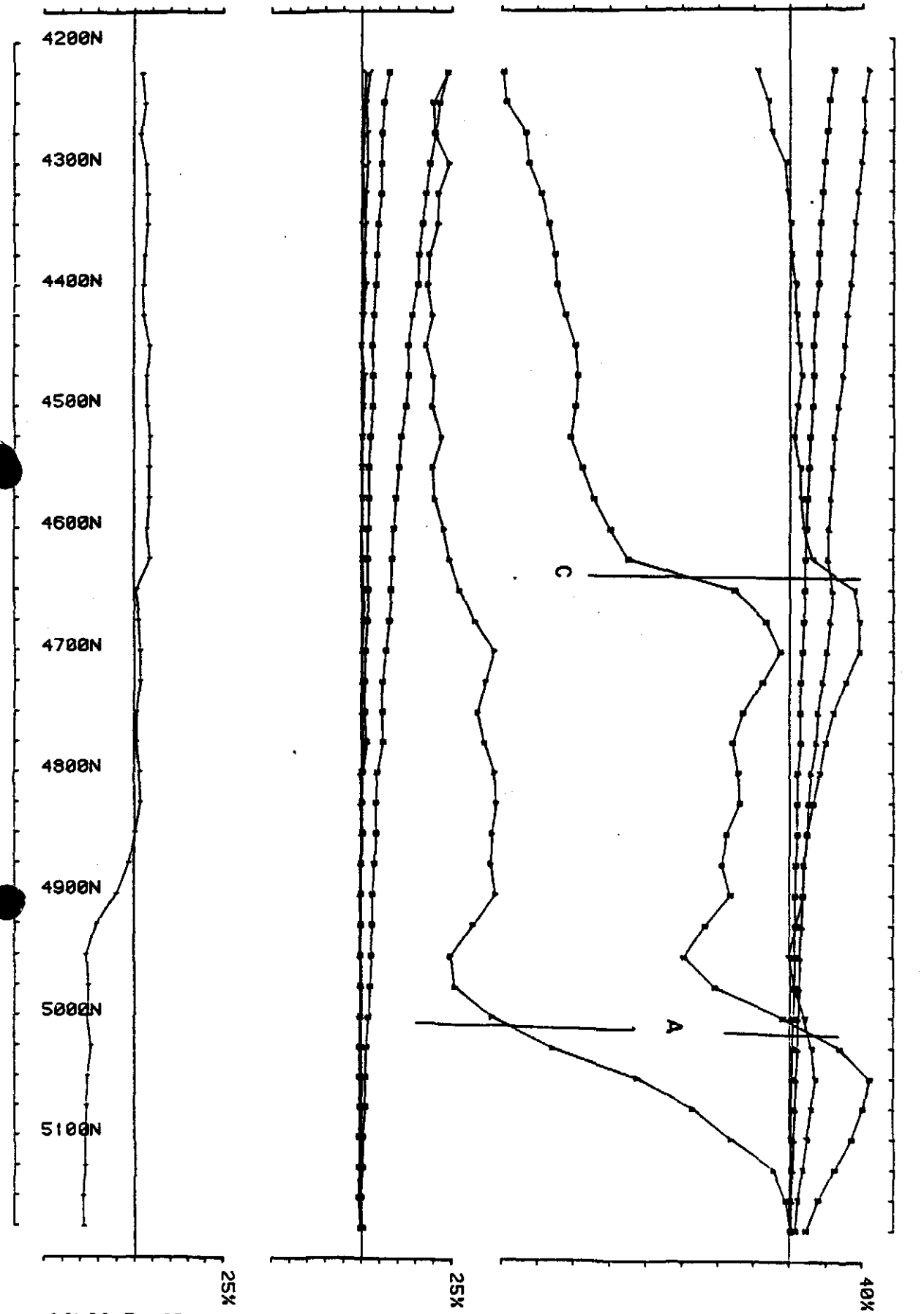

Area DOLCOATH GRANITE AREA SHEFFIELD TASMANIA CRA Job 007001 Freq(hz) 26.2(

Loop no 0711 Line 5600E component Hz secondary Ch 1

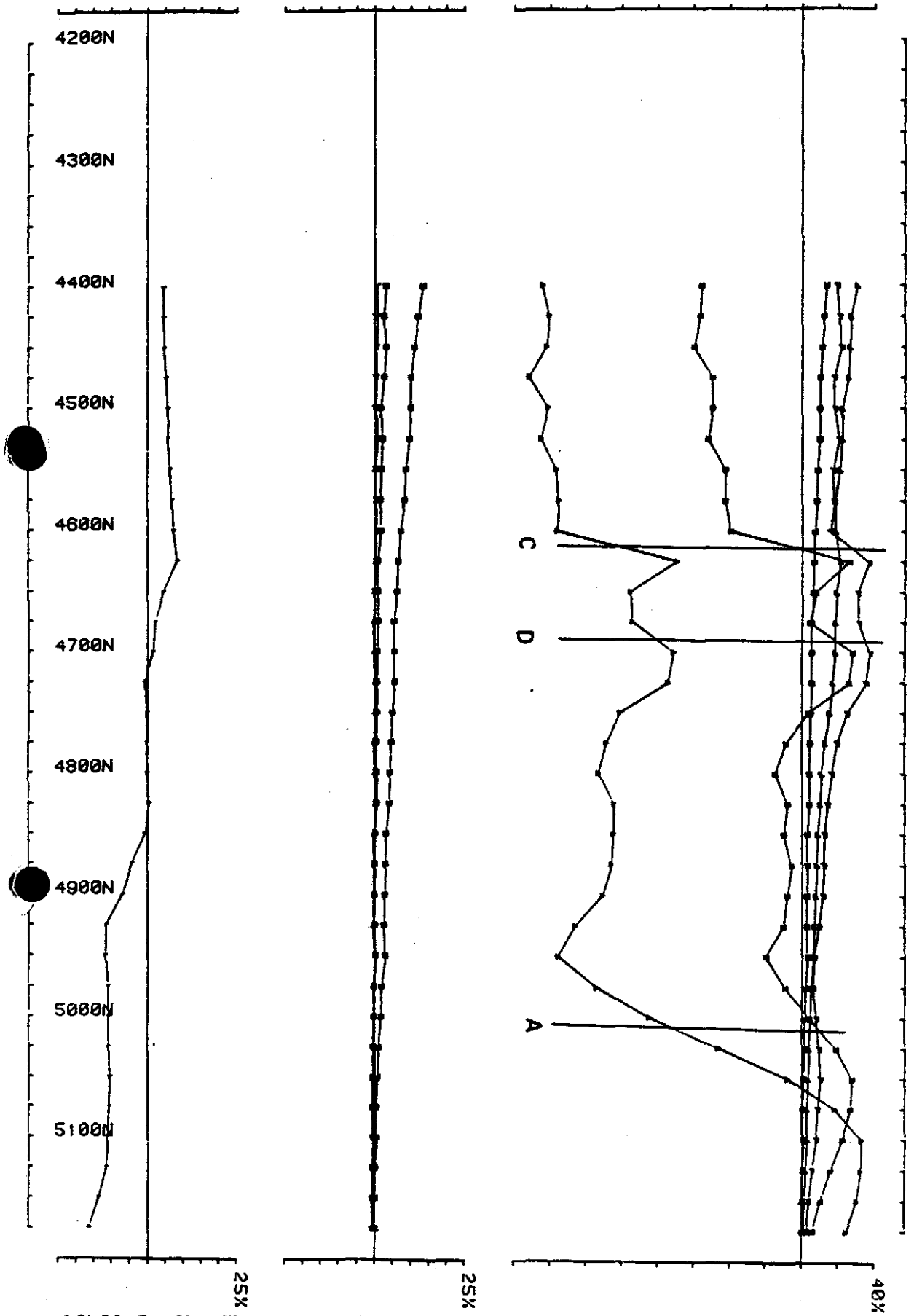

Area DOLCOATH GRANITE AREA SHEFFIELD TASMANIA CRA Jul 007001 Freq(hz) 26.20

Loop/w 0711 Line 5700E component Hz secondary Ch 1

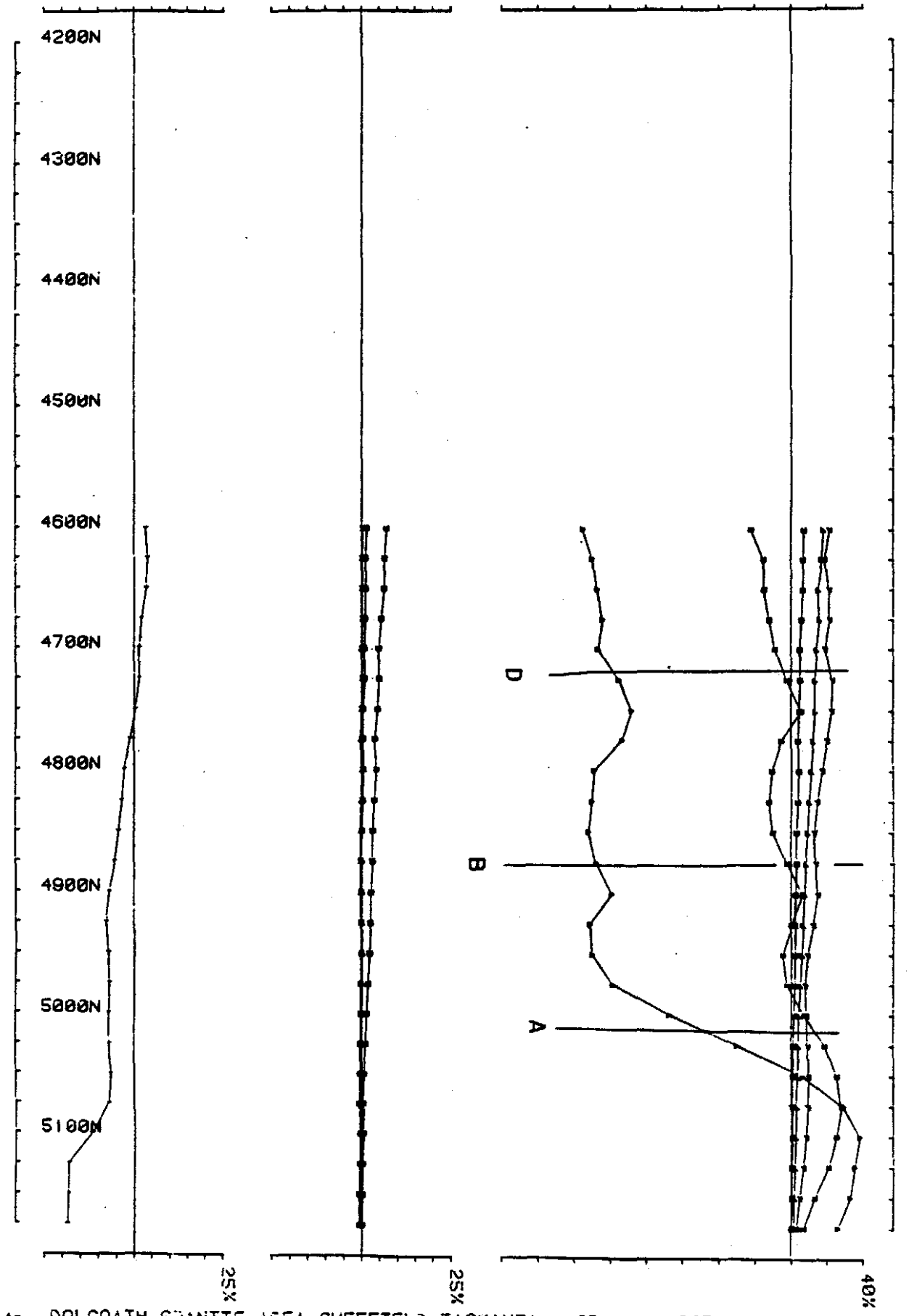

Area DOLCOATH GRANITE AREA SHEFFIELD TASMANIA CRA Job 007001 Freq(hz) 26.20

Loop no. 0711 Line 5800E component Hz secondary Ch 1

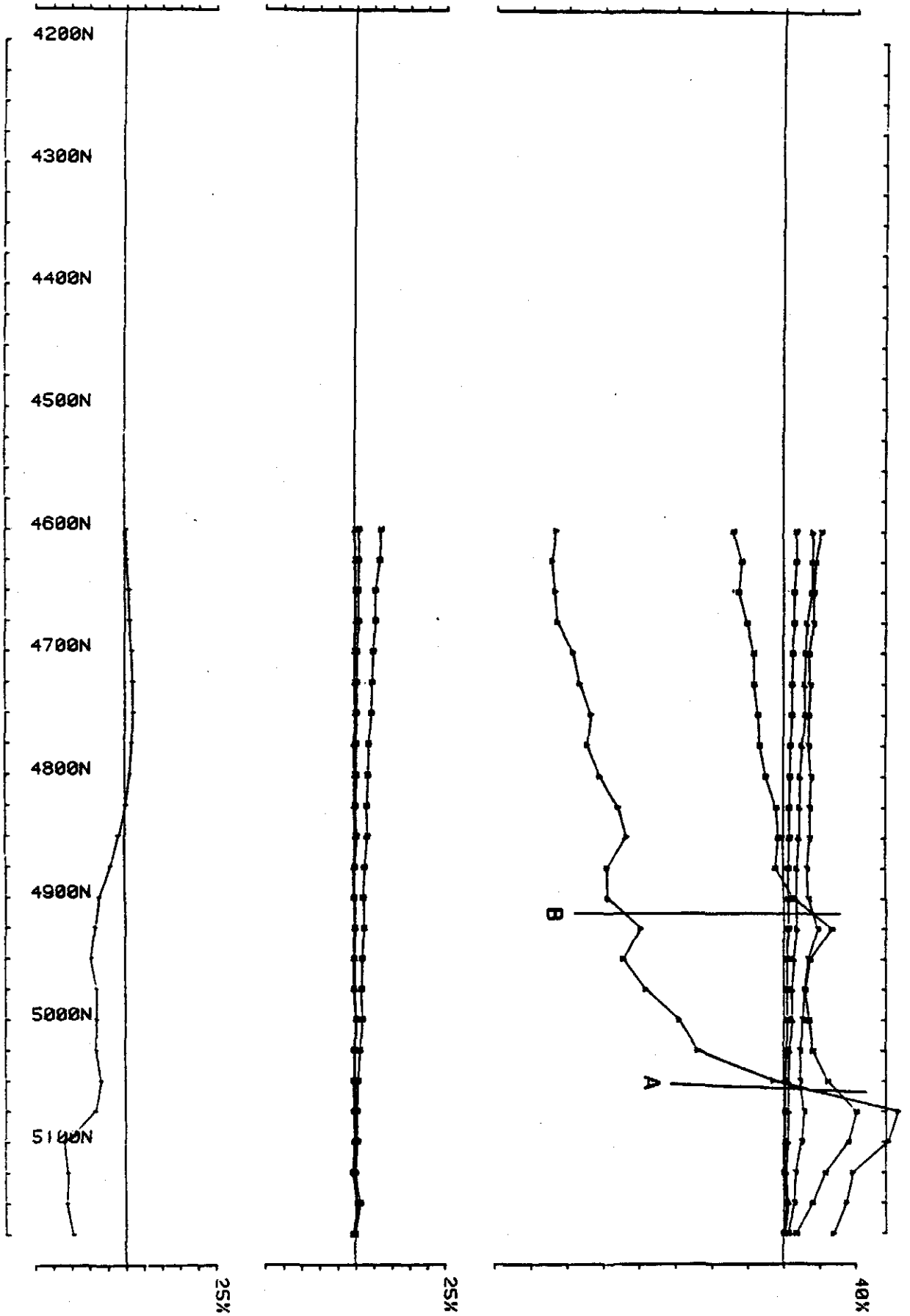

Area DOLCOATH GRANITE AREA SHEFFIELD TASMANIA CRA Job 007001 Freq(hz) 26.20

Loop 0711 Line 5900E component Hz secondary Ch 1

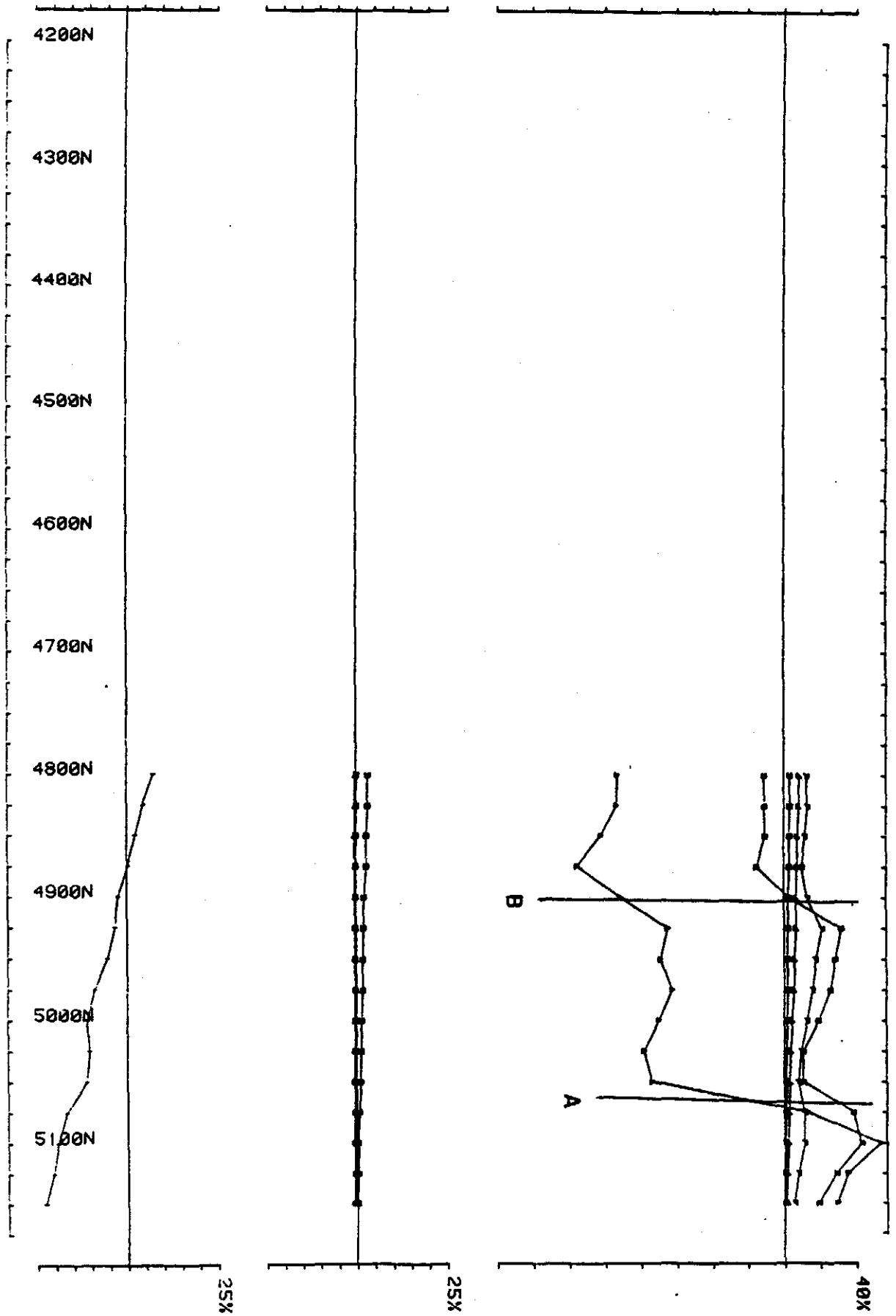

Area DOLCOATH GRANITE AREA SHEFFIELD TASMANIA CRA Job 007001 Freq(hz) 26.2C

Loopno 0711 Line 5950E component Hz secondary Ch 1

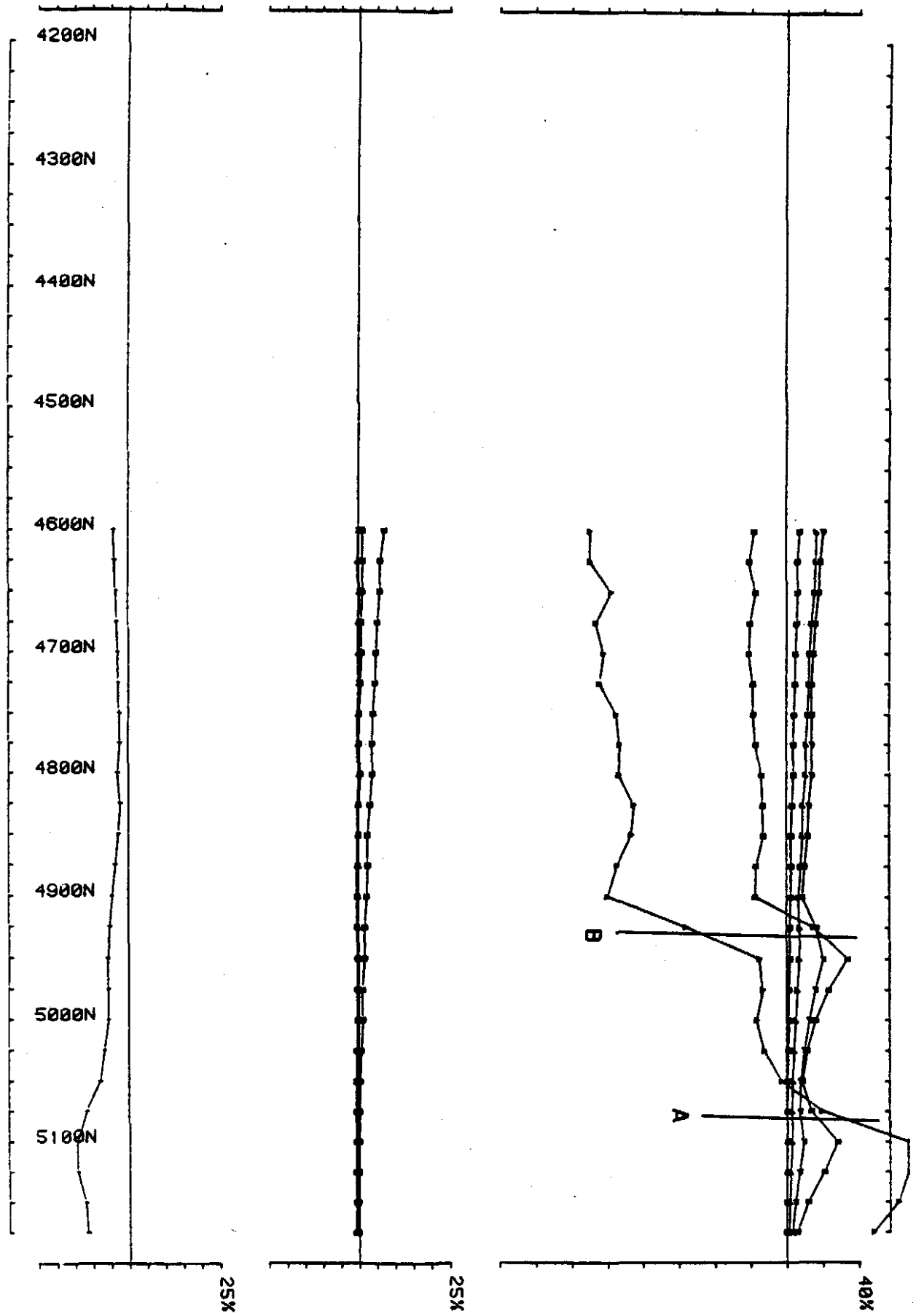

Area DOLCOATH GRANITE AREA SHEFFIELD TASMANIA CRA Job 007001 Freq(Hz) 26.20

Loopno 0711 Line 6000E component Hz secondary Ch 1

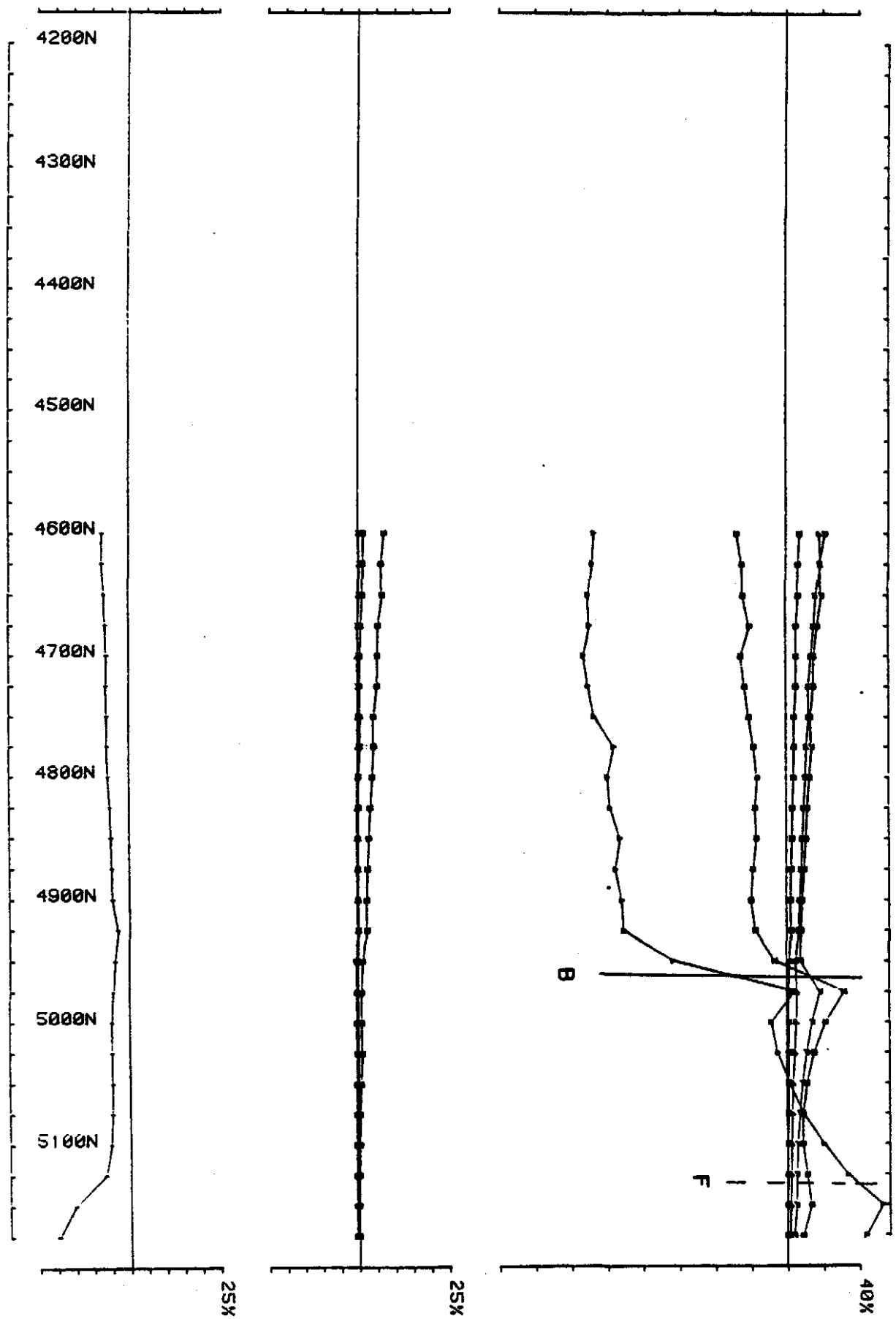

Area DOLCOATH GRANITE AREA SHEFFIELD TASMANIA CRA Job 007001 Freq(Hz) 26.2C

Line 0711 Line 6100E Component Hz Secondary Ch 1

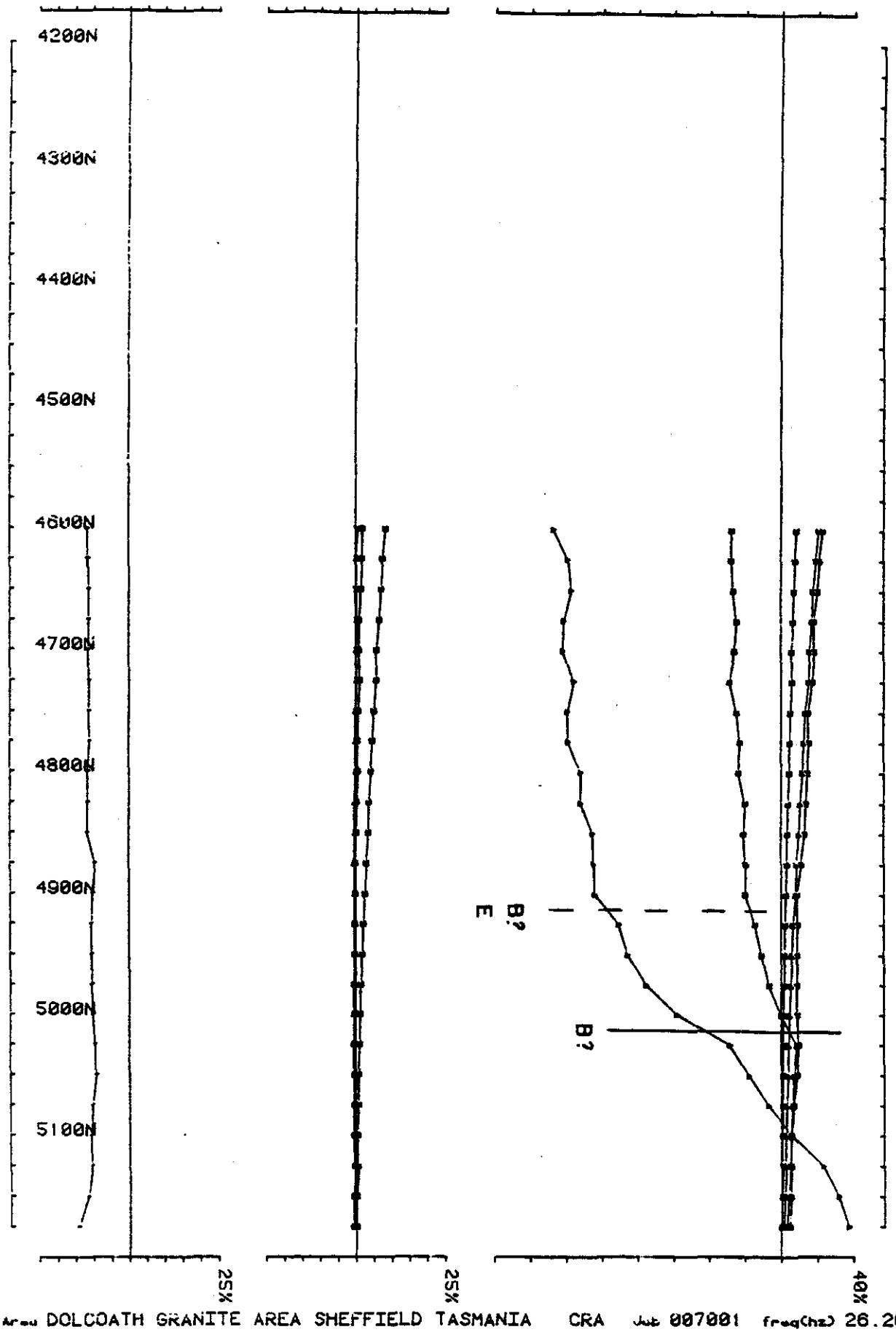

Area DOLCOATH GRANITE AREA SHEFFIELD TASMANIA CRA Job 007001 Freq(hz) 26.20

Hz

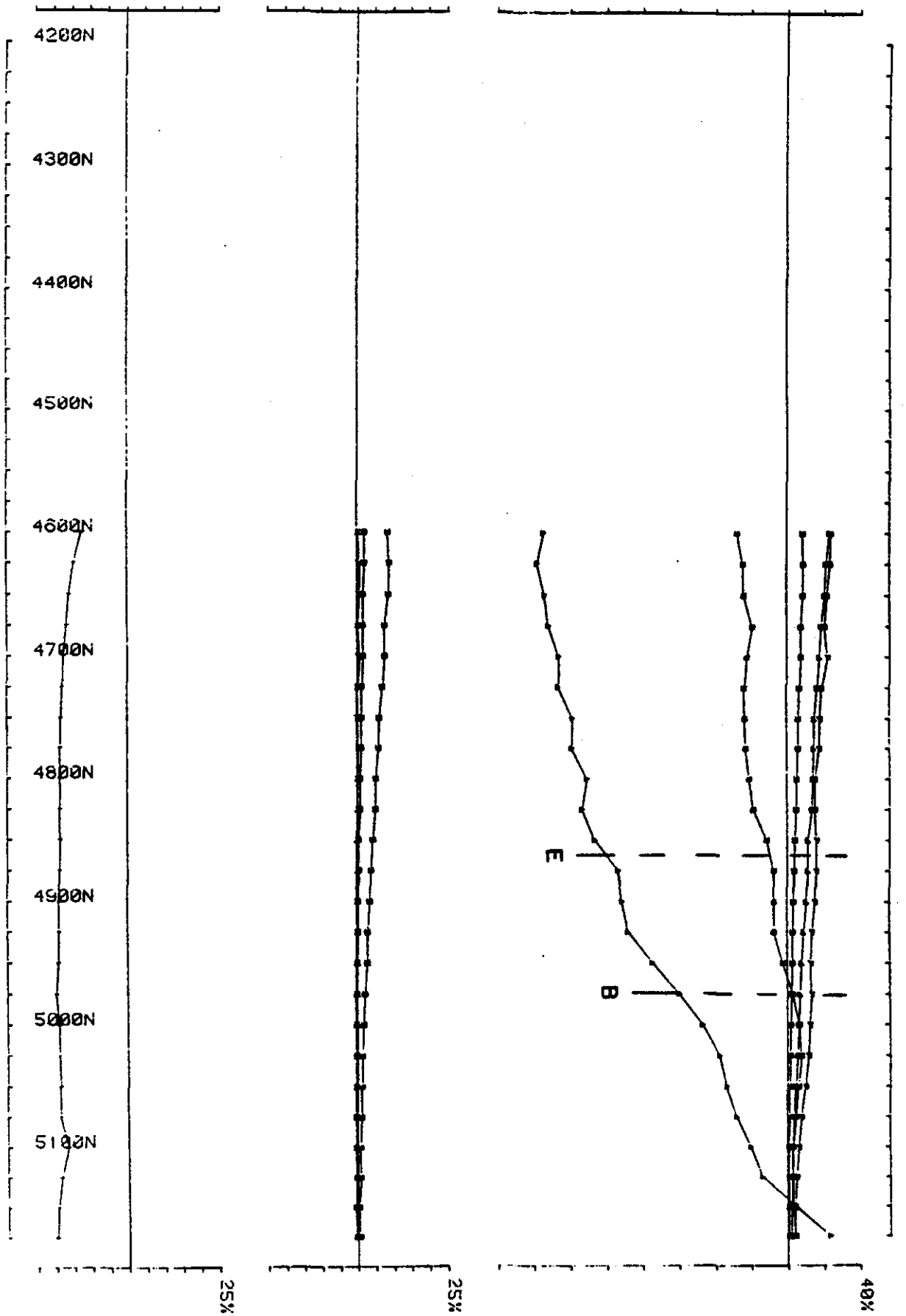

Area DOLCOATH GRANITE AREA SHEFFIELD TASMANIA CRA Job 007001 Freq(Hz) 26.20

Loop: XY11 Line 8300E Component Hz Secondary Ch 1

425 000E

426 000E

5200N

WILMOT LAKE
POWER TUNNEL

5 407 000N

LOOP 1

4800N

4600N

4400N

4200N

5700E

5800E

5900E

5950E

6000E

6100E

6200E

6300E

5000N

A

B

C

D

E

F

5 406 000N

UTEM MK III SURVEY

FOR

CRA EXPLORATION PTY. LIMITED

DOLCOATH GRANITE AREA

TASMANIA

5 cm

COMPILATION MAP — PLAN No.

SURVEY BY : FG — 1982 JAN

SCALE : 1:5000

DRAWN : FG, JM — 1982 FEB

78803

APPENDIX II

A WIDEBAND, TIME DOMAIN EM SYSTEM USING A FIXED TRANSMITTER AND MAPPING RECEIVER

788040

I

UTEM: A Wideband, Time domain EM System Using a Fixed Transmitter and Mapping Receiver

J.C. Macnae, Y.L. Lamontagne, G.F. West (1981)

1. Introduction

UTEM is a wideband, time-domain, ground EM system with a step-function system response which was developed in the Geophysics Laboratory, University of Toronto by Y.L. Lamontagne and G.F. West. It was designed to achieve the sensitivity and interpretability necessary to handle problems of deep exploration and conductive environments, in an economically viable manner. The UTEM method was conceived in 1970, and the first instrument UTEM I was operational in 1972. This analogue system was used in a number of surveys which were described by Lamontagne (1975). UTEM II (a digitally recording system) was then designed and constructed at U of T with financial aid from a consortium of mining companies. It was first used in 1976. To fall 1980, about 1000 line km had been surveyed with the system from 144 loops in 35 areas. UTEM III, which is a microprocessor controlled system with expanded capabilities is now (1981) being produced by Lamontagne Geophysics Ltd, 740 Spadina Ave, Toronto. Some of the field results obtained using the UTEM II system have been described in Lamontagne et al. (1977, 1980), Macnae (1977, 1980a, 1981), Lodha (1977), Podolsky and Slankis (1979).

2. The UTEM System

UTEM uses a large, fixed, horizontal transmitter loop as its source. The field of this loop is mapped in the quasi-static zone with the receiver system; the vertical component of the magnetic field is always measured, and in some circumstances the horizontal magnetic and electric field components may be measured as well (Figure 2.1). The size of the transmitter loop depends on the prospecting problem; loops may range from about 1.5 km x 1 km in resistive terrain to 300m x 300m in a conductive area. Lines are typically surveyed to a distance of 1.5 to 2 times the loop dimensions.

The large loop transmitter - field mapping receiver configuration was chosen because the system was to be made capable of the deepest

UTEM SURVEY LAYOUT

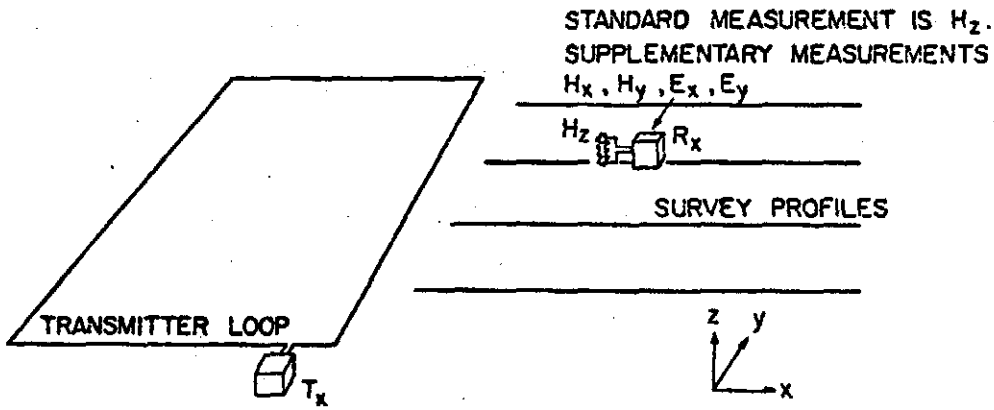

Fig. 2.1 Schematic layout of a UTEM survey.

UTEM WAVEFORMS

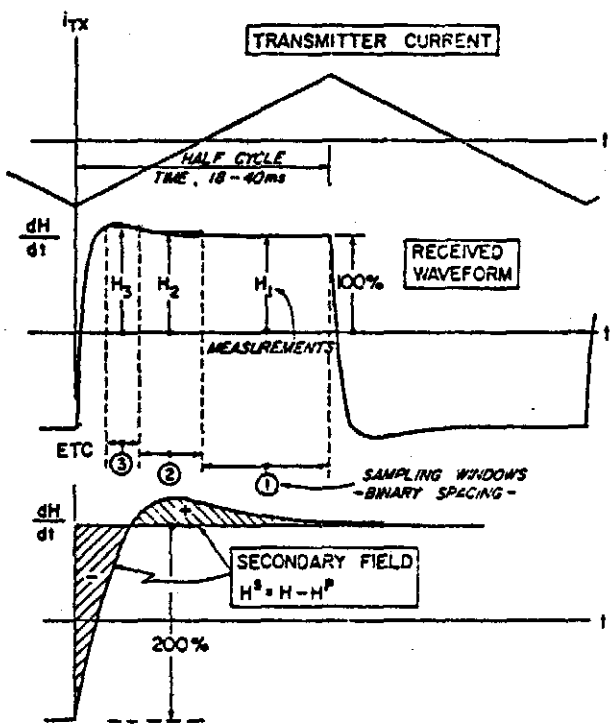

Fig. 2.2 Transmitted and received UTEM waveforms. Note that the measurement channels are numbered from the latest to the earliest.

possible exploration for ore-body sized conductors, without sacrificing the ability to resolve shallower structures (<50m). This dictates a very large transmitter moment, and makes a distributed source and/or a large separation between transmitter and receiver desirable. Then the transmitter-to-target and target-to-receiver coupling does not vary by many orders of magnitude within the zone of exploration.

Given a large transmitter and a large Tx-Rx separation, it is inevitable that extensive overburden and formational conductors will be more highly energized than with a small scale system. Also, it becomes increasingly likely that the system will be "seeing" several nearby conductors at once. The magnetic field of a fixed current system induced in the ground is a potential field, and if it is mapped on a profile or over a surface, there is a firm theoretical basis for separating it into parts and estimating the current systems which caused it. When the transmitter and the eddy current system moves for each observation, stripping of responses into component parts is more difficult.

There are negative aspects to using a fixed transmitter method. The transmitter can be positioned badly for induction in small plate-like conductors, and a large good conductor will screen a smaller, shorter time-constant conductor behind it. For these reasons it may be desirable to have survey coverage from more than one transmitter location. When the method is field efficient, the cost of this is not intolerable.

The UTEM transmitter passes a low frequency current of precise triangular waveform through the transmitter loop. The sensor of the magnetic field is a coil, which responds to the time derivative of the local magnetic field, so in "free space" a precise squarewave voltage would be induced in the receiver. In the presence of conductors the waveform is substantially distorted. The UTEM receiver measures this distortion by determining the amplitude at 10 delay times (average over time windows) located between the waveform transitions with binary spacing. The sampling scheme is shown in Figure 2.2. The base frequency of the system is selectable, usually 30 or 15 Hz, (25 or 12.5 Hz in 50 Hz countries). A common practice is to set the base frequency about 0.5 Hz from a sub-harmonic of the power line in order that power

line interference can be detected by slow beating in the data. The base frequency is usually low enough that the ground response has nearly vanished by the end of the half cycle. When this is the case, the UTEM system determines the step responses of the ground in the time range 25μs to 12.5ms (30 Hz base frequency).

3. Time Domain Systems

Time domain systems have some advantage over frequency domain systems in that simultaneous measurement is possible over the whole spectrum, and at the same time it is possible to check the synchronization of the transmitter and receiver time-bases. Most time domain systems employ an on-off type of transmitter signal and confine all measurements to the off period, as this automatically separates the secondary from the primary field. When a coil is used as a sensor, however, the time derivative of the signal is observed. Thus, if the transmitter loop is energised with a step current, it is the impulse response of the ground which is observed.

It is much more desirable for interpretation purposes to observe the step response than any other time response. The reason for this lies in the characteristics of eddy current decay. For the step response, the early time limit is identical to the frequency domain inductive limit, and for a simple conductor in free space this is a function of geometry alone. For the impulse response, the early time limit is scaled from the step response limit by the inverse of the transient decay time constant (Figure 3.1). Thus, the decay rate must first be determined in order to interpret amplitude information in terms of geometry. In simple cases this may present little difficulty, but when complex or over-lapping responses are observed it can be a serious problem. Also, even in the case of the step response, the overburden anomalies which generally are of short time constant have early time amplitudes which are very much larger than the anomalies of the long time constant of target conductors. Any further amplification caused by measuring the impulse rather than step response is clearly undesirable.

The sampling scheme of Figure 2.2 was chosen so that time scaling is permitted. In frequency domain, inductive responses may be characterised by dimensionless parameters of the form

$$\theta_f = \sigma\mu\omega L^2$$

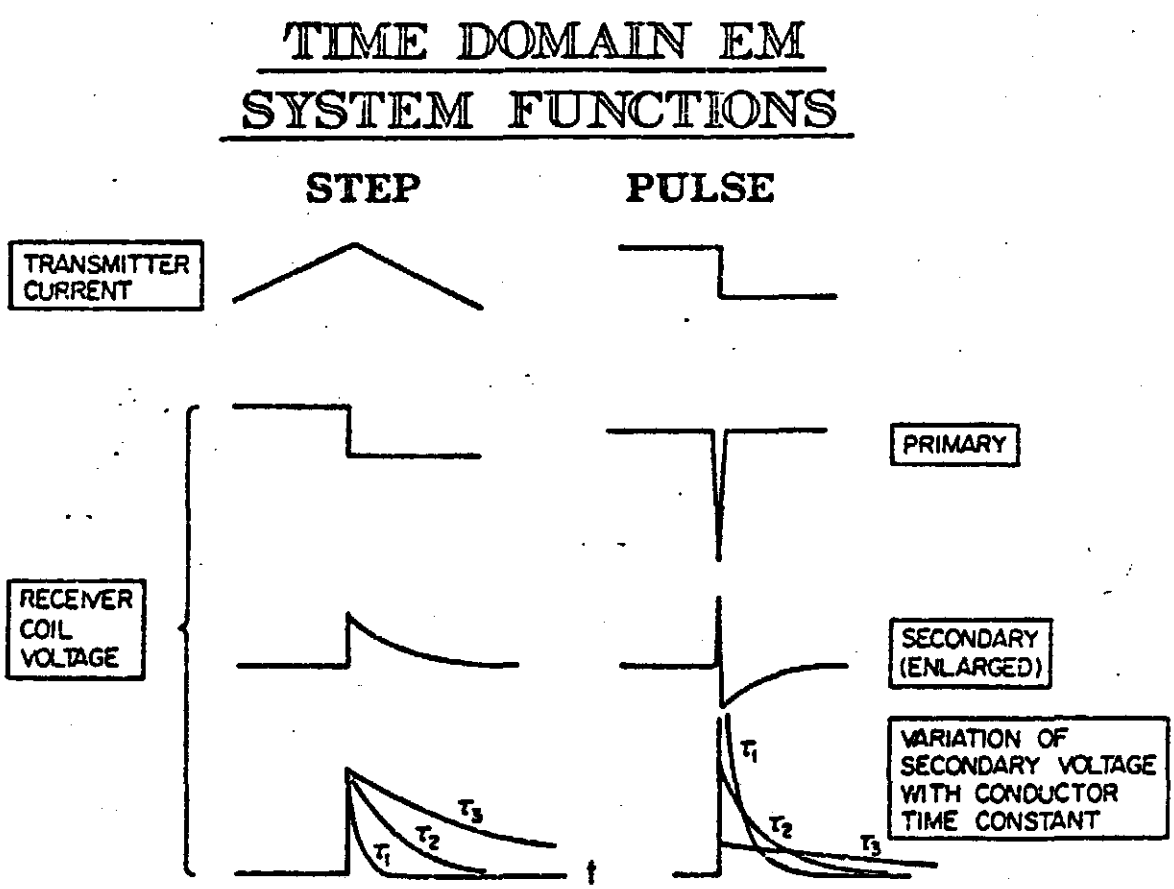

Fig. 3.1 Comparison of transient signals in step and pulse type systems.

which defines the equivalence in response obtainable by scaling conductivity, permeability, frequency and dimensions. In time domain, analogous scaling can only be performed for simple discontinuity system functions such as a step, impulse, or ramp which have changes in form at only one time (Lamontagne, 1975). The equivalent dimensionless parameter in time domain is given by

$$\theta_t = \sigma\mu L^2/t$$

To ensure that time scaling can apply to data that has been sampled and averaged over a time window, it is necessary that the window widths be proportional to time after the discontinuity. UTEM has such sampling. Time scaling should only be applied to anomalous responses which are short enough so as to vanish in the inverval between the two successive transitions of the step which form the square wave. The base frequency used in UTEM is usually low enough that this is the case.

4. Data Presentation

Because the field intensity falls off rapidly with increasing distance from the transmitter loop, it is desirable to normalize the secondary field observations in some manner. A suitable normalizing factor is the primary vertical magnetic field signal. If the position of the loop and the receiver is known reasonably accurately, a calculated value of H_z^P may be employed. If the ground response vanishes by late time, the channel 1 measurement is a direct measure of H_z^P. Normal survey practice encompasses both procedures.

Figure 4.1 shows one example of a standard UTEM H_z^S data plot. Channel 1 is plotted as an absolute secondary field (Ch 1 - H^P)/H^P and all other channels are normalized to Ch 1 to correct for errors in calculation of H^P due to position error, and also for static magnetic anomalies (for further details see Lamontagne, 1975). The late channels on the sample plot show a crossover type of anomaly, indicative of a concentration of induced current. The channel variation indicates that these induced curents are decaying with time. On the early time channels, the migration of cross-over location from one channel to another indicates that the secondary current flow at these times is not fixed in geometry, which is indicative of an extensive conductor (here extensive overburden) rather than a localized conductor such as that responsible for the late time crossovers.

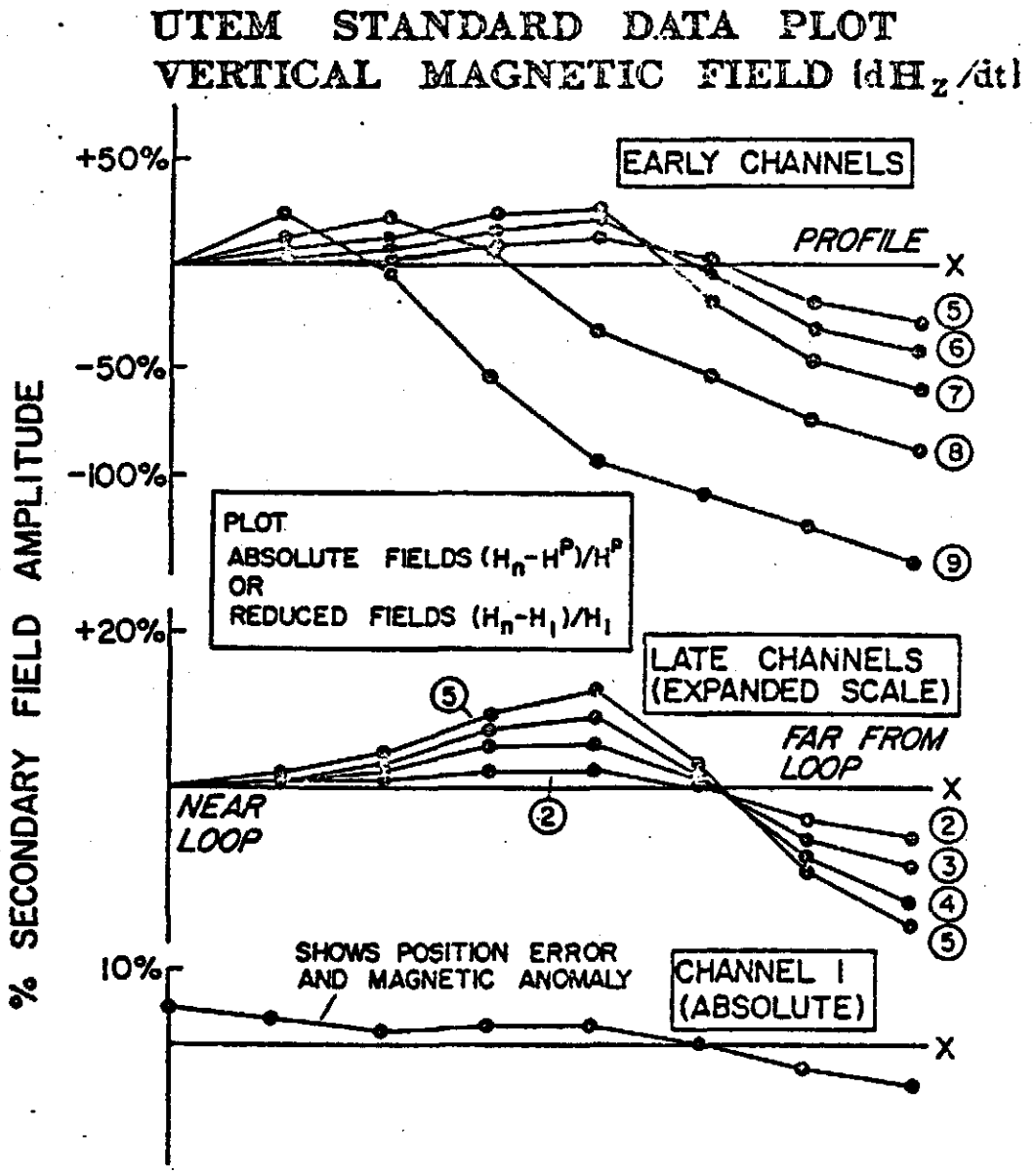

Fig. 4.1 Standard presentation of UTEM vertical component magnetic field data.

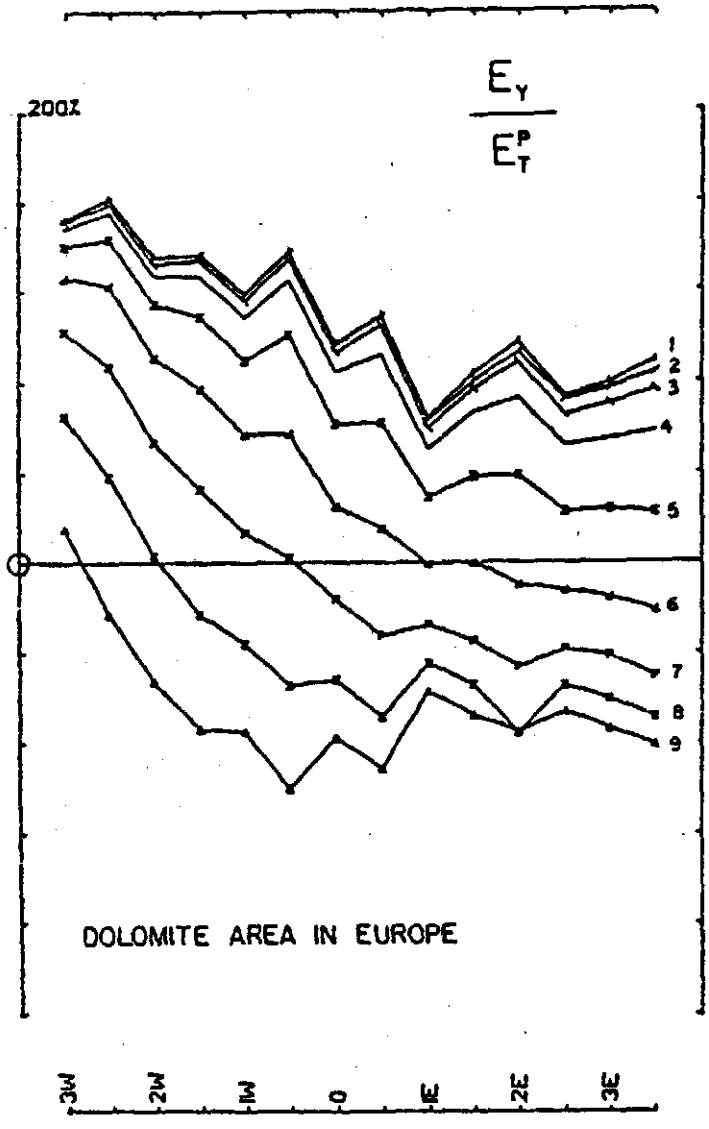

Fig. 4.2 Standard presentation of electric field data as observed component normalized to the free space field of the Tx loop.

The electric field wave form is, like the voltage from the coil sensor, a square wave if the ground is very resistive. It is distorted in much the same way as the H signal when the ground is conductive. Electric field observations are usually plotted as E_i/E_T^P - the observed channel voltage between the electrodes divided by the maximum expected late time voltage between electrodes at the observation point oriented in any direction $(E_x^{P2} + E_y^{P2})^{1/2}$. This normalization facilitates intercomparison of x and y component data.The geological noise level in electric field data is usually high, so expanded scale plotting is not required. All channel data are usually plotted on the same axes, as shown in Fig. 4.2.

The electric field converges to a fixed value, as the EM transients vanish at late time. However, the late-time E limit is usually different from the free space or uniform half space value, due to lateral inhomogeneity of the earth's conductivity structure. The late time electric field around a loop greatly resembles what is seen in a gradient resistivity survey. The field weaves about around the more resistive areas and through the more conductive ones. A vector display of the late time E field is an interesting reflection of the relative conductivity of various parts of the ground. It is impactical to plot the actual E vectors as the field intensity falls off too rapidly. The vector observations are therefore scaled to the calculated free space field of the loop, as for profile plots. Vector plots of the free space field of a loop are shown in Fig. 4.3. Examples of field data are given in the following section.

Errors caused by the presence of noise and poor geometrical control are discussed for the magnetic (H) field case in Lamontagne (1975). For the electric (E) case, details of the measurement and sources of error are discussed by Macnae (1981) in Appendix G. As for the magnetic fields, good geometrical control is important to minimize error in primary field calculation at individual stations. As in the DC resistivity method, topographic features can seriously distort local electric fields, and local conductivity contrasts such as overburden patches and minor lithological changes can have quite large effects on the amplitude of measured E fields.

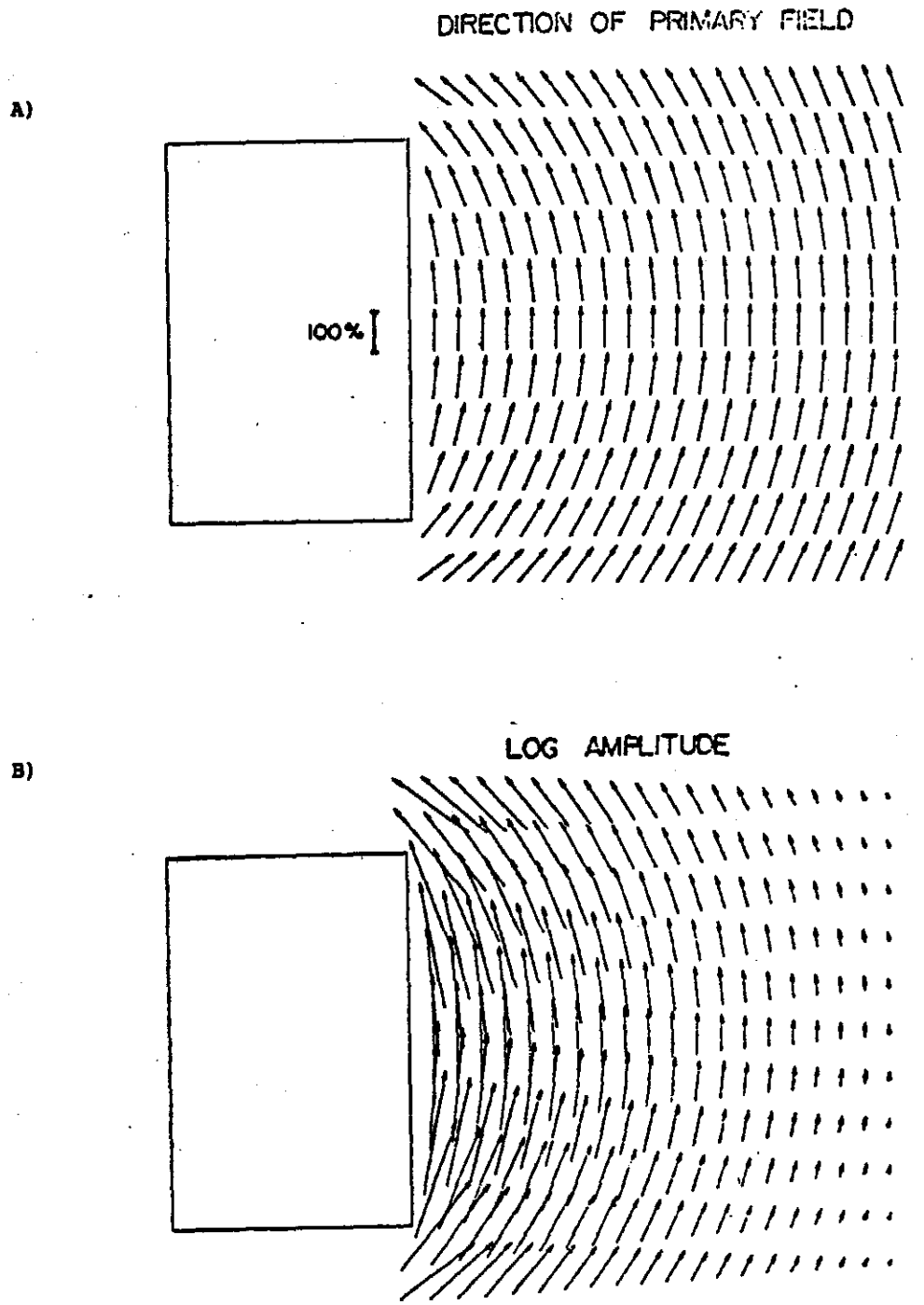

Fig. 4.3 Vector plots of late time electric field

A) Direction information only
B) Showing direction and intensity of the primary field.

5. Equipment. (UTEM III)

The transmitter consists of a 1.8 kW motor-generator (34kg) with fuel pump for unattended operation and the UTEM power signal generator (20.8kg). The power unit provides currents of up to 6A peak into loops of up to 40Ω and 3A into 80Ω. The transmitter loop wire is generally no. 17 AWG magnetwire, (≈10kg/km). A single turn is used in large loops, while two or more may be used in small loops.

The UTEM receiver consists of the measuring unit and an H and an E field sensor. The H sensor is a ferrite cored coil of 600m^2 equivalent area with internal preamplifier which is mounted on a rugged tripod (6.5kg). The E field sensor is just a pair of metal electrodes and wires to make a grounded dipole of about 25m length. The measuring unit (≈13kg) records the 10 channel measurements from the selected sensor on a magnetic tape cassette and also provides visual and aural indications for the operator. The measuring system is of integrator type (analogue within windows, digital from cycle to cycle), with automatic rejection of extreme noise pulses and compensation for systematic errors. Integration times vary with signal-to-noise ratio and are usually in the range 30 seconds to 3 minutes. In difficult circumstances such as in close proximity to noisy power lines where the signal-to-noise ratio is low, longer integration times are used to obtain good data.

Transmitter and receiver distortion and drift are very small. (Tx rise time 6μs; distortion <.005% above 10 Hz; amplitude regulation .2% >100μ, .05% > 1 ms; amplitude drift .02%/day, 100 ppm/^{o}C). The transmitter and receiver units are synchronised by use of precise crystal oscillators. These are normally reset once or twice per day. Drift is about 10μs/working day.

The tape recorded UTEM data can be played back into virtually any computer system for editing and plotting. The U of T UTEM II system employs a Tektronix 31 electronic desk calculator for data reduction and an 11 x 17 in. flatbed plotter. UTEM III has a more powerful custom computer and plotter. Either unit is sufficiently portable and rugged for use in all field camps. The new computer (GFC1) has a weight of 90kg together with all peripherals and transport case. The computer provides the obvious advantage of allowing interpretation to proceed during the survey.

The optimum field crew for a typical UTEM survey is three men: a geophysicist, a trained operator, and a helper. The geophysicist spends part of his time on the survey and part on data reduction and interpretation. Measurement is usually best done with a two man crew especially if E fields are to be recorded. However surveying can still proceed with a single operator. The helper is thus available for loop repair, layout and pickup. The transmitter is normally operated unattended.

INTERPRETATION

6. Layered Earth Responses

The problem of EM induction in a layered earth is very well treated in the literature, particularly for frequency domain systems (e.g. Wait, 1962). Time domain cases have also been studied for some specific problems, for example the thin sheet was solved by Maxwell (1891) and the half-space response has been discussed in Nabighian (1979). A general, layered earth solution for UTEM geometry and waveforms was given in Lamontagne (1975). Figure 6.1 shows 3 examples of computed responses for different a layer conductivities. Figure 6.2 shows 3 examples of a thin layer at different depths. There are several common characteristics of layered earth responses. The shape of the anomalous profiles are generally similar, becoming broader at later times. The migration of crossovers with time, with positive lobes towards the loop and negative lobes away from the loop indicates that the induced current system is migrating away from the loop. This type of behaviour was discussed in Nabighian (1979).

7. Finite Thin Plate in Free Space

A convenient modelling method for thin finite plate conductors in free space is the integral equation solution of Annan (1974). Annan computed the best set of polynomial eigenpotentials of order 4, and used these to represent the induced current flow in the plate as a sum of 15 "eigencurrents". The solution for the eigencurrents themselves is quite complicated, but needs only to be done once for a plate of given width to length ratio. After that, any induced current system can be described in terms of 15 coefficients in the eigenpotential summation. The secondary field at a receiver can then be simply computed in terms of these induced eigencurrents. One great advantage of Annan's method

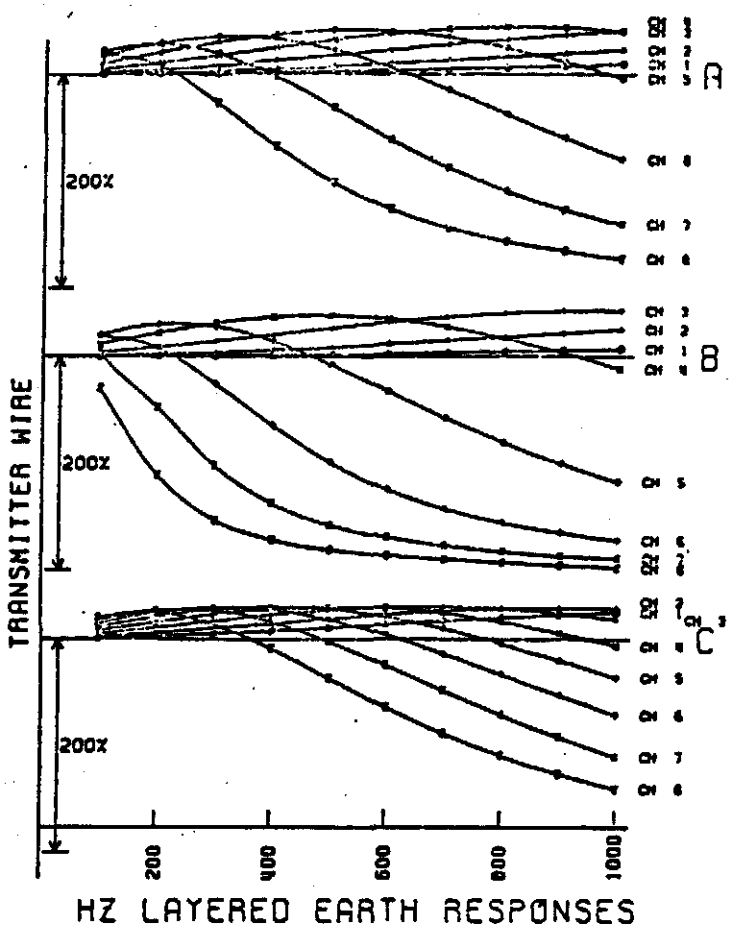

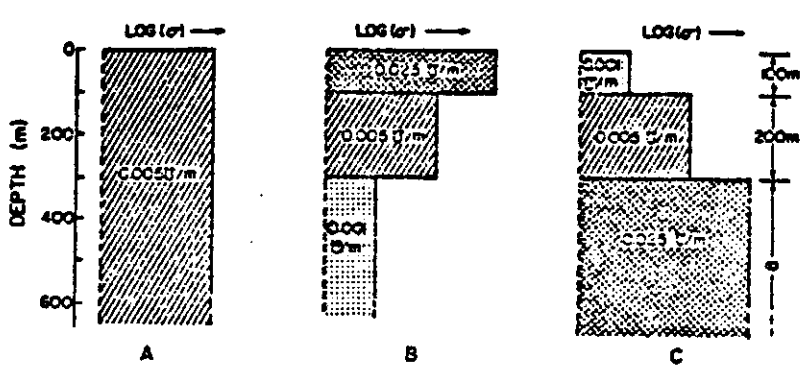

Fig. 6.1 UTEM layered earth response.

5 cm

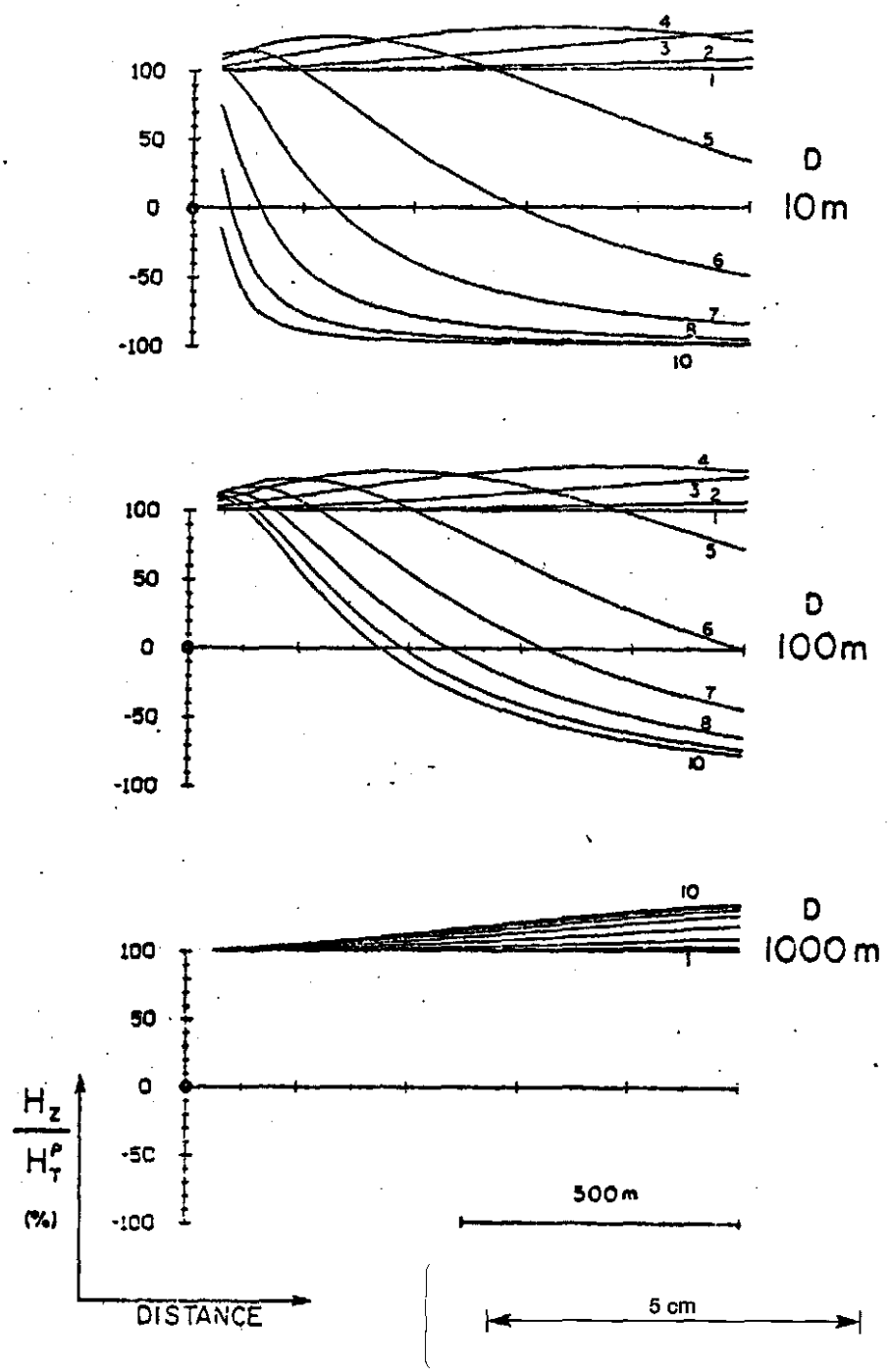

Fig. 6.2 Hz response of a thin horizontal sheet at various depths. The conductivity-thickness of the sheet is 2 Siemens. The front of the Tx loop is at the origin of coordinates.

is that each eigencurrent has a frequency or time domain response identical to a simple loop circuit. Thus the solution for a broad frequency range or many time windows is very easy to calculate. Routines for simple, interactive application of Annan's algorithms to a number of EM systems have been programmed by Dyck for the VAX computer in the Department of Physics, University of Toronto (Dyck et al., 1980).

Examples of type curves generated with Annan's solution may be found in Lodha (1977) and Lodha and West (1977). Figure 7.2 shows the results of a set of computed UTEM type curves for the geometry shown in Figure 7.1. Also shown on Figure 7.1 is the geometry of the primary magnetic field, which controls the nature of induction in the plate. For the zero dip case, the primary field is mostly perpendicular to the plate. The induction in the plate tends to cancel this field at early times, leading to a negative H_z anomaly directly over the plate. Positive shoulders on each side show the secondary magnetic field of the "forward current" near the front edge of the plate nearest the loop and the "reverse current" near the rear edge. The normalization scheme used in plotting this data is the total secondary field by the calculated primary the measuring point. This has the effect of making assymetric a secondary anomaly that is symmetric in terms of absolute amplitude by increasing the relative amplitude away from the loop. In fact, the absolute amplitude of the positive shoulder near the loop is almost always larger than the one on the side away from the loop. As the dip of the plate is increased, the positive shoulder moves away, and by the time a 30^{o} dip is reached the reverse crossover is off the end of the line plotted. From dips of 30^{o} to 135^{o}, the anomaly maintains a basic shape in the form of a simple crossover. The amplitude does vary somewhat however, being controlled by the primary field component normal to the plate which becomes a smaller and smaller fraction of the total field as the plate rotates from 30^{o} to 150^{o} (Figure 7.1). The case at a dip of 150^{o} shows a very interesting behavior. The primary field can be seen to be <u>down</u> in the upper half of the plate, and <u>up</u> in the lower half. The result of this is that the anomaly changes location and amplitude dramatically. For a very small plate, an anomaly could conceivably disappear completely - this phenomenon has been discussed by Bosschart (1964) for the Turam geometry. For a large planar conductor

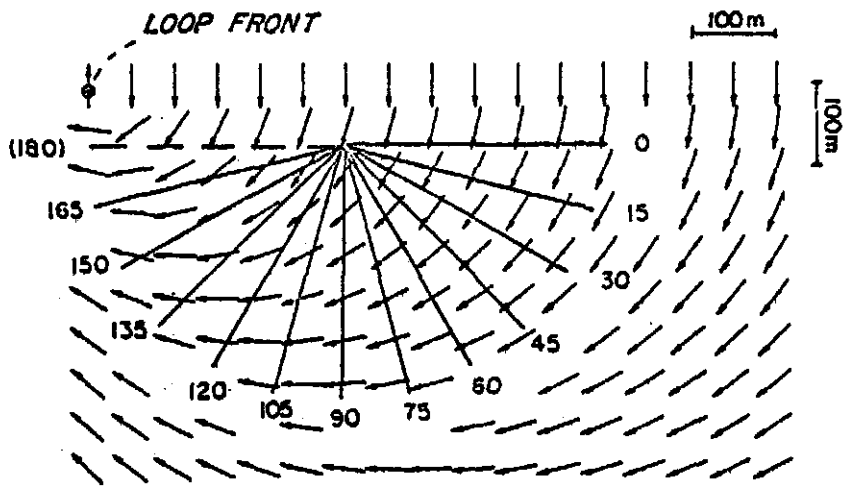

SECTION VIEW OF PLATE CONDUCTORS AND PRIMARY MAGNETIC FIELD

GEOMETRY FOR 90° CASE

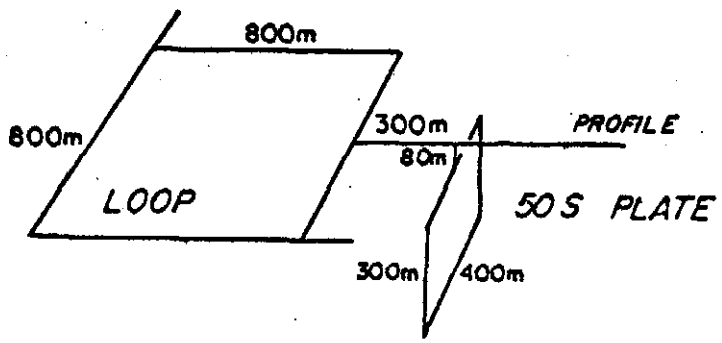

Fig. 7.1 Geometry and dimensions of the models shown in Fig. 7.2. Also shown is the configuration of the primary field in the vicinity of the target conductor.

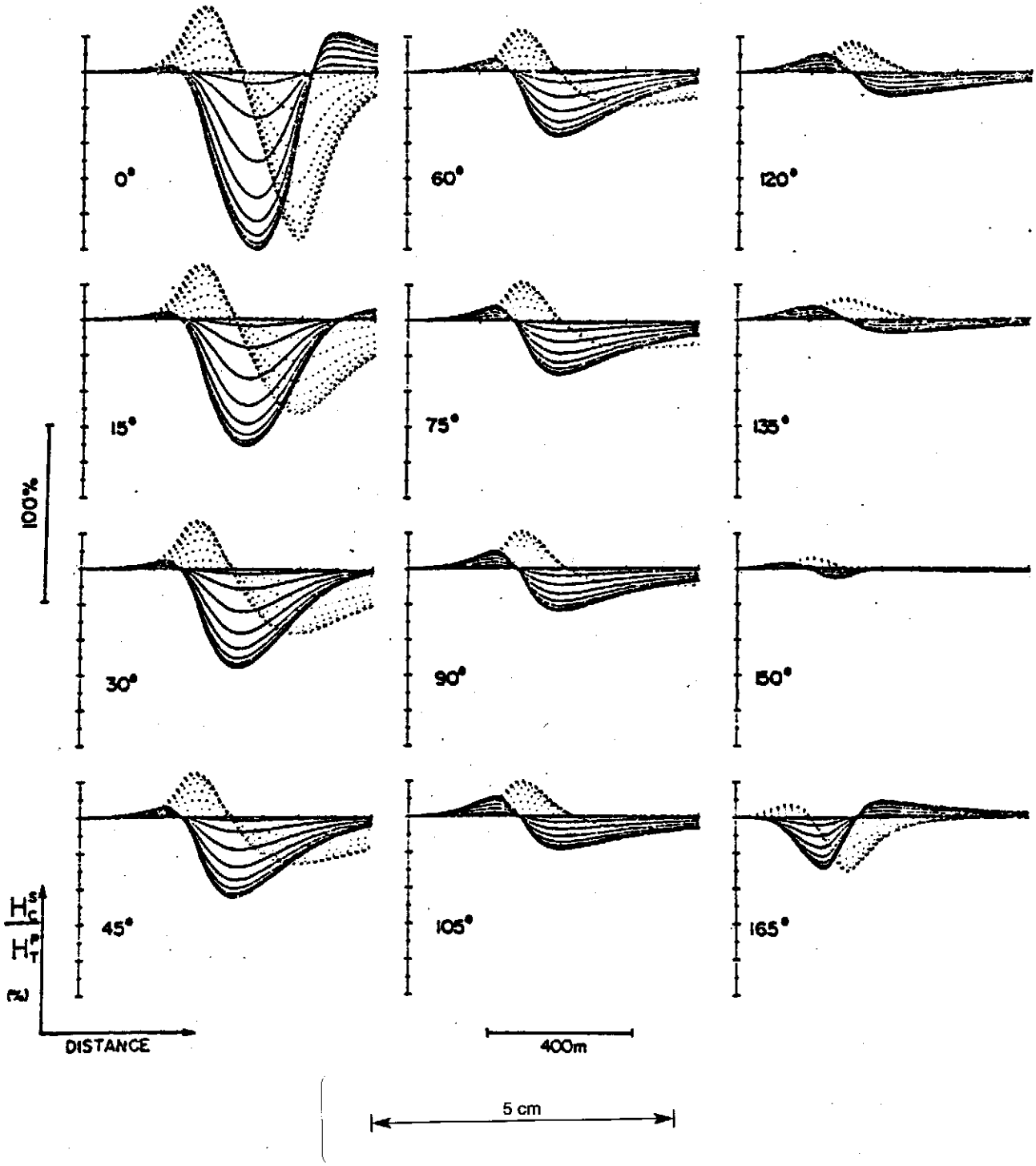

Fig. 7.2 UTEM H_z (solid) and H_x (dotted) profiles over a dipping plate. (Geometry shown in Fig. 7.1).

however, an anomaly is always present as a curving primary field must cut it somewhere. The only case where this might not be true is that of a vertical conductor directly located under the centre of a horizontal transmitting loop. The 165° dip case of Figure 7.2 shows a clear reverse crossover on the edge of the conductor far from the loop. The normal crossover is very small due in part to the reduced induction at the near edge as shown in Figure 7.1, and also to the large primary field used as a divisor for normalization.

The electric field anomaly generated by a plate conductor is affected by the earth-air interface, so analogue scale modelling methods must be employed to produce type profiles. Fig. 7.3 shows an example for a vertical plate. The longitudinal electric field is greatly reduced over the body at all times (i.e. there is a strong reduction in the late time limit). The dynamic (time-varying) part of the anomaly has the same time variation as the magnetic field but has a different geometrical pattern. Because the electric field is highly vulnerable to any conductivity boundary, the static, late-limit part of the anomaly over a conductor may be much reduced by any stratification between the conductor and the surface.

8. Other Simple Anomaly Shapes

A set of simple models is shown in Figure 8.1, for each of which the main features of the vertical magnetic field are sketched. The set of sketches was derived from scale model experiments by Lamontagne (1975). For the simple models illustrated where the host rock is completely non-conducting, the general anomaly shape for one body remains quite constant for the whole time range. The changes in anomaly from one channel to another are mostly in the amplitude and smoothness of the anomalies.

Thin dyke. A conductive, steeply dipping body gives an H_z crossover shape similar to the plate model just discussed. The point where the anomaly changes sign indicates approximately the top edge of the conductor. The anomalies at later times tend to be broader and shifted slightly down dip from those at early times. The inductive decay rate of the anomalies will be discussed shortly.

Surface horizontal finite conductor. A thin horizontal conductor of limited dimensions (not extending under the loop) produces an anomaly

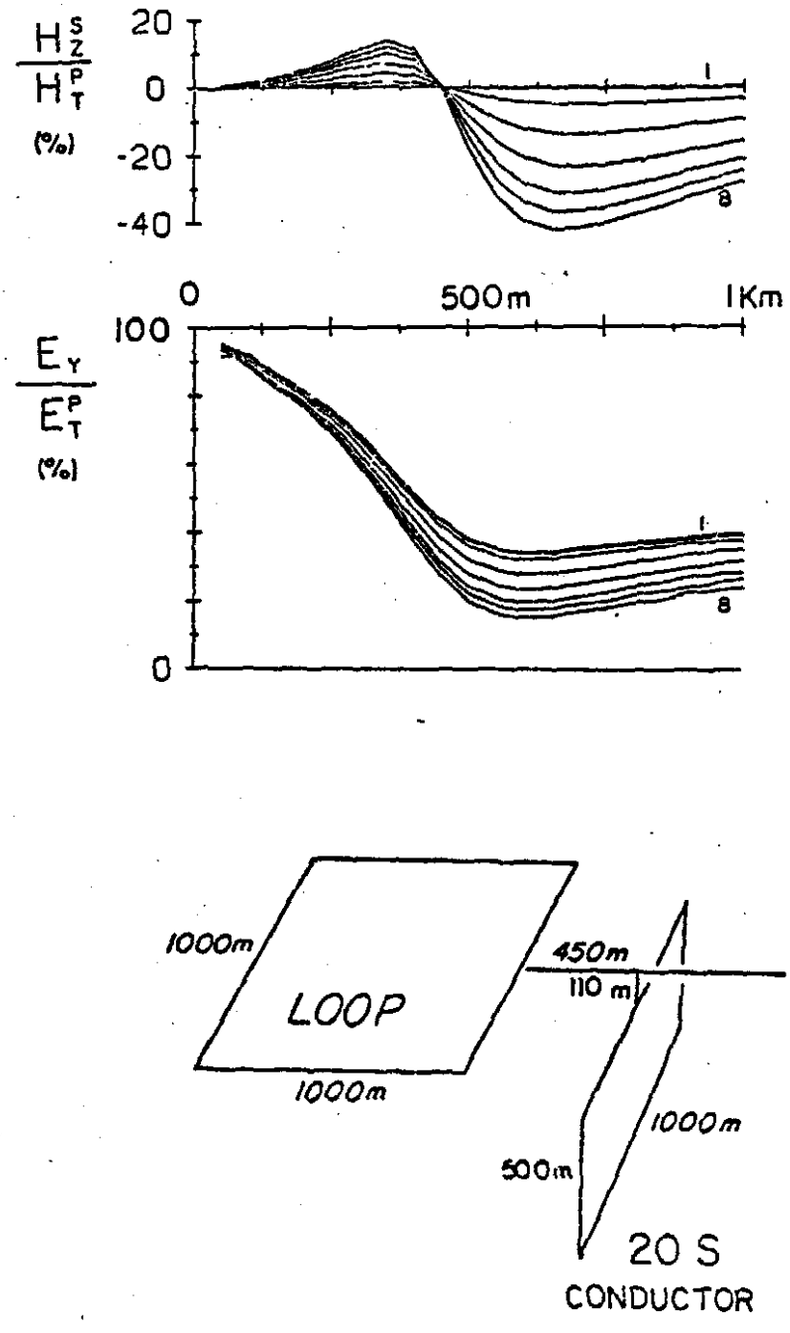

Fig. 7.3 Scale model UTEM H_z^s and Ey data over a vertical plate conductor.

consisting of a low over its central area, with large positive shoulders near its edge. The shoulders become rounded at later times and migrate towards the centre of the conductor. Note that the thin horizontal plate shown in Figure 8.1 has a fairly deep location and thus the inwards migration of the crossover points is less evident, although present.

Shallow Block conductor. This type of conductor produces a negative anomaly over its top having an amplitude of close to 200% at early times. An important characteristic of a block-like conductor is the absence of large positive flanking anomalies. The amplitude of the positive shoulders is less than 1/10 of the central negative, in contrast to the thin horizontal layer where the shoulders have amplitudes of order half the central negative. The sharpness of the cross-overs at early time can be used as an indication of depth of burial. This type of anomaly is called a top anomaly.

Thick dyke. As might be expected, this is an intermediate case between a block and a thin dyke where the width of a tabular body is of the same order as its depth of burial. In such cases the response is a combination of a crossover and a top anomaly, the top anomaly being more evident on the early time channels, and the crossover anomaly on later time channels. This behavior results from the different scales of induced current flows, the top anomaly being controlled by the width of the dyke, and the crossover by the depth extent.

Extensive horizontal conductors. All the models with finite horizontal extent give rise to localized anomalies which just change amplitude with time (approximately). The response of a very large conductor such as that shown in Figure 8.1E is included for comparison. In this case, the induced currents are not confined and they migrate horizontally with time.

Time response of simple finite models. The response shown in Figure 8.2 are the UTEM sampled step responses, and thus are only strictly valid for interpretation of actual field data when the observed anomalous response has effectively vanished at late times. Time scaling is permitted for these cases as previously discussed. Full discussion of the applicability of these time decays is given in Lamontagne (1975), and the table in Fig. 9.3 shows how characteristic parameters may be

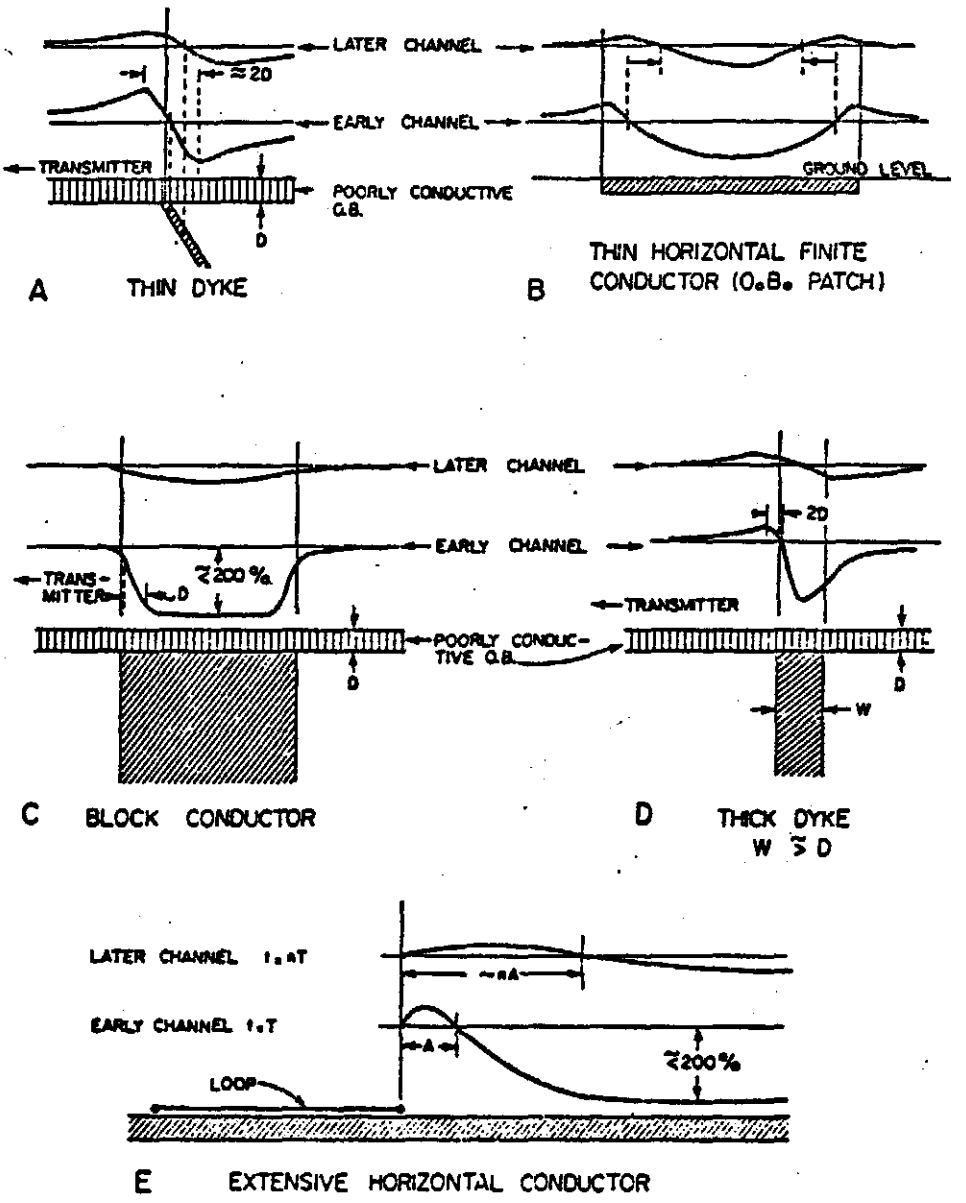

Fig. 8.1 The form of UTEM H_z^s anomalies over some simple shapes. All conductors are in free space.

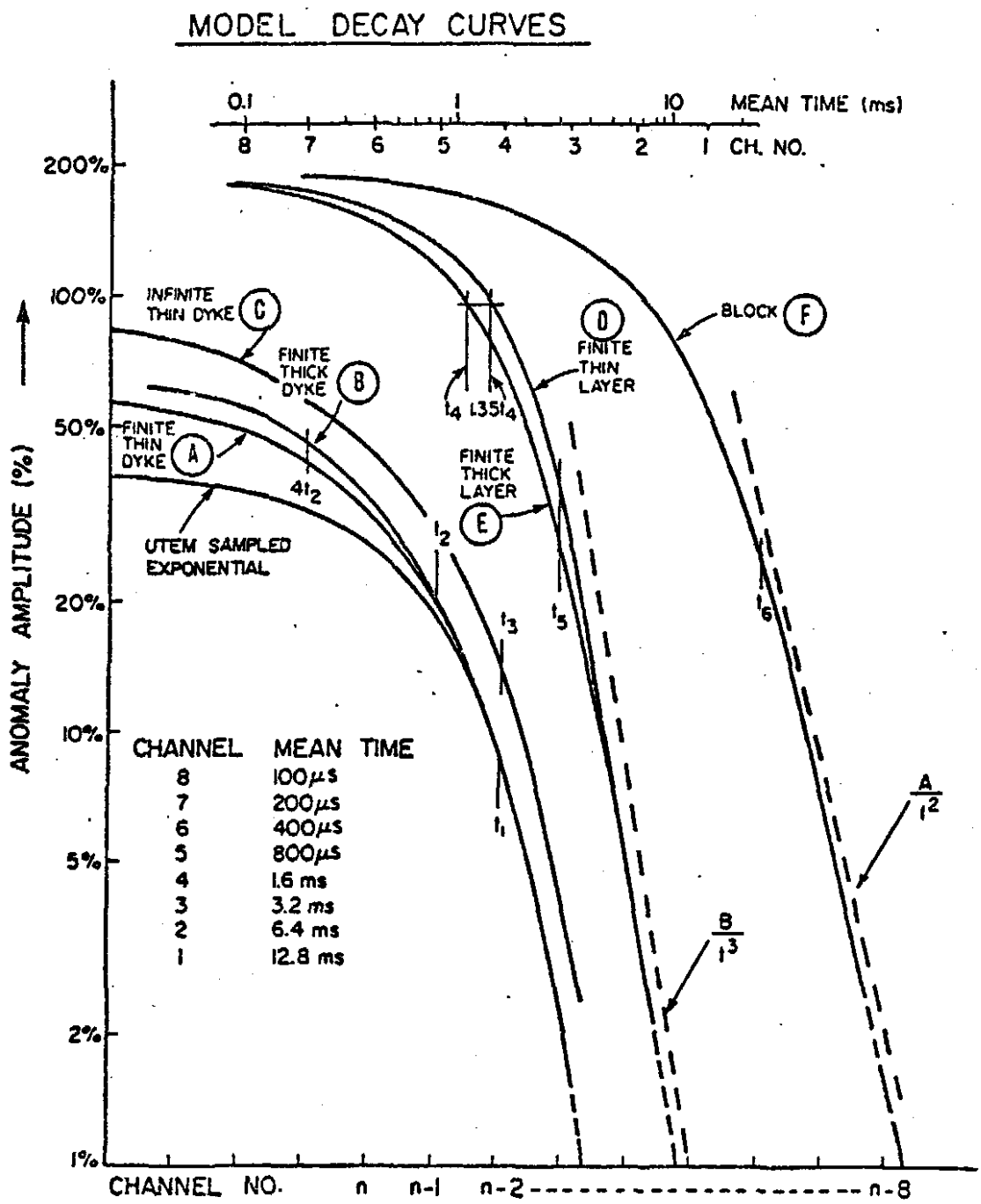

Fig. 8.2 *The amplitude decay curves for the simple modes of Fig. 8.1. The time reference points* t_1-t_6 *are used with the interpretation formula of Fig. 8.3.*

INTERPRETATION OF TIME DECAYS USING SIMPLE MODELS

Use in conjunction with Figure A9
Mks units used everywhere

A. Finite Thin Dyke: Plot peak-to-peak anomaly and use curve A with horizontal and limited vertical shifting to find t_1. An estimate of the conductance is then obtained by:

$$\sigma d = \frac{4t_1}{\mu L}$$

L = strike length,
d = dyke thickness
σ = dyke conductivity

B. Finite Thick Dyke: First interpret as a thin dyke by fitting latter part of decay to curve A to find t_1. Then estimate t_2 as shown on Curve B. t_2 is the time at which there is a 3% relative amplitude enhancement from the thin dyke response. Alternatively, $1/4t_2$ corresponds to a 10% enhancement. A rough thickness estimate is then obtained from

$$d = \frac{t_2 L}{10\, t_1}$$

C. Infinite Thin Dyke: When a dyke is much more extensive than the transmitter loop, the decay differs from the finite strike length case. Use curve C to find t_3 and calculate σd from

$$\sigma d = \frac{4\, t_3}{\mu B}$$

B = effective length of the conductor; in practice use

$$B = (S^2 + D^2)^{1/2}$$

where S is the length of the transmitter loop, D is the distance between the conductor and loop

The formula is valid only for strictly continuous dykes; in such cases, the anomaly amplitudes should be consistent with the effective length.

D. Finite Thin Horizontal Layer: Plot negative centre of anomaly and fit to curve D (time shift only) to find t_5.

$$\sigma d = \frac{4t_5}{\mu W}$$

W = width of conductor (smallest horizontal extent)

E. Finite Thick Horizontal Layer: First interpret as a thin layer using later part of decay curve. Then find time t_4 when observed decay curve deviates a factor of 1.35 earlier than the thin layer curve. This gives a rough thickness estimate from

$$d = \frac{Wt_4}{4t_5}$$

F. Block Conductor: Plot centre anomaly and fit to curve E (time shift only) to find t_6

$$\sigma = \frac{16t_6}{\mu W^2}$$

W = width of block

Fig. 8.3 Formulae for interpretation of time decays.

interpreted from observed decay shapes. The use of the geometrical shape of anomalies to identify the shape of the conductor has been previously discussed.

9. Overburden Effects

We will restrict the discussion of overburden and host rock effects to the case of a simple finite dyke conductive target, which was studied using a scale model by Lamontagne (1975). Conductive overburden cover can modify the responses of underlying conductors in two main ways. Let us consider a dyke target whose response in free space is given in Figure 9.1D. If overburden is now placed over this target conductor, the resultant response (Figure 9.1B) is not just the sum of the overburden and dyke response. At early times it can be seen that there is very little response from the dyke. This is because the magnetic field has not yet penetrated the overburden, and it leads to the name "overburden blanking" for this characteristic. At later times (Ch 6-1) when we can see from Figure 9.1A that the field has completely penetrated the overburden layer, the dyke and overburden response (B) is virtually indistinguishable from that of the dyke alone (D). The time decay pattern of the peak-to-peak amplitude of the crossover is plotted in Figure 9.2. It clearly shows the blanking effect of the overburden at early times. The minute negative response at earliest time is present only when the overburden extends under the loop, and is the result of the dyke "seeing" a field which has still not had time to reverse from the last cycle. Lamontagne's scale model studies showed that the overburden effect generally is quite complex in a quantitative sense, as the observed response will depend on the overburden extent, transmitter size, and size and shape of the target conductor.

The second effect that may occur is when the dyke is in contact with the overburden. The results are quite different from those where the dyke was not in contact (Fig. 9.1C). In this case, regional current flow in the overburden has been gathered into the dyke which is of higher conductivity. This accounts for the large amplitude crossover anomalies at early times. The amount of current gathering is virtually independent of the dyke's depth extent, as the effect at early times of just a "line conductor" attached to the overburden in place of the dyke was over 80% of that of the complete dyke. At later times, when the

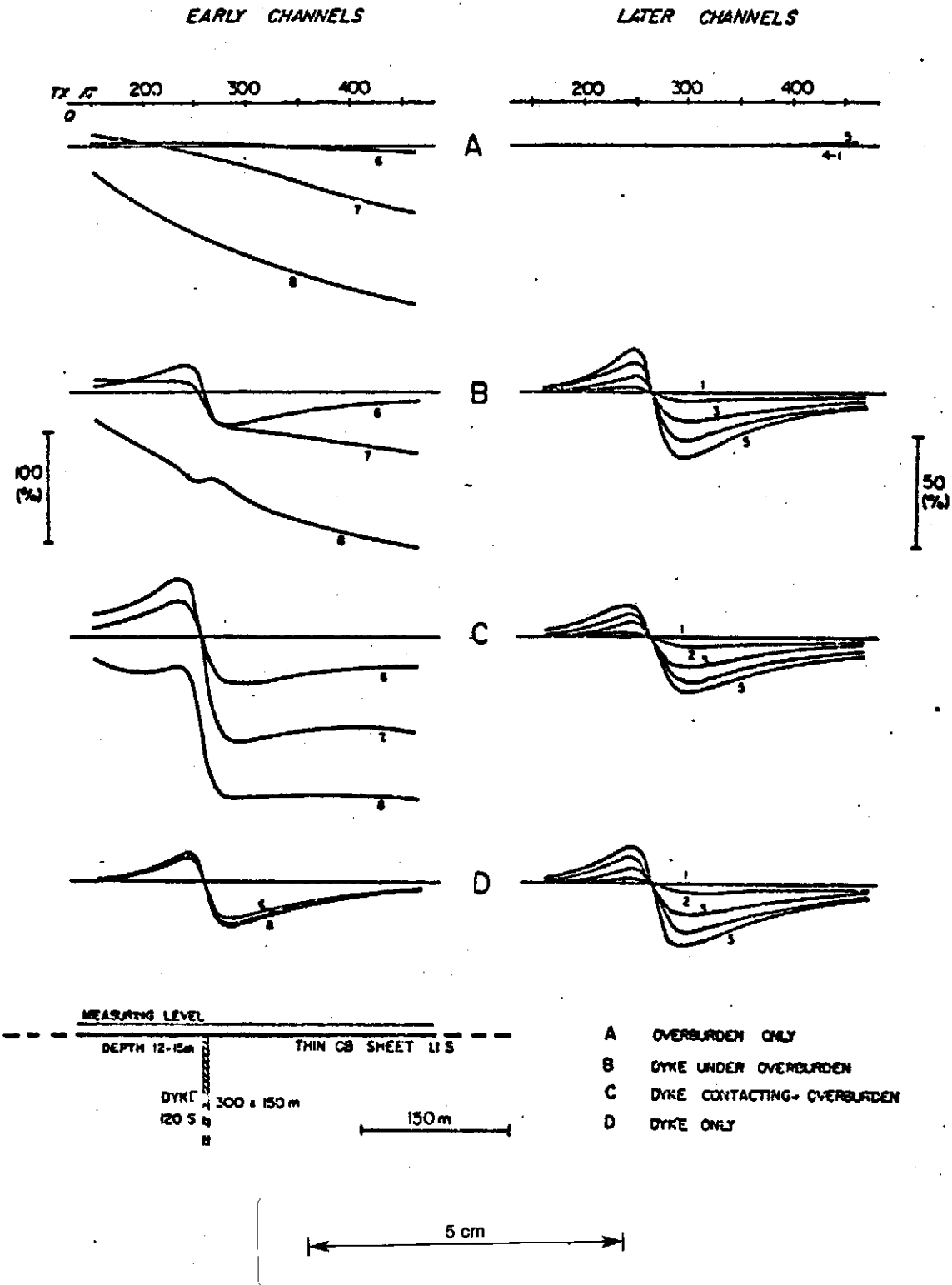

Fig. 9.1 Scale model UTEM H_z profiles over a conductive thin dyke with overburden present.

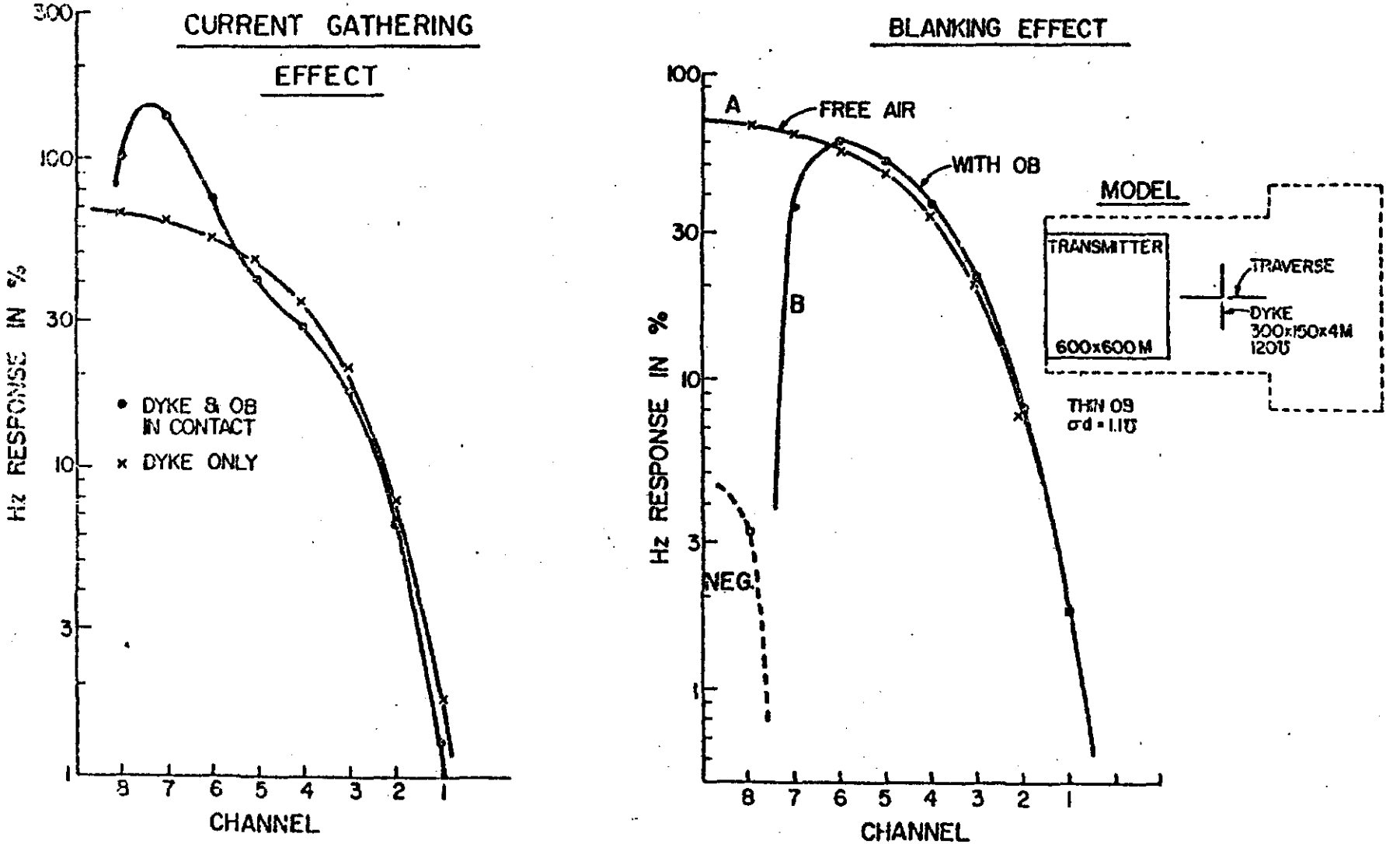

Fig. 9.2 Decay plots for the H_z anomalies of Fig. 9.1.

I.26

C90880

current flow in the overburden is no longer time-varying, the response is again almost identical to that of the dyke alone. The time decay of the response is plotted on Figure 9.2, and in addition to the enhancement at early times a slight attentuation of the response at intermediate times can be seen.

10. Host rock effects

Figure 10.1 shows the time variation on response or a 60 S vertical plate located in a half space. The results were transformed by Lamontagne (1975) from frequency domain numerical modelling of Lajoie (1973). At early times the response is reduced from the free air response: this corresponds to blanking by the conductive region above the target. At later times the response is enhanced indicating that the regional host rock current is being gathered into the plate at these times. For poorly conducting host rock, the response at late times is close enough to the free air response that simple interpretation of the target using a plate in free air model is valid. For the higher host conductivities (cases 4, 5) this is no longer the case.

FIELD EXAMPLES - LAYERED EARTH

11. Pinawa, Manitoba

This is an area of granitic Precambrian bedrock overlain by a glacial overburden which consists of sandy, pebbly detritus in which quite highly conducting clay layers occur. The overburden stratigraphy is quite complex both vertically and laterally on a local scale (1-10 m), but its nature changes only gradually on a larger scale. The area is flat, and the Precambrian surface is thought generally to be featureless. The objective of the survey was to check if any fault structures in the bedrock might be evident, perhaps through by having subcrop valleys along them. The bedrock resistivity in unfractured rock is known to be sc high as to be difficult to measure (>30 kΩm).

The survey consisted of a single transmitter loop 1130 x 600 m on the south of the survey area from which 13 lines 800 m long and spaced 100 m were read. Vertical component magnetic field and orthogonal horizontal electric field data were collected at 50 m intervals. Lines were numbered A to M from west to east.

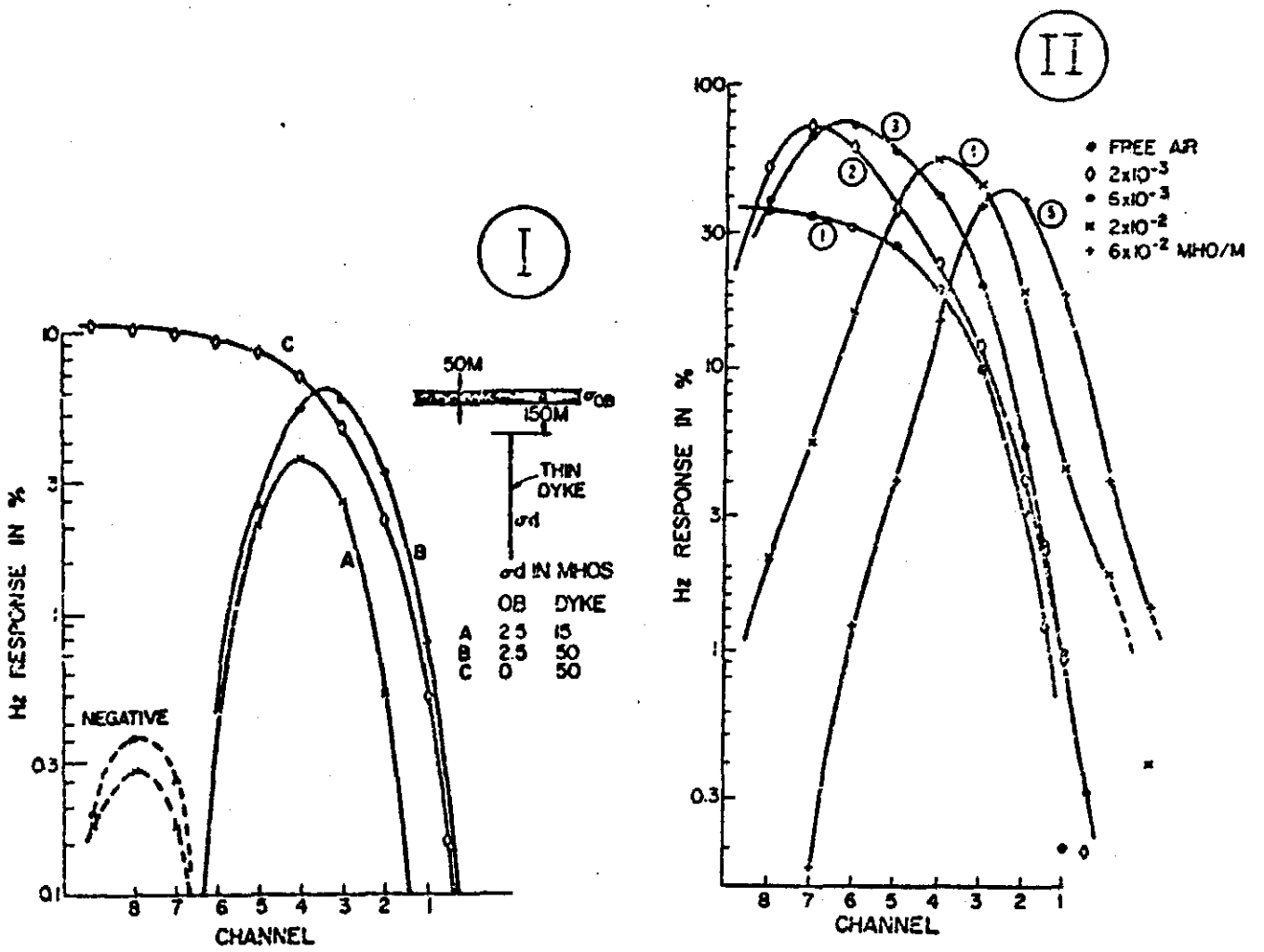

Fig. 10.1 Decay plots of H_z^s anomalies over a thin dyke (I) under a conductive overburden and (II) in a conductive half space.

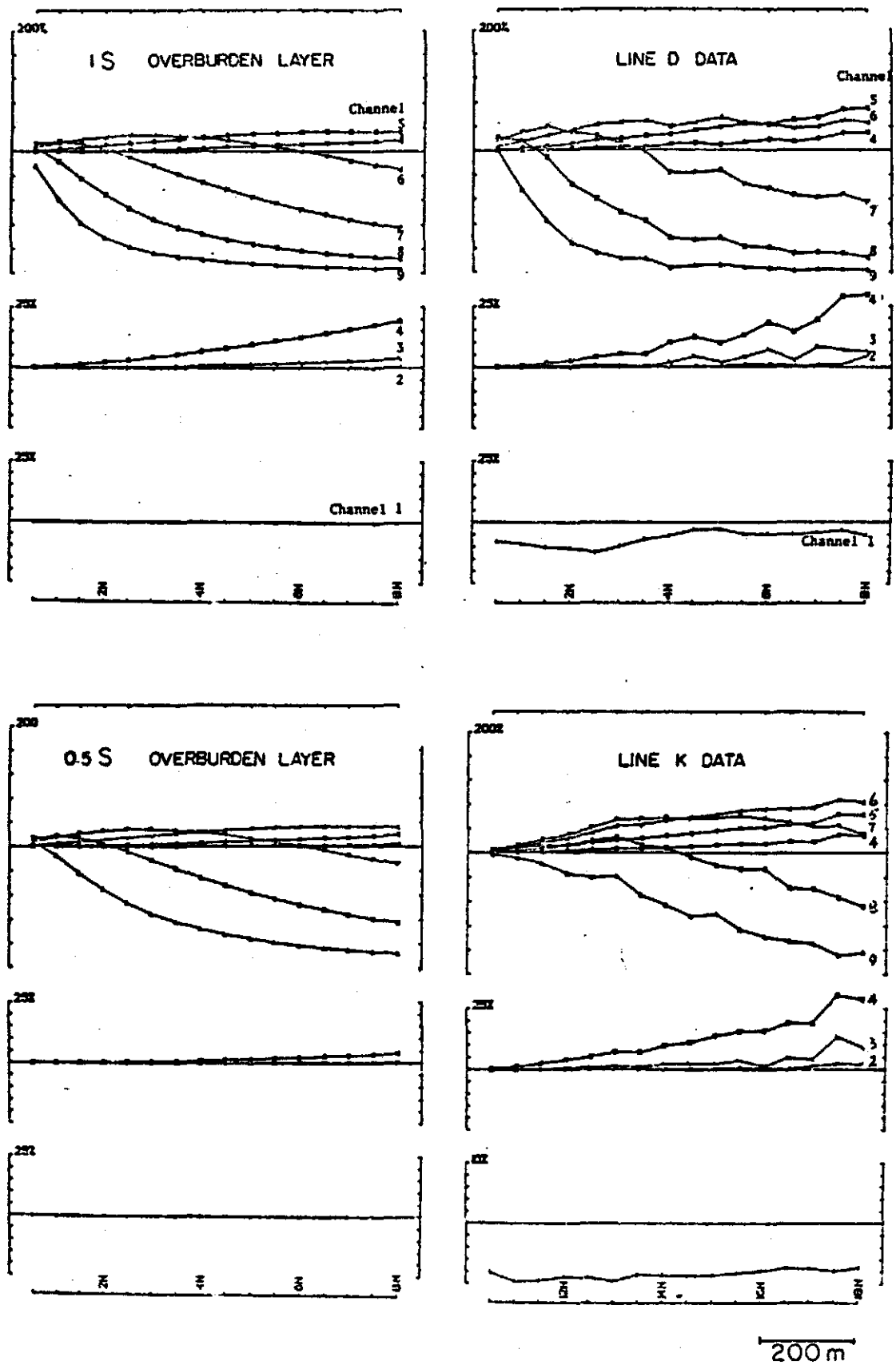

Fig. 11.1 Profiles of H_z^s from two lines of the Pinawa survey compared with a thin sheet overburden model.

5 cm

Fig. 11.1 shows two lines of the vertical component magnetic field data. For comparison, model data for an infinite, thin, horizontal, near-surface conductive sheet is also shown. There is a very strong resemblance between the observed and model data, although the fit is by no means excellent in a quantitative sense. A systematic difference is seen in the data, moving from lines A (west) to M (east). The westerly data resembles more conductive models than the eastern data, changing from a conductivity-thickness of 1.5 to 0.3 s. In such a case, the late-time positively anomalous data (ch 6-1) should be regarded as a near field anomaly, due to the regional average structure out to about 1.5 km in radius, while the active region data (ch 9-6) where the anomalous intensity changes rapidly with time indicates relatively local structure, i.e., averaging over a lateral scale of a few hundred meters. Very local heterogeneity in the overburden shows itself as small but repeatable wiggles in the profiles (e.g. line D, 3.5-4N) which reflect local irregularity in the current system which is predominantly sweeping around the transmitter loop under the stations at these times (ch 9-6).

Fig. 11.2 shows a vector plot of the data-time electric field data (with free-space amplitude normalization). The general circulation of the electric field is plainly displayed. The systematic lateral change in overburden conductance is apparent from the relatively small amplitudes over the conductive part and the enhanced amplitudes over the more resistive area. An ideal model for fitting to both the magnetic and electric field data would be a thin horizontal sheet with a laterally varying conductance, but this was not available. However, model data could be obtained for a thick, blocky, overburden layer, and it is included for comparison.

12. Milton, Ontario

This area was surveyed to demonstrate what a highly conductive, well stratified earth looks like. The area is one where 650 m of flat-lying Paleozoic sediments overlie the Precambrian basement. The predominant member of the stratigraphy is a uniform and thick sequence of clay-shale. Other beds are mostly relatively resistive calcareous and sandy formations. The survey area is a natural reserve of mixed forest and marshy streams, with occasional outcrops. The bedrock is a

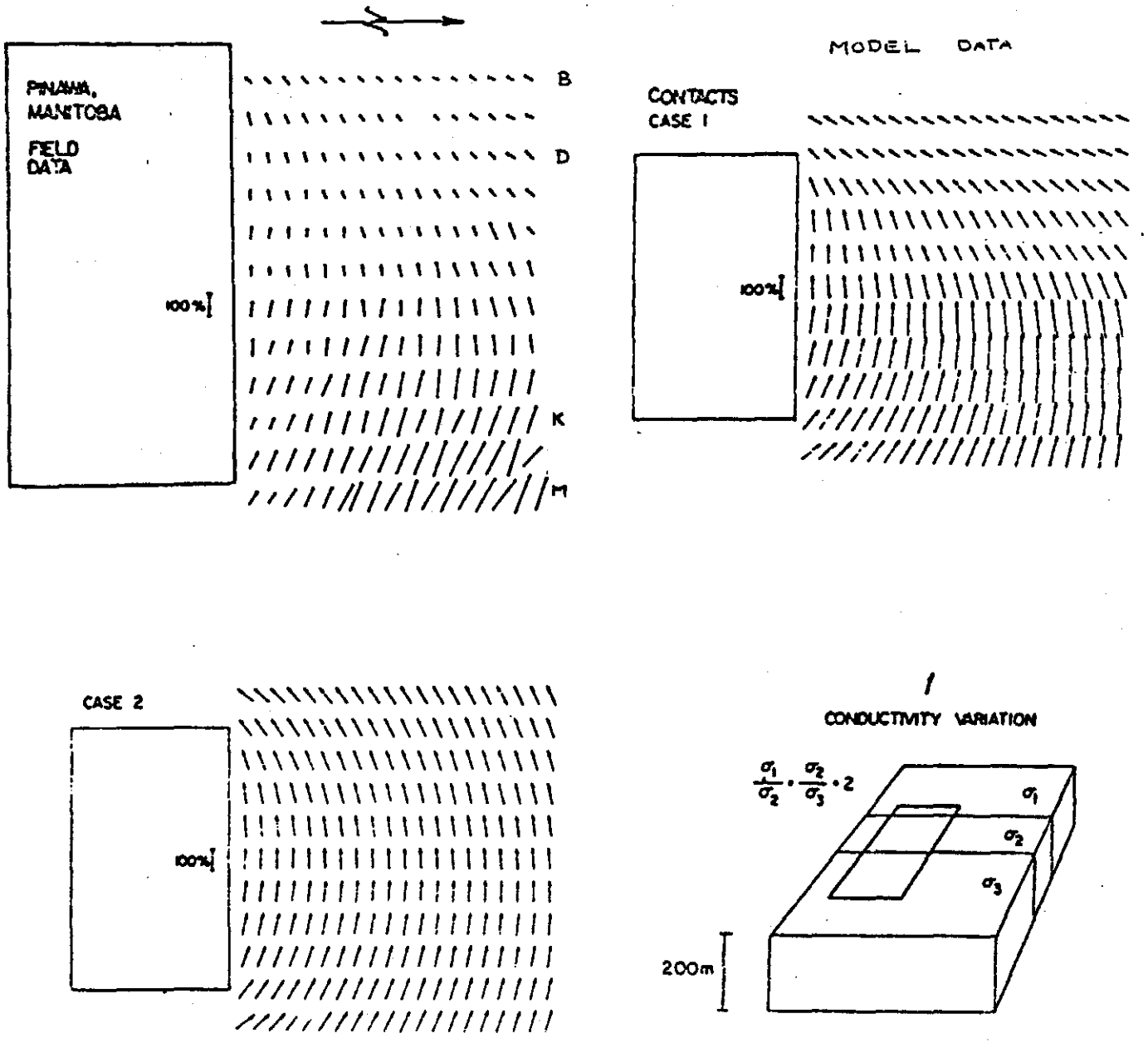

Fig. 11.2 Vector plot of late time E data at Pinawa compared with a simple model.

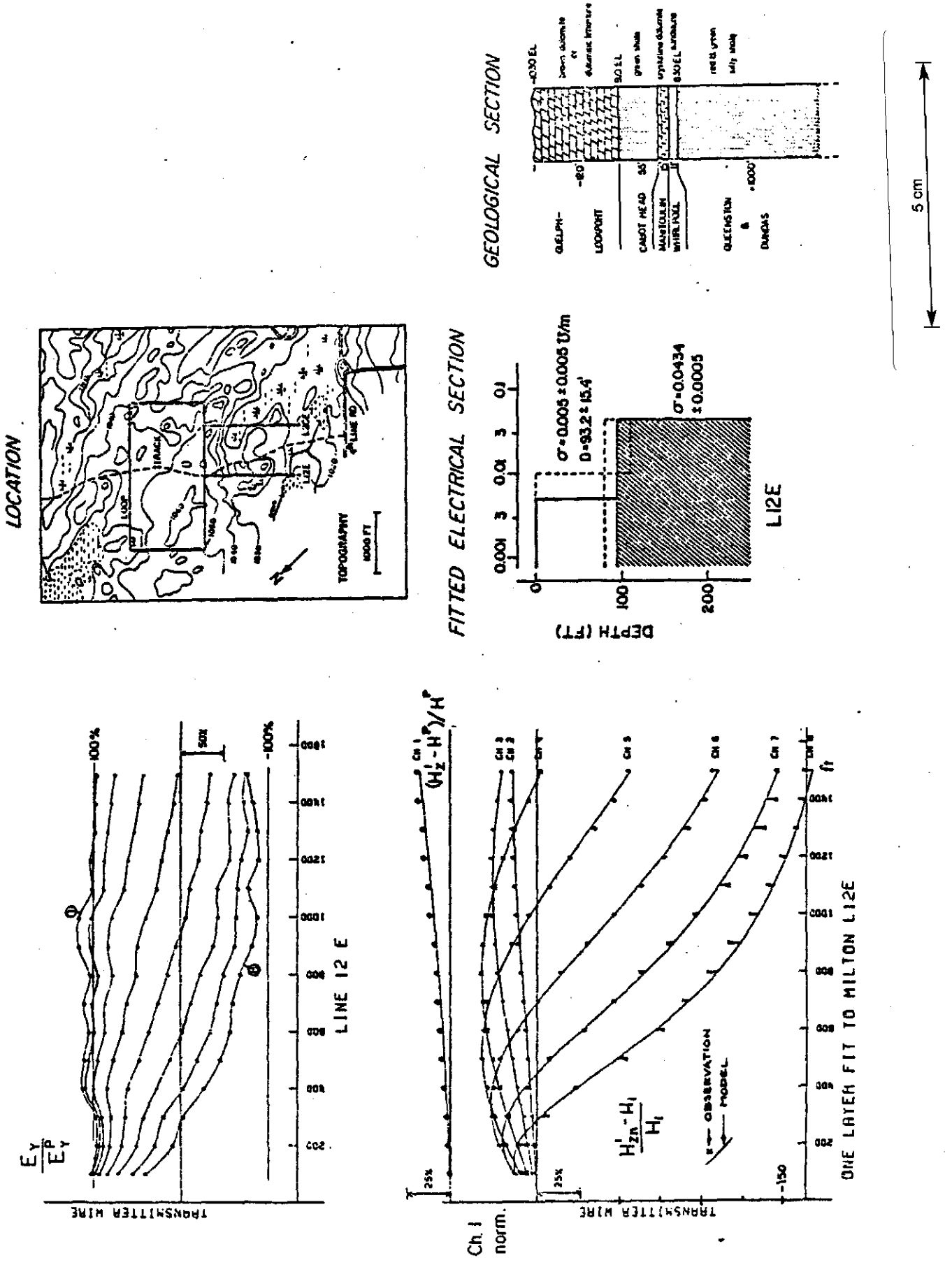

Fig. 12.1 Field example of Ey and H_z^s data from a well stratified earth. The electrical section was obtained from inversion of the H_{NN}^s data. The geological section is from nearby drilling for gas exploration.

thick dolomite formation. Topographic relief is relatively minor, with occasional rough spots near outcrop. Overburden is probably less than 10 m everywhere and much less on average. It is mostly humus or thin glacial soil. Surface water is fresh, and likely quite resistive (>100 Ωm). Fig. 12.1 shows some of the data with a quantitatively fitted model, and the stratigraphic section. The dolomite layer is too resistive for its conductivity to be determined by data that includes only 8 channels. (The survey was done with UTEM I). At first glance, the data looks like that for just any conductive earth as the early time, distant data has the usual strong negative anomaly, and there is a regular outward progression of crossovers to positive response as time progresses (decreasing channel number). However, the resistive surface layer does reveal itself in the slow approach of the early time curves to -200% anomaly. The convergence of Ey at late time to 100% of the primary field confirms the excellent lateral homogeneity of the site.

BEDROCK CONDUCTORS

13. Prosser Township, Ontario

This survey is over a typical, steeply dipping, graphitic-sulphidic formation in the Archean Shield near Timins Ontario. The target body has a very long strike length, and it was originally located by the vertical loop, fixed transmitter method. The overburden consists of a glacial lacustrine clay formation over till, sand and gravel. The Precambrian subcrop surface may be rough, but the ground surface is quite flat. Overburden depth at the drill intersection is about 200 ft (60 m). The clay fraction of the overburden is moderately conductive (resistivity ≈30 Ωm). Bedrock away from the graphitic-sulphidic formation is likely very resistive.

One of three UTEM H_z profiles is shown in Fig. 13.1. All are similar. A strong cross-over anomaly which has constant geomerical form and a very regular decay from channel 6 to 2 is observed. The data shown is reduced to channel 1, and channel 1 data normalized to the primary field shows a clear positive bump over the sulphides which cannot be due to positional error. The feature is a simple static-type induced magnetic anomaly.

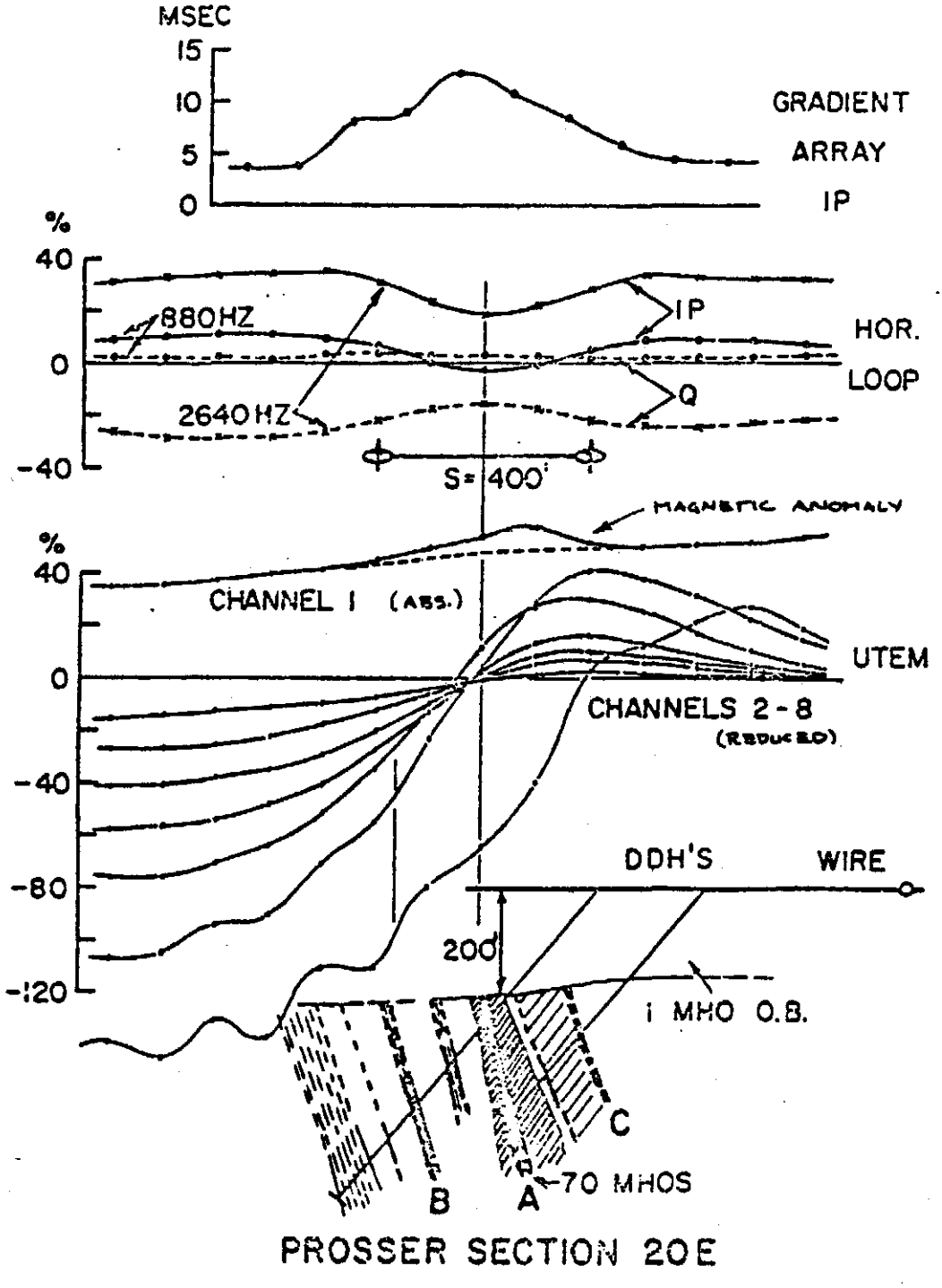

Fig. 13.1 A UTEM H_z^s profile over a dyke-like conductor compared with other survey data. Zone A is the main conductor.

At the earliest time on this survey (Ch 8 ≈100μs), the crossover of H_z is between the Tx loop and the conductor, indicating that field penetration through the overburden is just beginning. No inflection of the ch 8 response profile is seen over the target body. The figure also includes HLEM profiles at 880 and 3520 Hz which show a clear response from the target and, in the higher frequency example, a clearly offset base line due to the overburden response. The anomaly at the higher frequency shows an inverted polarity of quadrature response, due to the phase shifting effect of the overburden.

In the interval 200-400 μs (ch 7,6), the UTEM response settles down to a simple decay (Fig. 13.2) which is well fitted by a free-space plate model, leading to a 70 S estimate of conductivity-thickness. Geometrical interpretation of the conductor depth and dip can be facilitated by plotting profiles where the amplitude normalization is the same all along the profile, so the undisturbed field of the induced current is seen (Fig. 13.3). It is interesting to note that the geometrical form of the anomaly is somewhat different in the 200-400 μs time range (ch 7-6) and so is the decay rate. The enhancement in response is very probably a poloidal induction as sketched in Fig. 13.4.

14. Thomas Township, Ontario

This site has become an interesting test range for electrical methods. It is a graphitic zone that has many of the characteristics of a massive sulphide body. It is covered by 83 m of only moderately conductive overbuden. It was found originally by airborne EM and has been drilled twice.

A UTEM II survey with 30 Hz base frequency was carried out on 6 lines of length 2200 ft and spacing 400 ft using transmitter loops to the north and south of the grid. Fig. 14.1 shows a profile across the middle of the conductive zone.

At 50 μs (ch 9), the active region is only 500 ft from the loop. The field has not penetrated the overburden at the target site. From 100 μs to about 500 μs (ch 8-6), a crossover response is observed over the target. At about 500 μs the response changes to an assymetric negative anomaly which decays more slowly than the crossover response. The crossover response is a poloidal anomaly with current flowing along

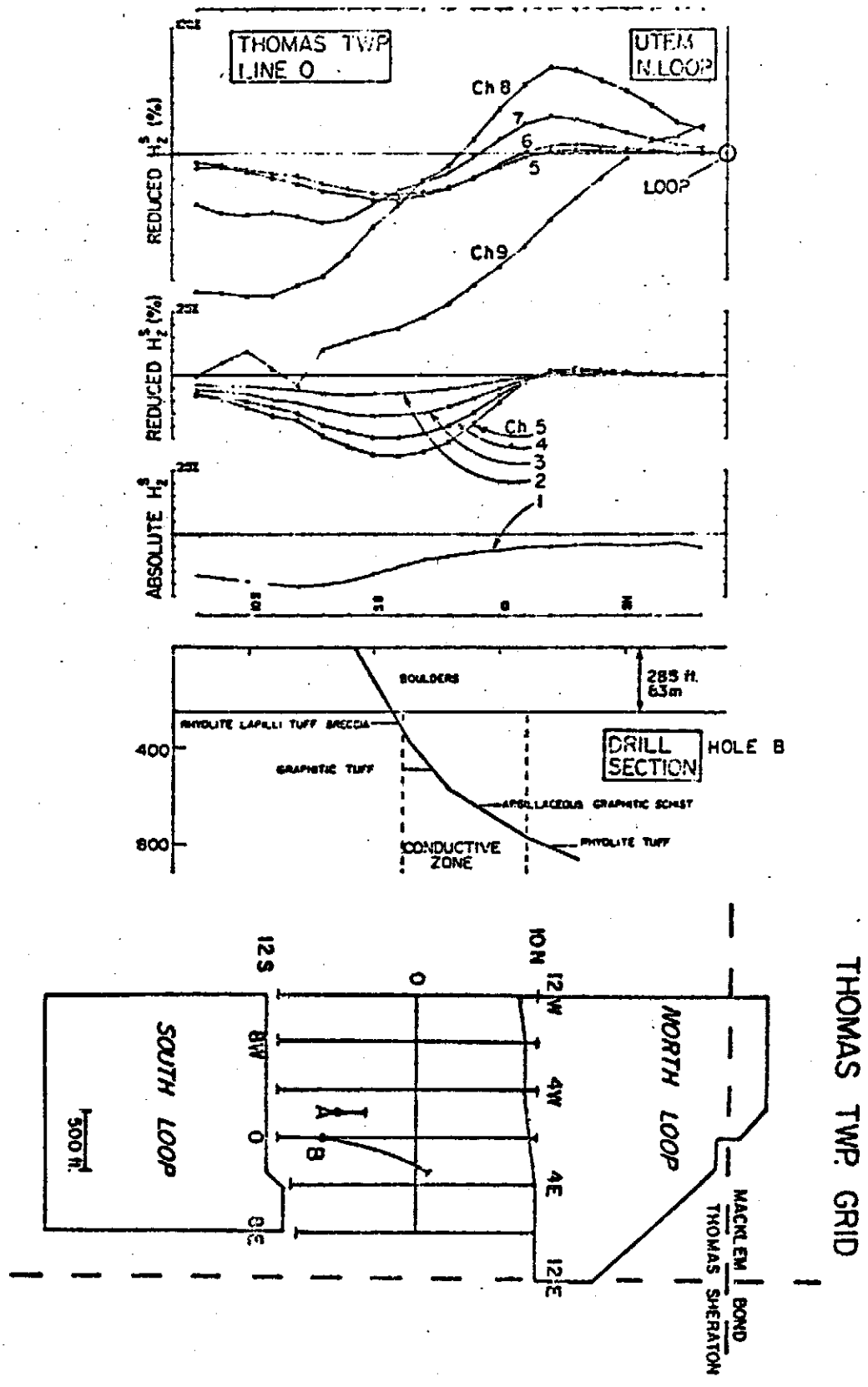

Fig. 14.1 A profile of H_z^s data from the north Tx loop across the Thomas Twp test site. A map of the survey is included (different scale).

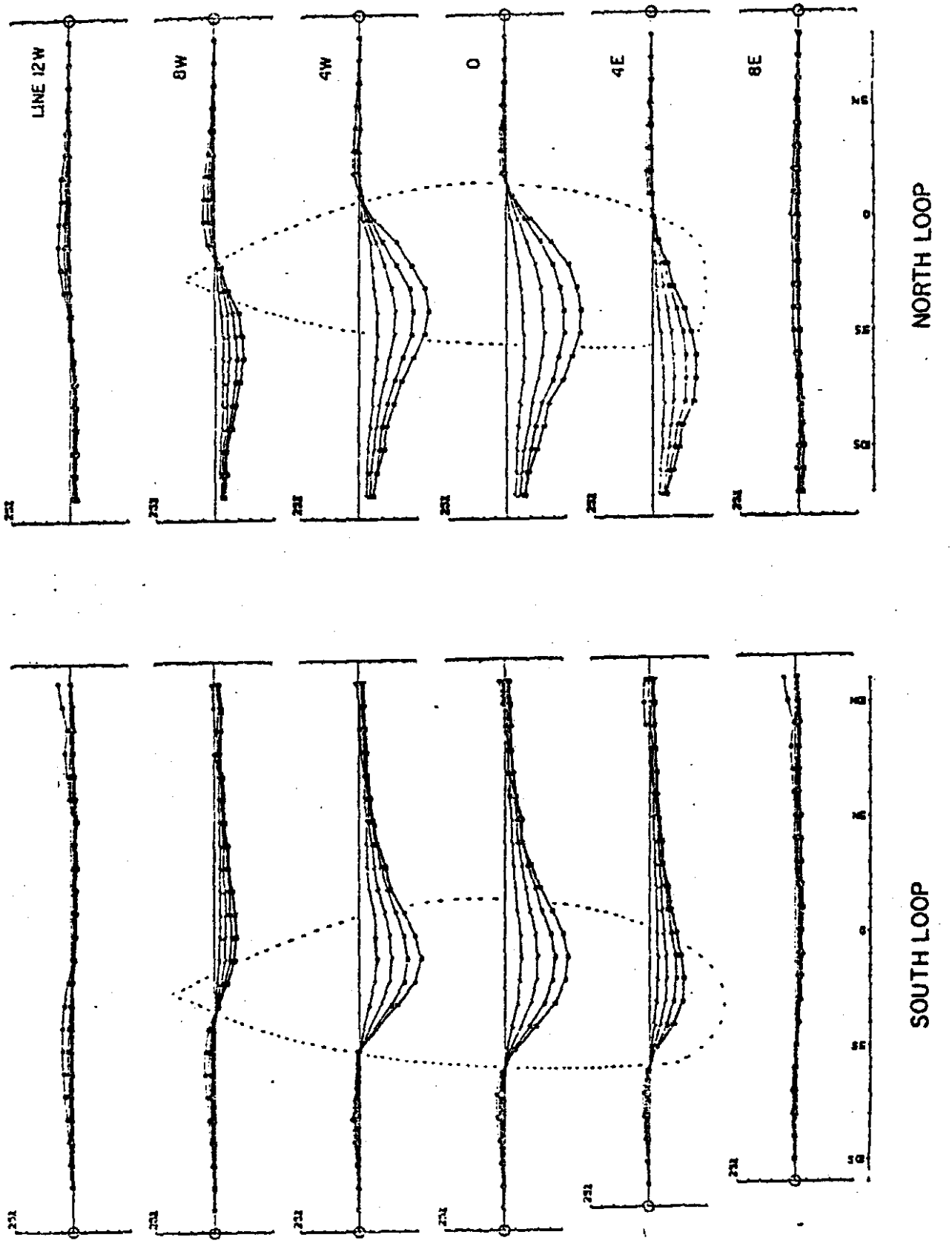

Fig. 14.2 Later time H_z^s profiles outline the perimeter of the conductor.

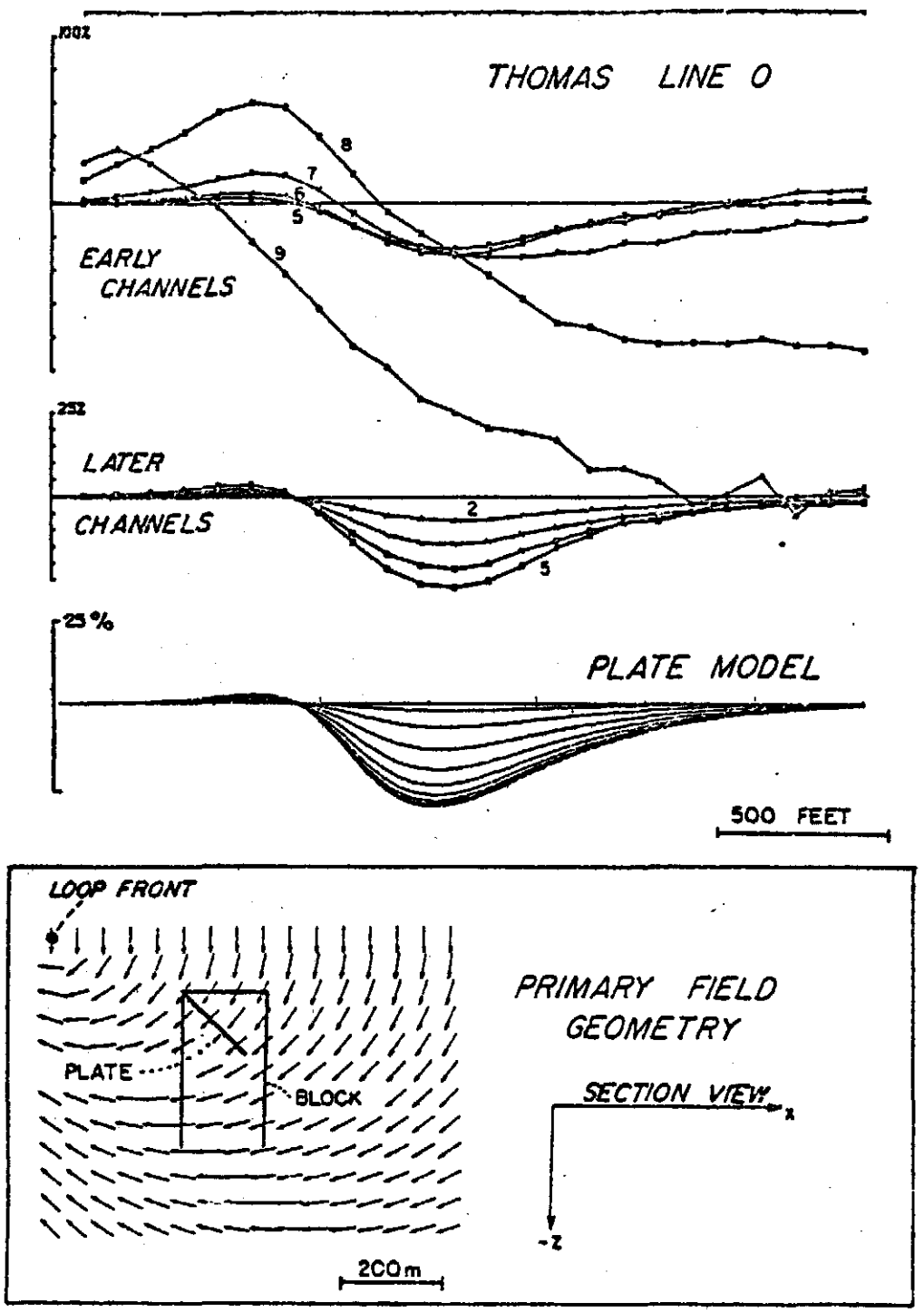

Fig. 14.3 Comparison of H_z^s data from the south Tx loop with a free space plate model. The configuration of the primary field is also shown.

5 cm

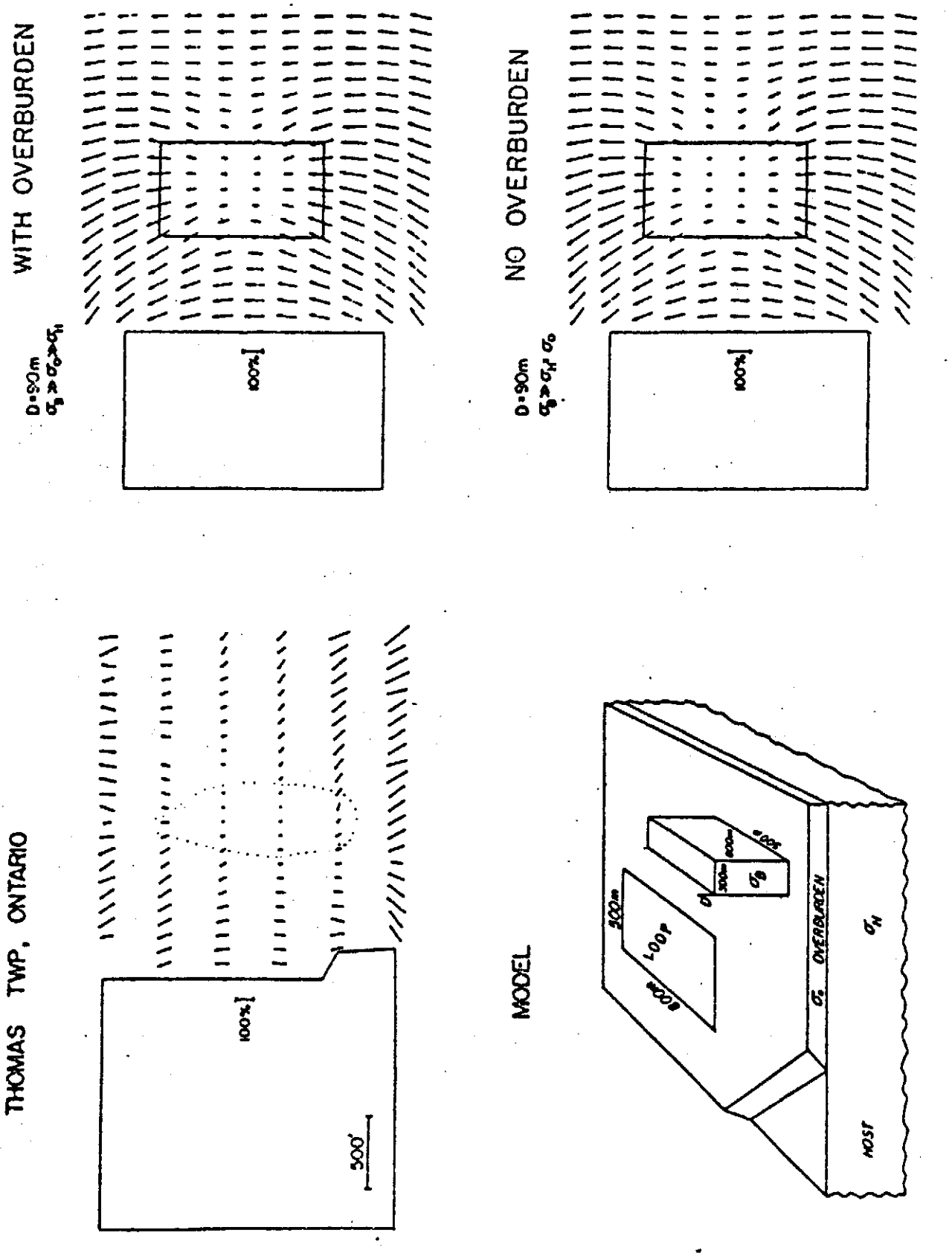

Fig. 14.4 Vector map of the late-time E field at Thomas Twp. A block model is included for comparison.

5 cm

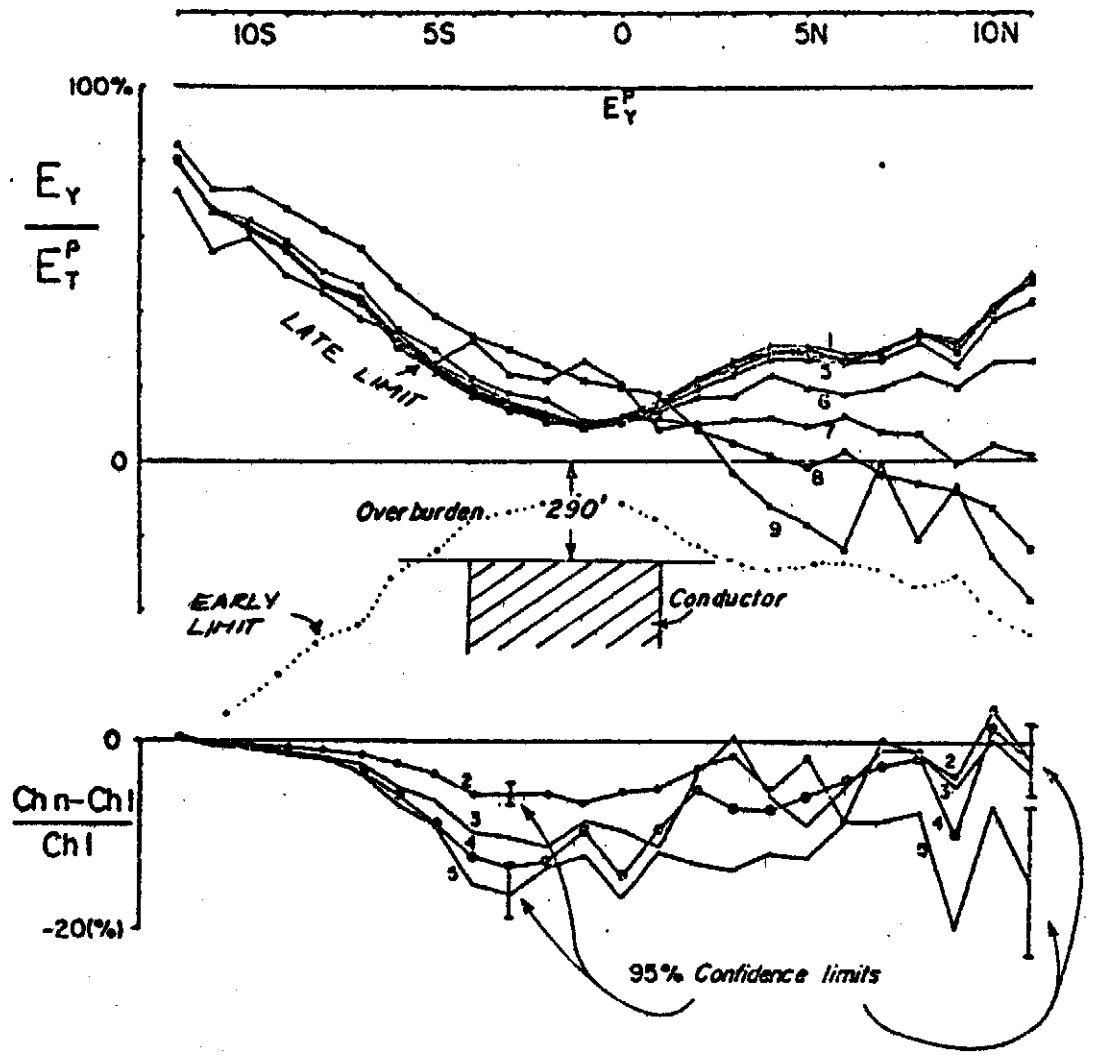

Fig. 14.5 Thomas Ey data for line 0 from the south Tx loop. The expanded scale data on the lower axes shows that a very weak dynamic E field anomaly is associated with the main H_z^s late time response (ch 5-1).

the zone, while the longer time constant response is a toroidal anomaly, where normal and return induced currents flow in the target conductor.

Fig. 14.2 shows a map of all the late-time profiles. They clearly delineate the edge of the target body. Fig. 14.3 shows how a rectangular plate model can be found which models the observed results from one Tx loop quite accurately, but which has to be rotated in order to match the results from the other loop. The induced current system in the actual conductor is obviously a tightly defined normal current in the front upper (near-loop) edge of the conductor with a more diffuse, return current deep in the rear of the body.

Electric fields were measured at the Thomas site. The late time vector map is shown in Fig. 14.4, along with a rough numerical model. The conductive zone shows very clearly, although its edge is ill defined. Fig. 14.5 shows a profile of the longitudinal component of electric field over the body. The field intensity is almost constant from channel 6 onwards, and the main feature of the response is the aforementioned broad reduction in the field strength over the conductor. It is helpful, when looking at E field profiles, to imagine a plot on the same axes of the negative of the observed channel 1 response. This is the value the field starts from at the step instant. Even as early as 50 μs (ch 9), the electric field has made most of its polarity reversal. In fact, from the loop to the target body it has overshot, while from the target body outwards it is changing relatively slowly. The time changes in E are actually very similar to those in H. There are two dominant decay times, a short one corresponding to the overburden on poloidal target response (ch 8-6) and a long one corresponding to the toroidal target response (ch 5-1). Also, the two have a different geometrical form corresponding with the different forms of the magnetic anomalies. The scaled up version of the E data in Fig. 14.5 shows the slowly decaying anomaly. There is considerable noise in the data at this magnification.

15. Izok Lake, N.W.T.

This is a well known new discovery by Texas Gulf in a remote area of the Canadian Shield. Only very thin gravelly overburden is present with a shallow lake covering much of the deposit. Permafrost is encountered at shallow depth. The geophysics of the deposit has been

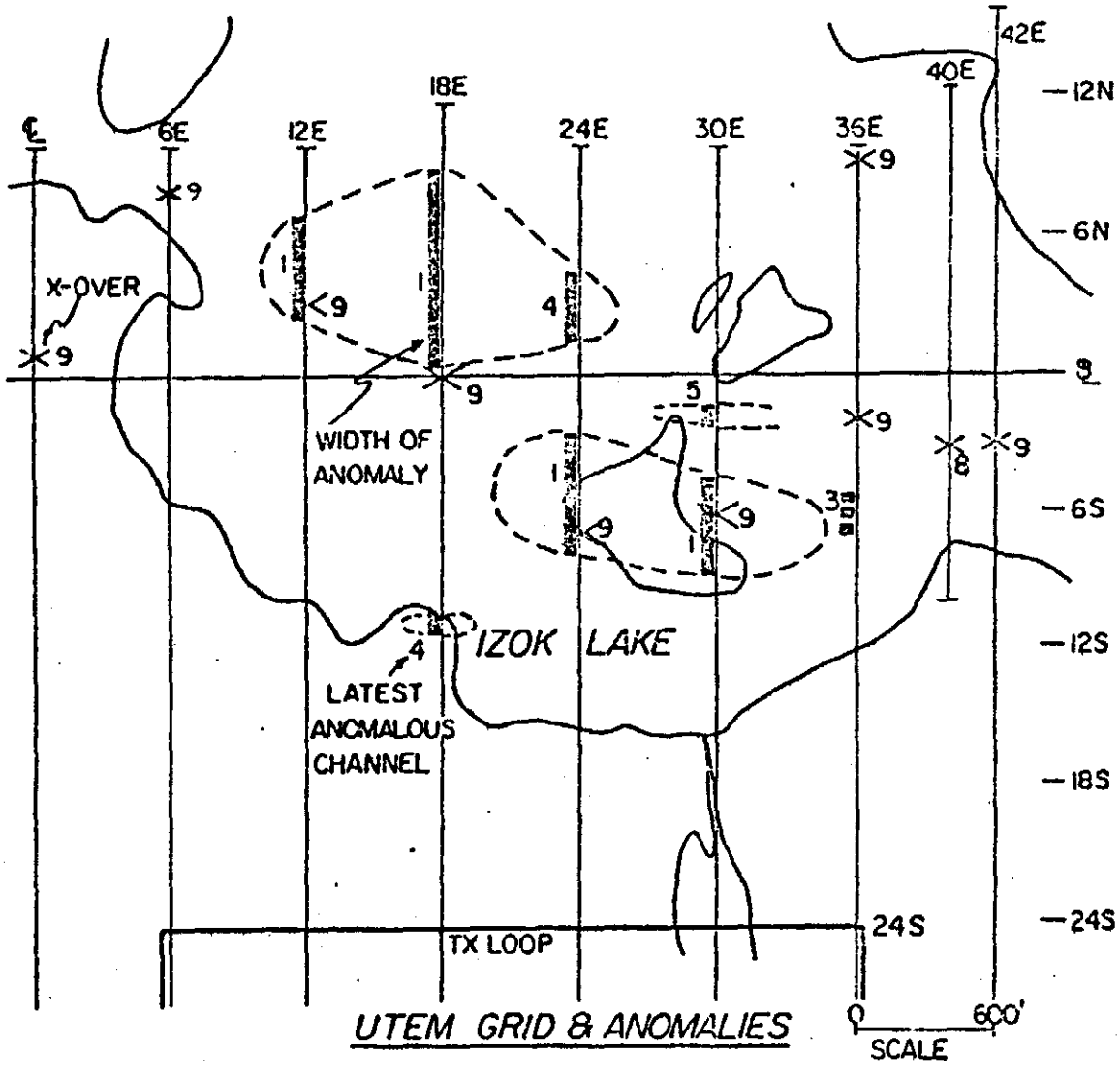

Fig. 15.1 Map of the UTEM survey over the Izok Lake deposit. The grid, lake outline, and position of anomalies is shown along with the interpreted vertical projection of the conductors.

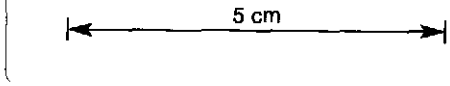

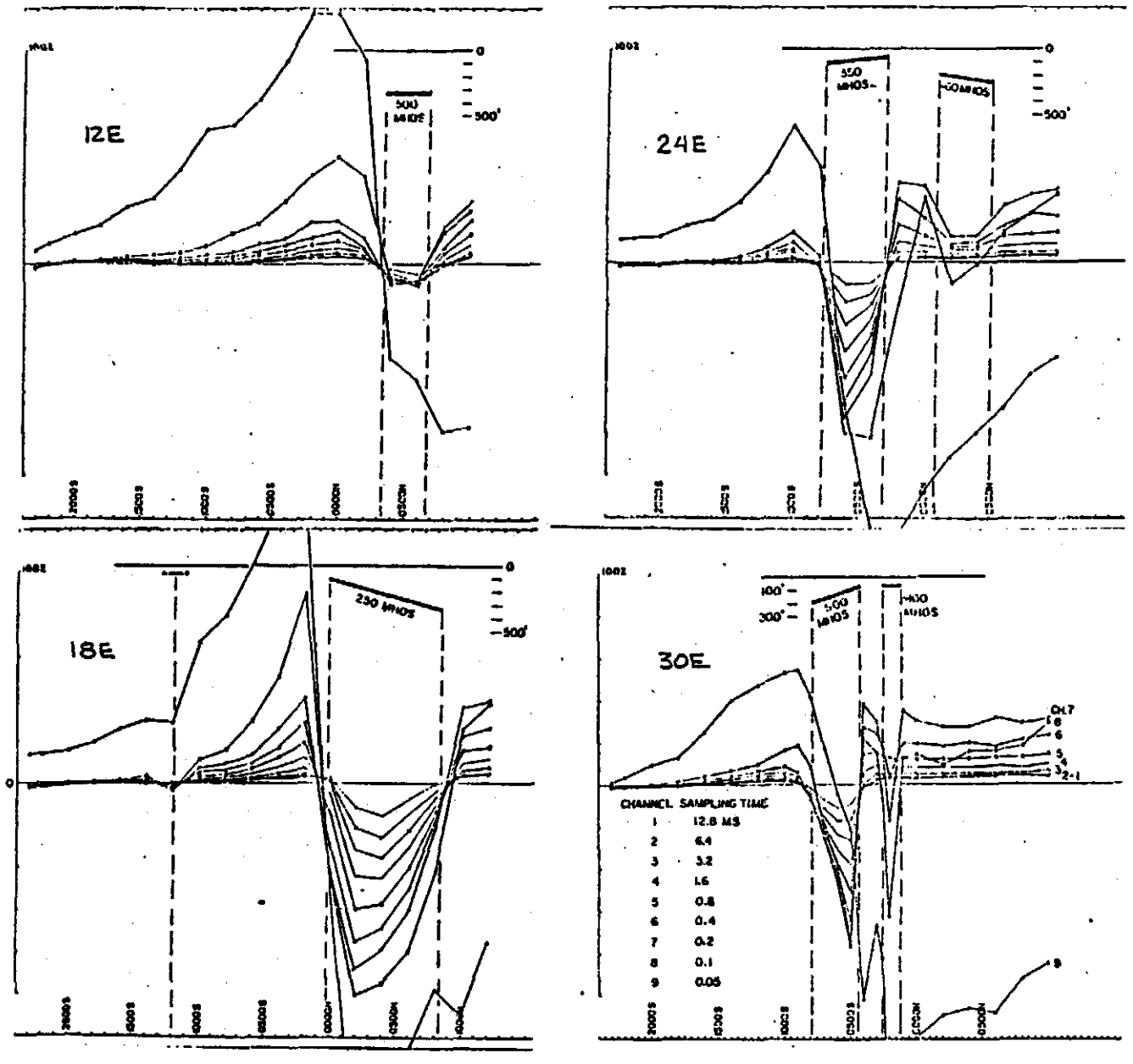

Fig. 15.2 UTEM H_z^s profiles over the Izok Lake deposit.

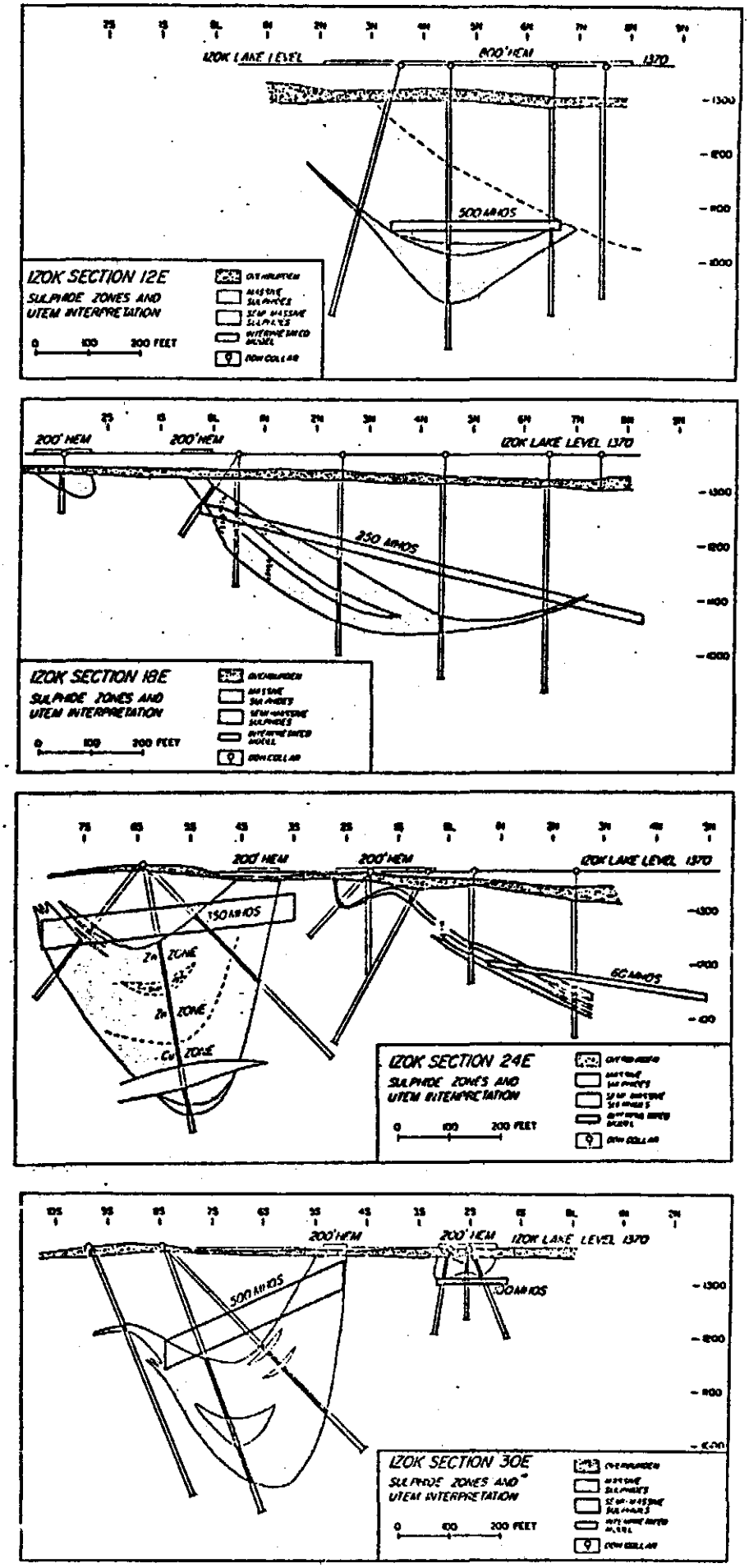

Fig. 15.3 Izok drill sections.

5 cm

described by Podolsky and Slankis (1979). The sulphides occur as several massive pods at various depths. None outcrop, but several pods do subcrop. The host materials are highly resistive and topography is minimal.

Fig. 15.1 shows the loop position and survey grid with markings showing anomaly location. This survey is similar to Thomas Twp, in many ways except that there are several bodies and they have shallower depth extent and variable depth-to-top. Several profiles are shown in Fig. 15.2. At the earliest time, a crossover response is observed which traces a single current line through the chain of conductors. This response vanishes rapidly. It is replaced with slowly decaying, mainly negative anomalies which are due to vortex (toroidal) currents circulating around each conductor. Drill sections are shown in Fig. 15.3.

16. Athabaska Basin, Saskatchewan

There is much interest in mapping steeply dipping graphitic metasediments in the early Proterozoic basement beneath the flat lying Athabaska (late Proterozoic) sandstone in northern Saskatchewan because these formations control uranium minealization. Excellent discoveries have been made around the edge of the basin with sandstone depths up to 100 m or so. The INPUT airborne EM system has been remarkably successful in tracing zones at depths of 200 m and more, but drilling requires precise location of the bodies from the ground.

The UTEM survey consisted of a transmitter loop and four profiles in an area where an INPUT survey had traced a conductor as a weak but distinct chain of anomalies. A later UTEM survey expanded on the initial test, but that data is proprietary. Fig. 16.1 shows the survey grid and the H_z profile data on two lines.

COMPLEX CASES

17. Europe I

This survey was over a sedimentary lead zinc sulphide deposit in unmetamorphosed Phanerozoic carbonate and marl sediments. The target body is a long, thin, horizontal, flattened cigar-shaped deposit which varies from about 100 to 160 m depth. The ground surface is strongly sloped and quite rough. Although the survey grid is in an undeveloped

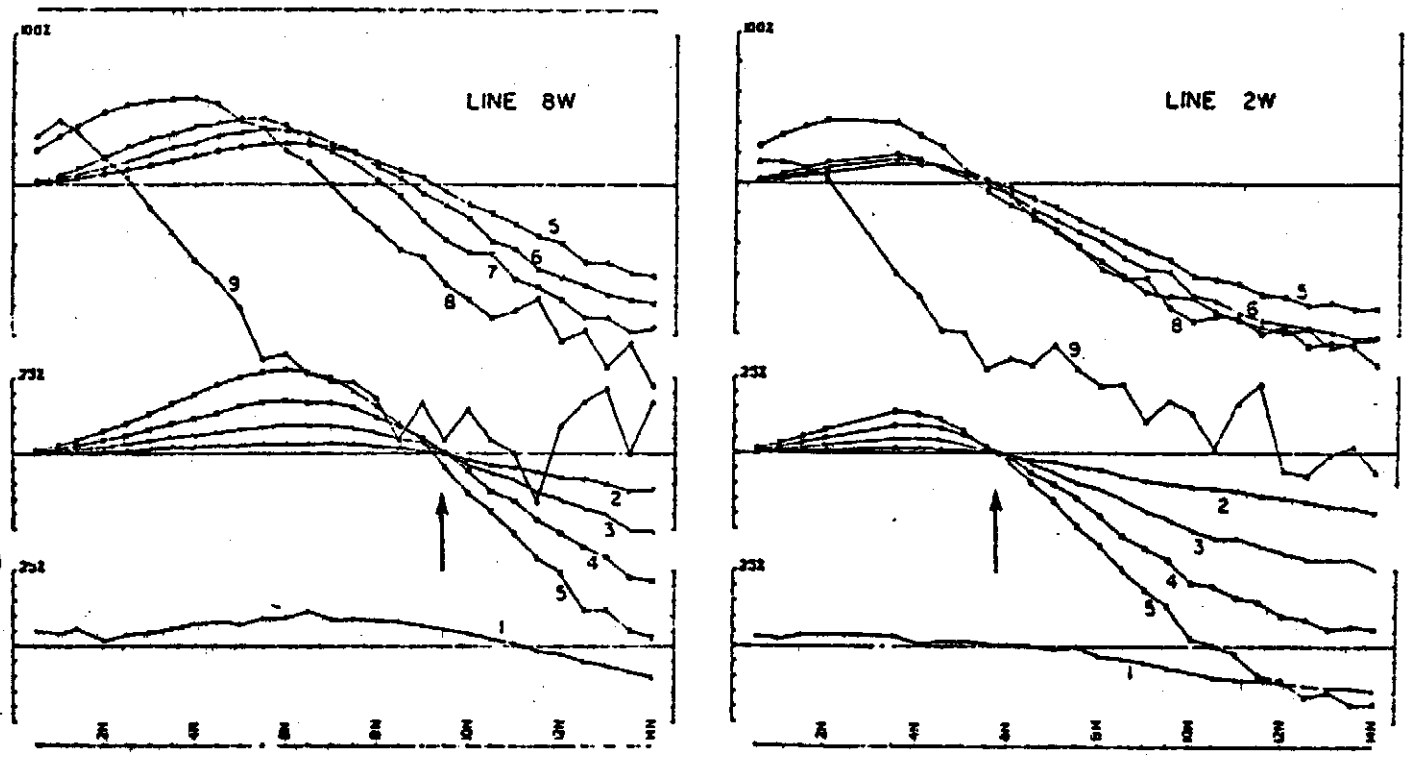

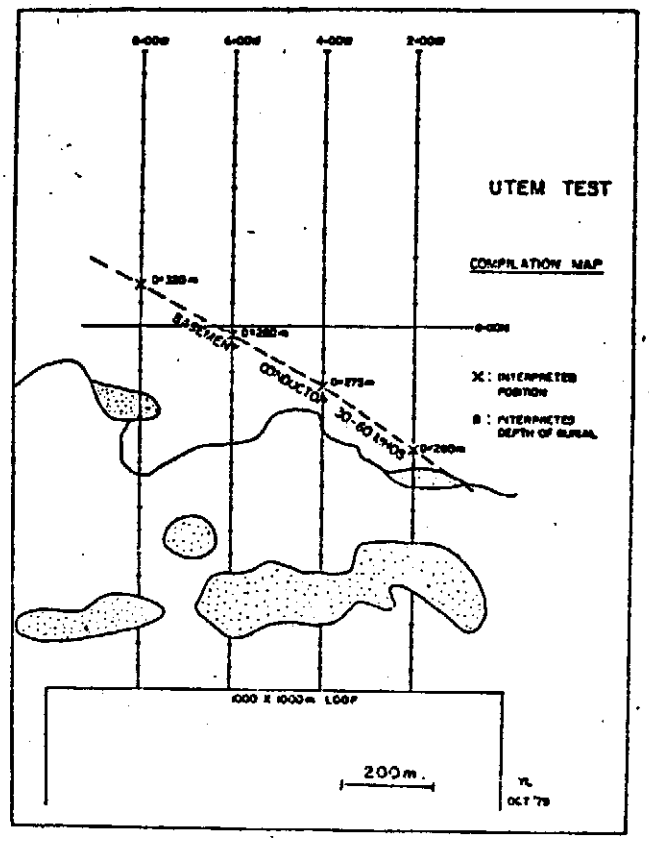

Fig. 16.1 Two UTEM H_z^s profiles over a deep graphitic conductor in the basement complex under the Athabaska sandstone. A map of the survey is shown. The interpreted depths exceed drilling depths by about 15%.

5 cm

area except for the entrance to an exploration decline into the deposit, there are several power lines through the grid to nearby industry. One is a major transmission line. An IP test survey was unsuccessful in recognizing the body, at least in part due to high noise conditions. The UTEM II survey proceeded slowly, with long averaging times near the power lines. The grid was surveyed from two transmitter loops (Fig. 17.1).

All H_z profiles have the same aspect (Fig. 17.2). The main response is from the conductive host rocks and it strongly resembles the theoretical response of a 167 Ωm half space (Fig. 17.2). Over the shallower parts of the body (which are also the most highly mineralized) an additional response component is found superimposed on the main host response. Just in the time range (ch 7-4) when the active zone sweeps down and past the target area, a distortion of the main respnse is found. If the expected response from the host rocks is sketched in (dotted on profiles), one can see that a crossover response which has a fixed location is superimposed on it. The crossover occurs at the same place for both transmitter loops, and it clearly reveals a temporary line current concentration which arises just as the peak intensity of the smoke ring passes the target zone.

The anomaly generating process found here is a good example of the kind of unidirectional induced current flow seen in two-dimensional modelling. An examination of the data shows no trace of any long time-constant symmetrical negative anomaly bifilar current which would indicate a bidirectional current flow due to local eddy current induction. This sets limits on the possible conductivity of the mineralization. To produce a significantly enhanced induction flow, the longitudinal conductance (σ_t x cross-sectional area) of the target must be much greater than that of the energized zone of host rock surrounding it. On the other hand, the time constant $\sigma_t \mu_o$ x thickness x width for bifilar induction must be small (<2 ms). These conditions lead to a conductivity-thickness estimate of about 8 siemens, which correlates with the dirty, unmetamorphosed condition of the ore.

18. Robinson Property, Ontario

This is an example of a simple, moderately conductive overburden on resistive bedrock. Profiles of H_z are shown in Fig. 18.1. On one of

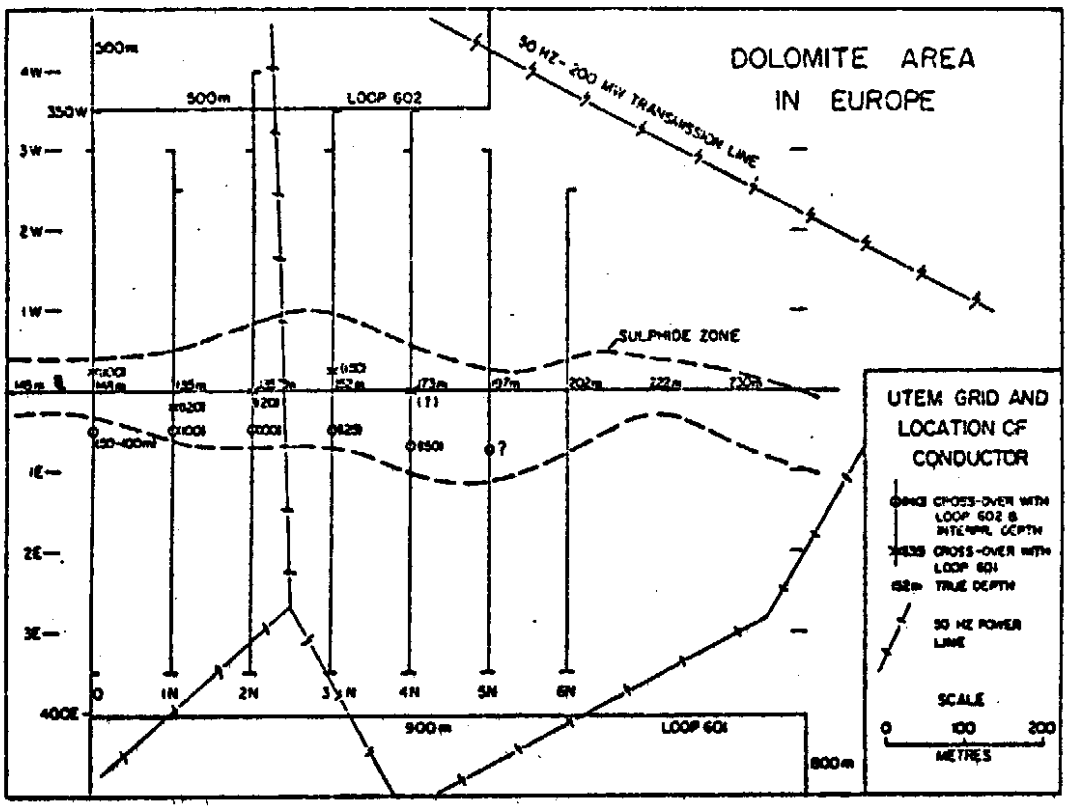

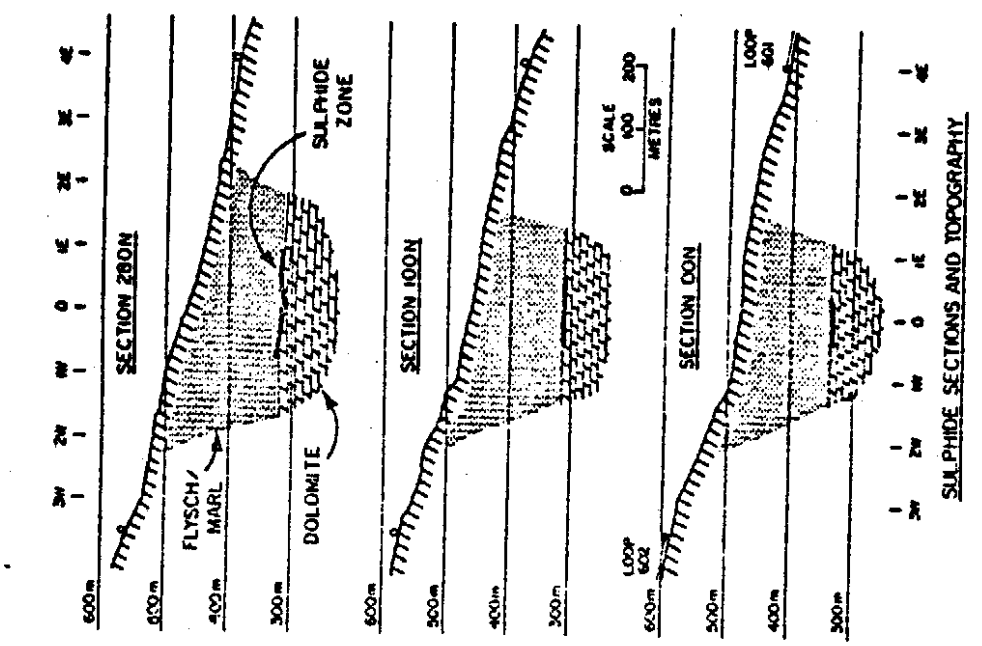

Fig. 17.1 Location map and geological section for a UTEM survey in Europe. The target conductor is a horizontal ribbon-like body.

5 cm

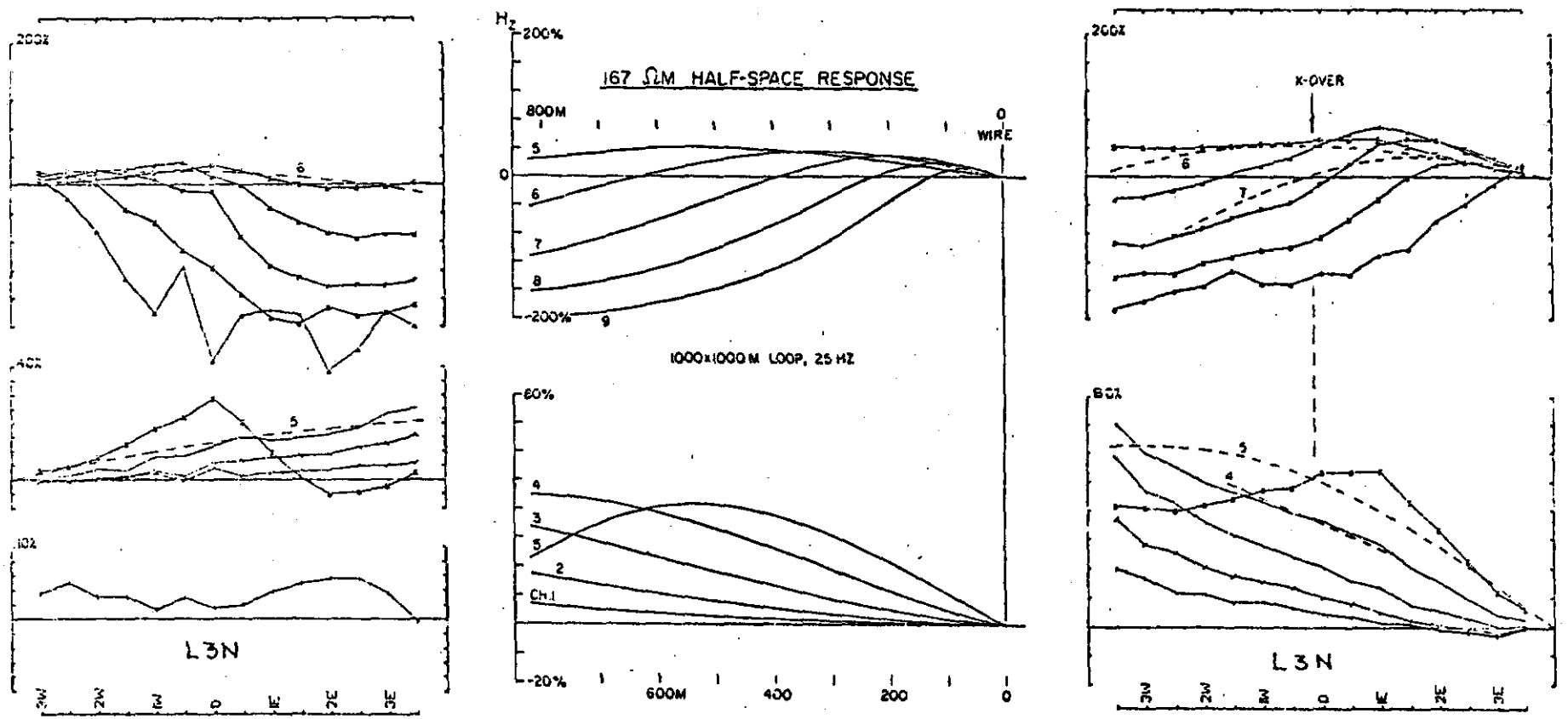

Fig. 17.2 UTEM H_z^s profiles over the area shown in Fig. 17.1, along with a theoretical profile for a half-space. Estimates of the stratified earth response for the area are dotted in on the field profiles. Note the residual crossover on channels 5 and 6.

880881

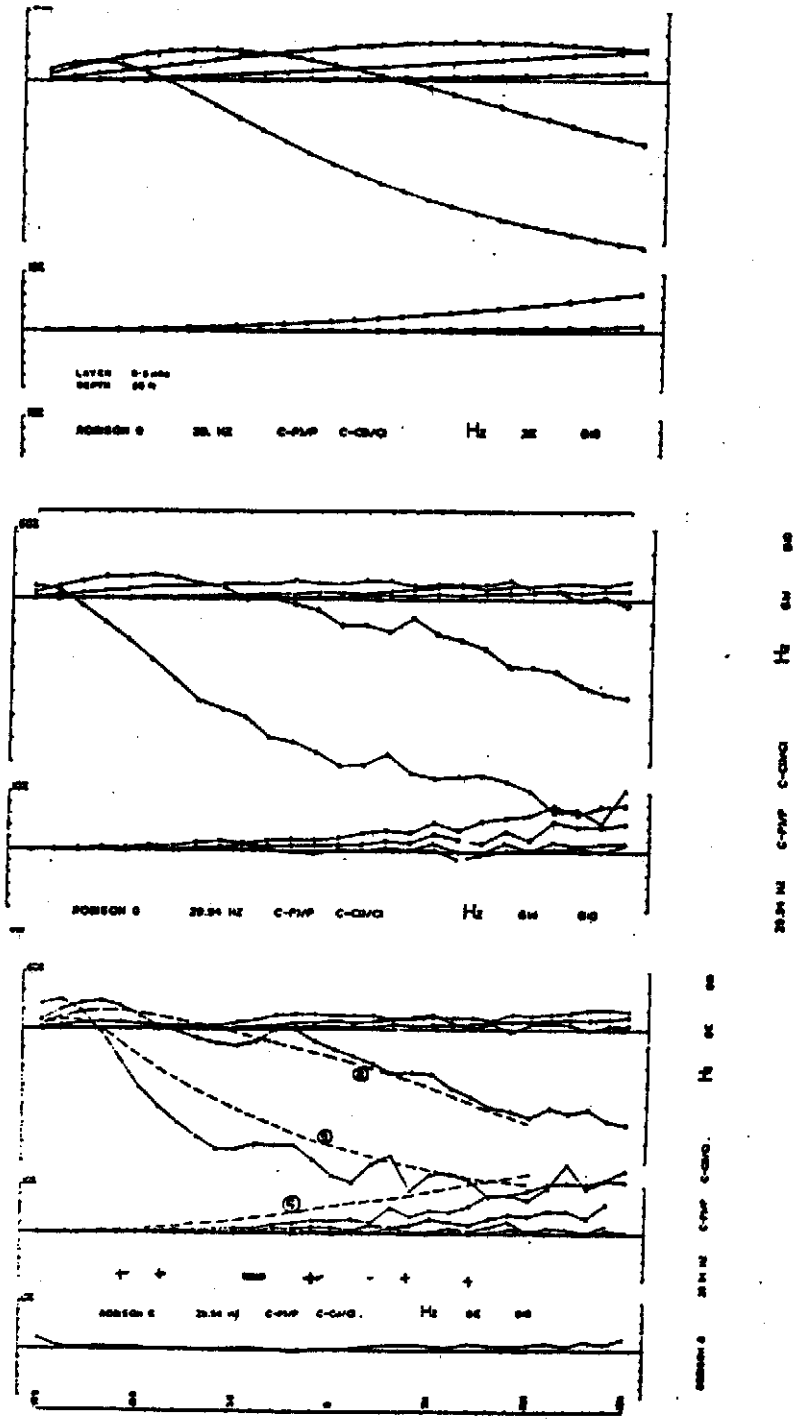

Fig. 18.1 Robison. This survey shows the effect of irregularities in a conductive overburden on a resistive subspace. A model response for a uniform 0.3S overburden is shown in A. The data on Line 6W(B) is quite similar. Data from L8E(C) show strong local perturbations. A negative current axis (i.e. missing current) is clearly defined at 4S, apparently due to a thin spot in the overburden. The local anomaly is visible on all channels for which there is an appreciable overburden response (9-7). Because this overburden is not very conductive, the field is already penetrating it at the earliest observed time. Thus early time blanking is not observed, even though the cause of the anomaly is undoubtedly in the bottom of the overburden layer.

the lines, the response closely resembles the theoretical response of a uniform overburden. On one of the others we see perturbations superimposed on the uniform layer type of respnse. The perturbations are fixed in space indicating fixed curent systems which in this case are produced by irregularities in depth of the overburden layer.

The data do reveal by examination of the changing amplitude of the perturbations that the conductivity irregularities are either in the base of the overburden or are closely linked to it. Firstly, the main response is that of a thin conductive layer, not a more uniform ground like a half space. The perturbations arise only in the time range when the active zone of overburden and host induction is moving out of the survey area. Thus their cause is at or below the base of the overburden. Because the bedrock reveals itself to be relatively resistive, a conductive feature surrounded entirely by resistive host rock would generate only a very weak poloidal (current gathering) anomaly, whereas a feature that is attached as part of the overburden could generate a much stronger one. No toroidal (inductive) anomaly with a different time constant pattern from the overburden response is observed. Thus an interpreter must attribute the responses to zones at the base of the overbuden which are not vastly more conductive than the overburden. At best, they could be due to minor mineralization at the subcrop surface.

19. Salt Creek, Western Australia

This is a survey carried out over a nickel sulphide prospect in the Precambrian Shield. The bedrock is well stratified but dipping almost vertically. The target was strata-bound sulphides. Weathering is deep and variable in the area and the conductivity of the overburden is extremely high. Fig. 19.1 shows some of the profiles. Only on the later time channels has the magnetic field achieved substantial penetration of the area. The main conductivity does appear to be near the surface, as expected. A rough estimate of the overburden conductance is 20 S.

Superimposed on the general response are a number of stationary perturbations. They have greater amplitude on some lines than other, but they correlate well from line to line. By examining how early in time they occur, one can estimate at which depth their source lies

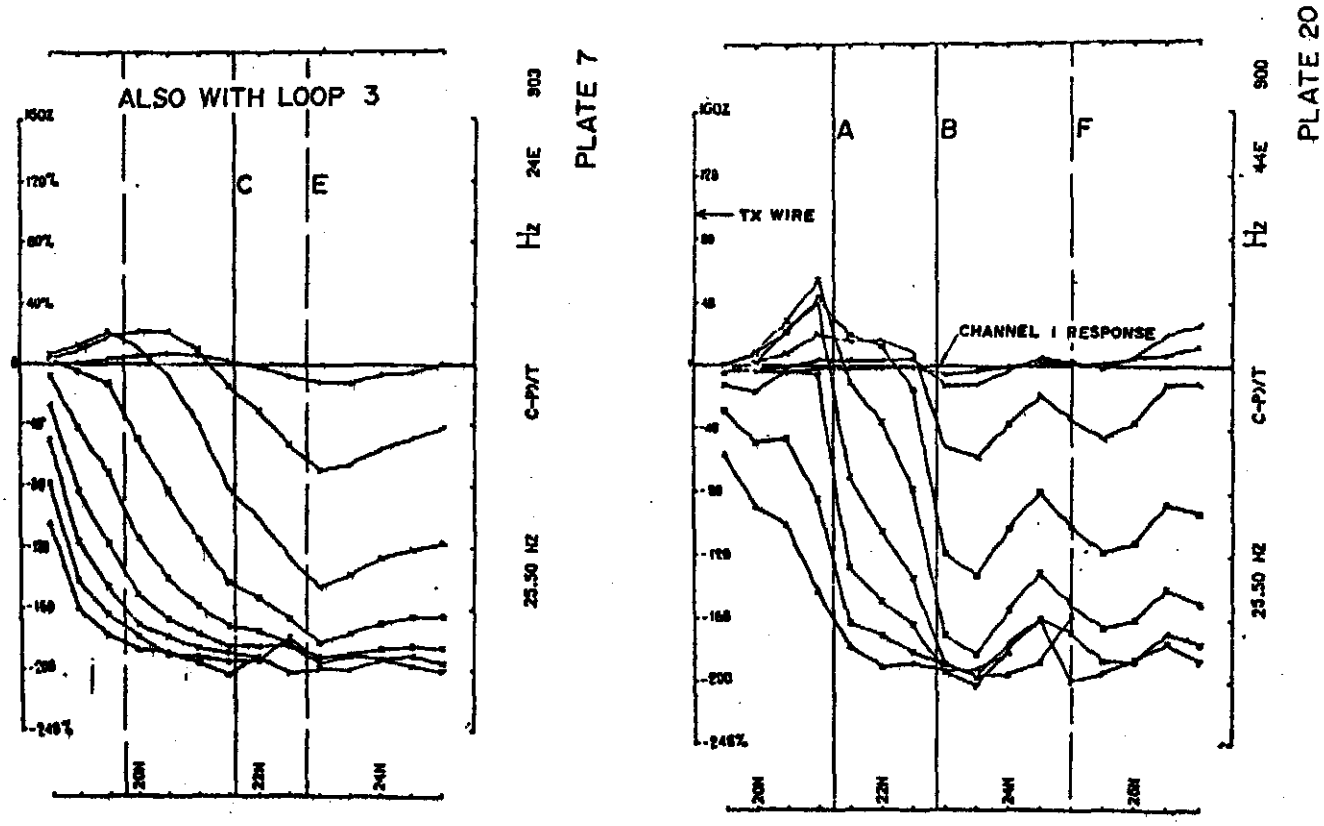

Fig. 19.1 Salt Creek. The profiles are from different Tx loops but cover the same stratigraphy. Full penetration of the source field into the earth is achieved only on Ch 1 (≈15 ms). The observed response on L24E approximates a layered earth down to about Ch 4. L44E is generally similar to L24E but has much stronger local perturbations. Axes of current enhancement are shown on both profiles. Zones A and B are very strong features, with the current in zone B dominating all other at late time. The B anomaly is blanked at early time, but the shape of the Ch 1 anomaly indicates the current axis to be only 10-20 m deep. The conductance associated with the feature must be large, however (>50 S). It is either the loop side of an exceptionally conductive wide strip of overburden or the top of a stratigraphic conductor that projects close to the surface.

relative to the overburden. A number of the current axes have been marked and correlated from line to line.

References

Annan, A.P., 1974, The equivalent source method for electromagnetic scattering analysis and its geophysical application: PhD thesis, Memorial University of Newfoundland.

Dyck, A.V., Bloore, M., and Vallee, M.A., 1980, User manual for programs PLATE and SPHERE; Research in Applied Geophysics #14, Geophysics Laboratory, Department of Physics, University of Toronto.

Lamontagne, Y.L., 1975, Applications of wide-band, time domain EM measurements in mineral exploration: PhD thesis, University of Toronto, available as Research in Applied Geophysics - Geophysics Laboratory, University of Toronto.

Lamontagne, Y.L., Lodha, G.L., Macnae, J.C. and West, G.F., 1977, Towards a deep penetration EM system: Paper presented at 79th annual meeting of the CIMM, Ottawa, April, 1977; published in: Bull. Austral. Soc. Expl. Geophysicists, v.9, 1978.

Lamontagne, Y.L., Lodha, G.S., Macnae, J.C. and West, G.F., 1980, UTEM, "Wideband Time-domain EM Project 1976-8, Reports 1-5"; Research in Applied Geophysics #11, Geophysics Laboratory, Department of Physics, University of Toronto.

Lajoie, J. and West, G.F., 1975, The electromagnetic response of a conductive inhomogeneity in a layered earth, Geophysics, v41, n13(supplement); p1133-56.

Lodha, G.L., 1977, Time domain and multifrequency electromagnetic responses in mineral prospecting: PhD thesis, Department of Physics, University of Toronto, available as Research in Applied Geophysics, # , Geophysics Laboratory, University of Toronto.

Macnae, J.C., 1977, The response of UTEM to a poorly conducting mineralized environment: MSc thesis, University of Toronto.

Macnae, J.C., 1980a, The Cavendish test site: a UTEM survey plus a compilation of other ground geophysical data: Research in Applied Geophysics #12, Geophysics Laboratory, Department of Physics, University of Toronto.

Macnae, J.C., 1980b, An atlas of primary fields of fixed transmitter EM loop sources: Research in Applied Geophysics #13, Geophysics Laboratory, Department of Physics, Univerity of Toronto.

Macnae, J.C., 1981, Geophysical prospecting with electrical fields from an inductive source, PhD thesis, Department of Physics, University of Toronto, 279p, available as Research in Applied Geophysics, #18, Geophysics Laboratory, University of Toronto.

Maxwell, J.C., 1891, A Treatise on electicity and magnetism: London, Clarendon press.

Nabighian, M.N., 1979, Quasi-static transient response of a conducting half-space - an approximate representation: Geophysics, v44, p1700-1705.

Podolsky, G. and Slankis, J.A., 1979, Izok lake deposit, Northwest territories, Canada; a geophysical case history; in Geophysics and Geochemistry in the search for metallic ores; Geological Survey of Canada, Economic Geology report 31, p.641-652.

Addendum

20. Brouillan Twp, Quebec P.

This survey was over the eastern part of the Selco's Detour sulphide deposit. The zone was discovered by an INPUT AEM survey, because one part is a relatively massive pyrite-rich zone. However, the economically important mineralization is disseminated over a broad area in Archean metavolcanic rocks that are locally flat-lying. Overburden is thin and resistive and the site is flat. The purpose of the UTEM survey was to trace the main conductor under a tongue of granitic rock which invades horizontally from the east. This was accomplished, but the most scientifically interesting results came from the disseminated-stringer mineralization on the western part of the grid.

Fig. 20.1 shows the survey grid and the location of the main conductor. Fig. 20.2 shows H_z^s and E profiles on L6W. Fig. 20.3 shows the late limit E vector maps from one of the Tx loops.

The main conductor is a large, vertical plate with a short time constant (<1 ms). Its response has vanished by Ch 4. At later times, we expect no magnetic field response or change in the electric response, to the level of measurement error. However, this is not what is observed. Slow, irregular variations in E and H persist to latest time (Figs. 20.3, 20.4).

The main static part of the electric field anomaly is a strong reduction in intensity over the principal zone of disseminated mineralization. The zone is independently delineated on the map by the 100 Ωm apparent resistivity contour of a dipole-dipole IP survey. The late-time E field is well predicted by a block model, as is also shown in Fig. 20.3

The unexpected late-time behaviour of the fields is shown in Fig. 21.4A. The inset graphs show how a weak slow decay persists to very late time in both the E and H_z data. The profile form of this effect is quite erratic in strength but of constant polarity. The E data when normalized to the late time total field bear a striking resemblence to the dipole-dipole IP PFE profiles (Fig. 20.4B). The H_z effect is found over most of the survey grid, not just the low resistivity zone. Macnae (1980) has shown how an IP spectral model

can be fitted to the E data. The H data is more enigmatic, as it is difficult to explain it quantitatively on the basis of a simple polarizable, moderately conductive block of ground. However, the time decay is the same as observed for E and it is so similar in character that it must be closely related. Similar effects have been noted in an H_z survey over another disseminated, stringer type sulphide zone in a resistive host environment.

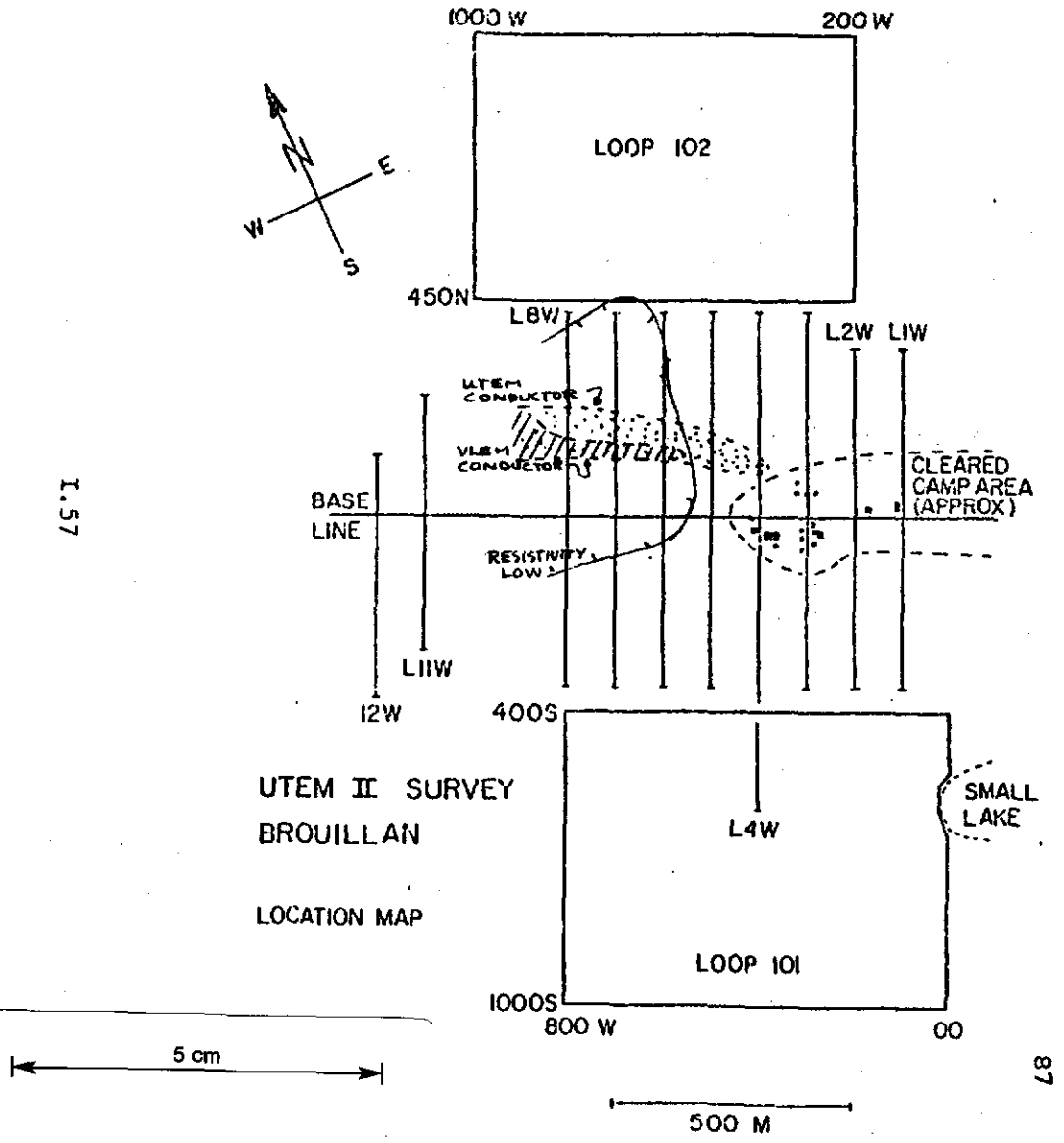

Fig. 20.1 Brouillan survey grid.

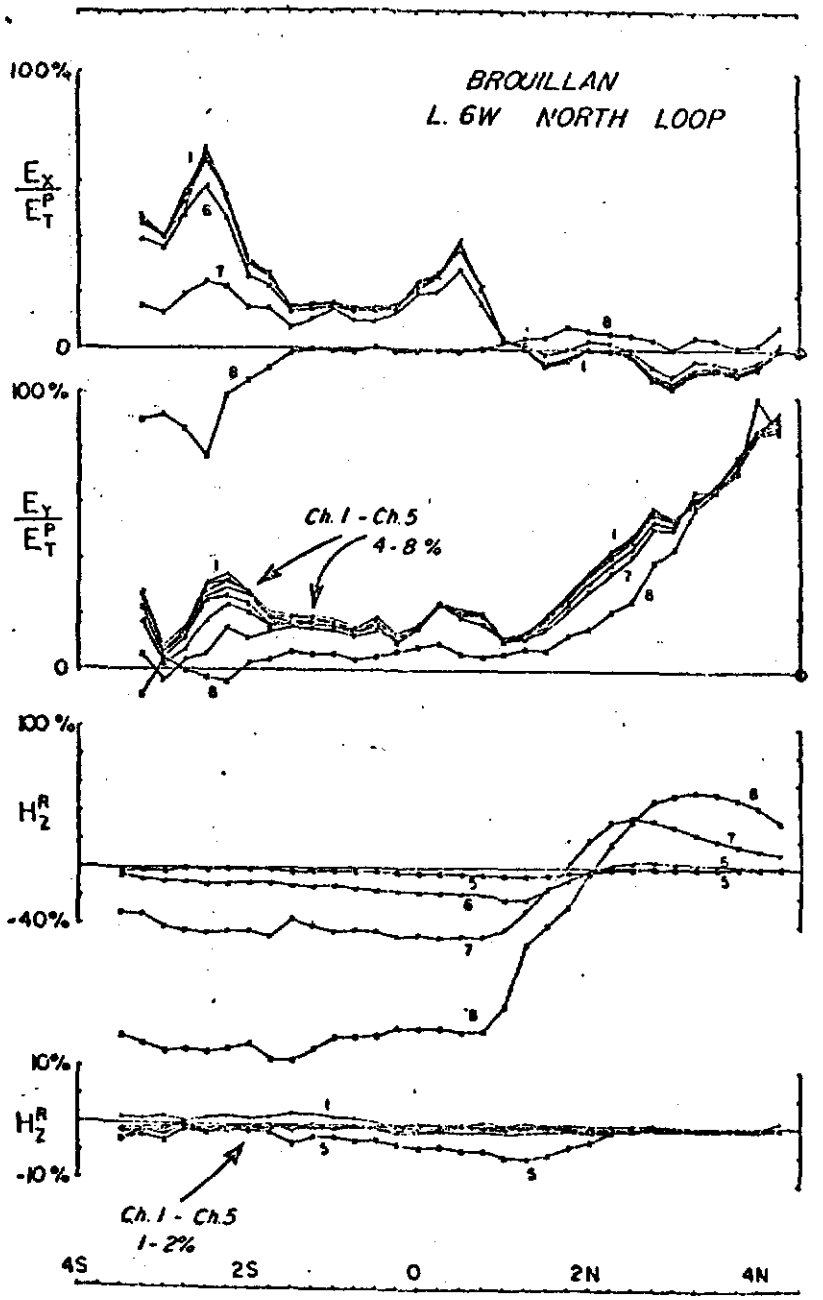

Fig. 20.2 An example of the profile data.

7880096

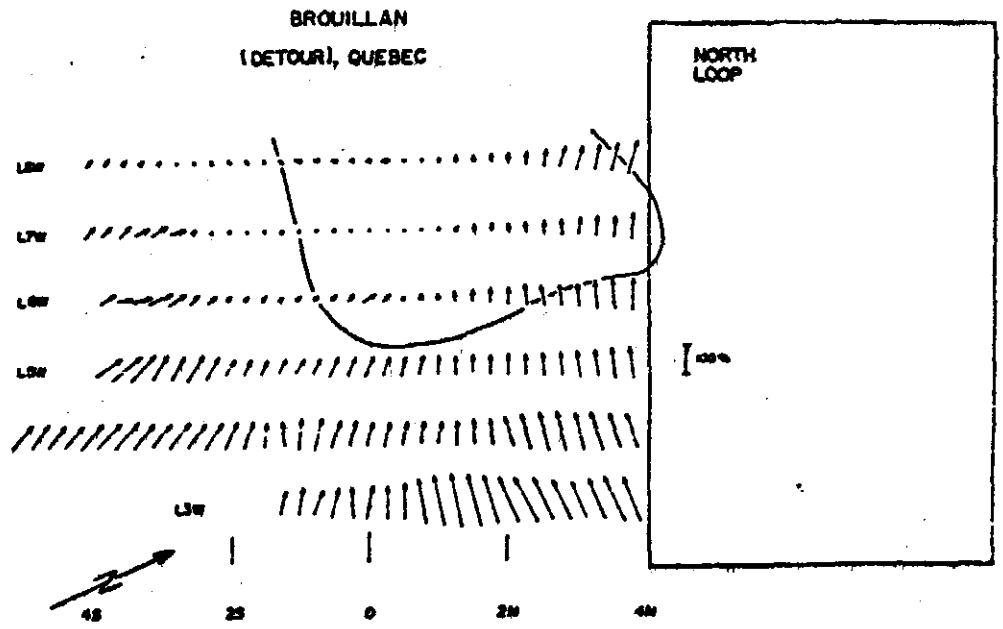

RLE MODEL OF SHALLOW BLOCK

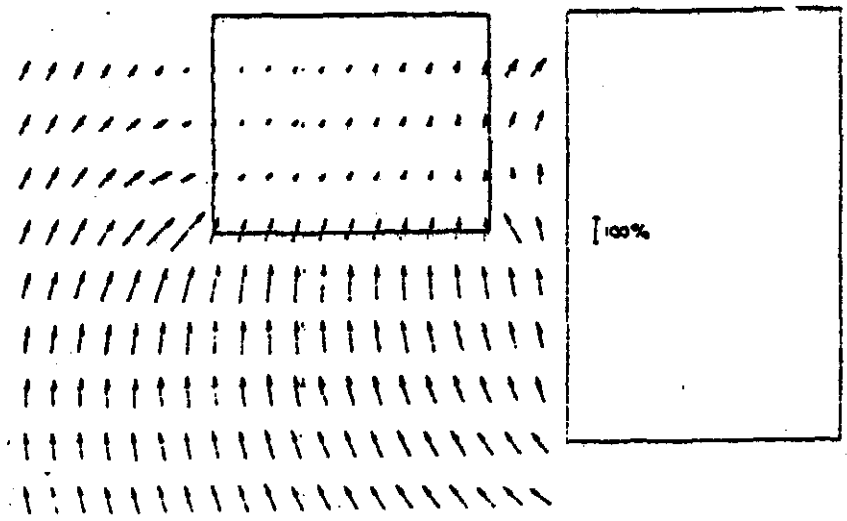

Fig. 20.3 Brouillan late time E vectors from the north loop compared with model data.

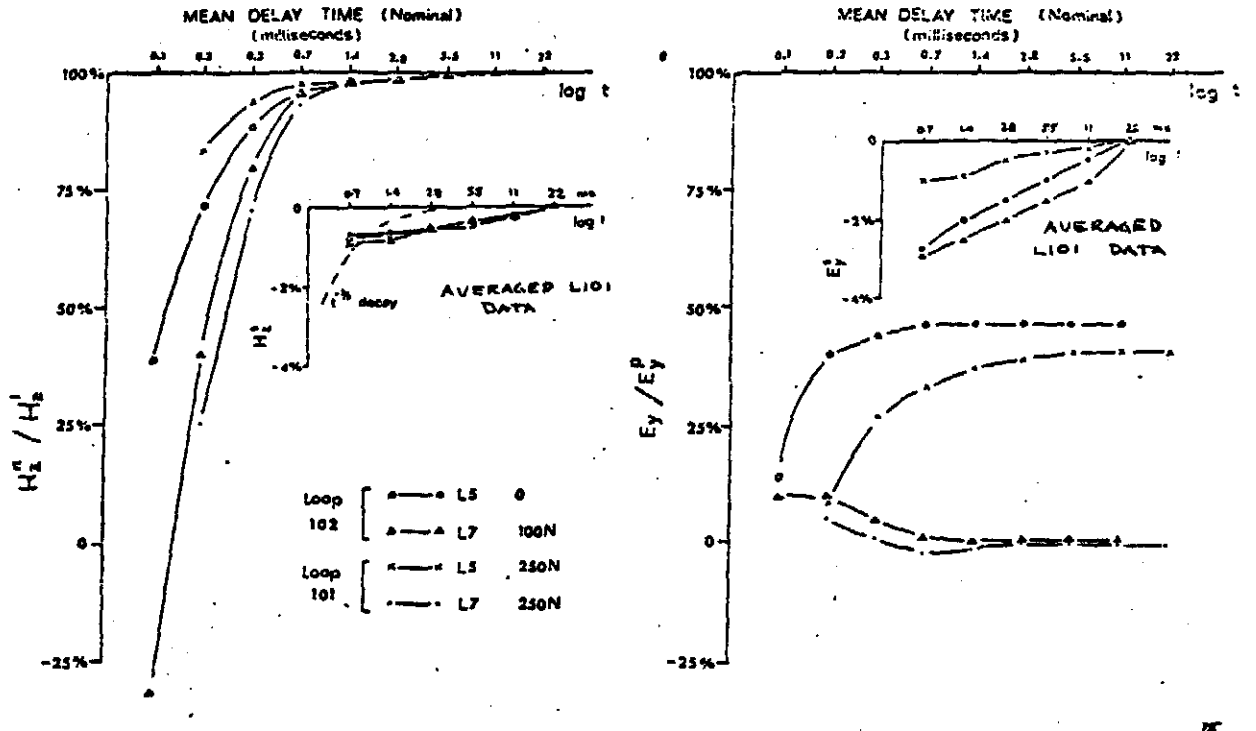

A.

Late time transients of Hz' and Ey at Brouillan.

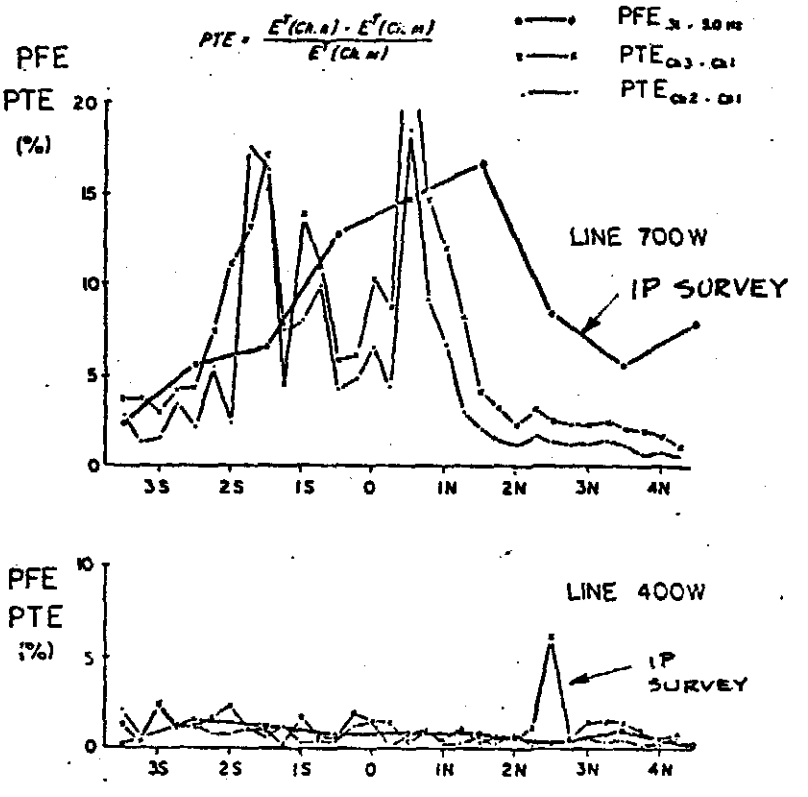

B

Dipole dipole, a=100', n=1 PFE profiles from galvanic IP survey, and TTEM E field late time effects to show that the anomalous areas correspond in location.

Fig. 20.4 Induced polarization effects.

A) Observed decays at a few stations shown at normal plotting scales and with high magnification (5 pt averages for magnified data).

B) Profiles of the total field normalized late E decay comparing with the dipole-dipole IP data.

TUNNEL POSITION

DH 4573

BASELINE 5000 N

5400 N
5200 N
4800 N
4600 N
5000 E
5100 E
5200 E
5300 E
5500 E
4400N
5400 E
5600 E
4200 N
5700 E
5800 E
5900 E
6000 E
6100 E
6200 E
6300 E
6400 E
6500 E

Shed

MIN

5 cm

0 25 50 100 200 metres

SCALE 1 : 2500

788099

CRA EXPLORATION PTY LIMITED

DALCOATH GRANITE GRID

GROUND MAGNETIC SURVEY

Base value 62 000nT Sensor height 2.5m

REF.	SK55-3		
SCALE.	1 : 2500	DRAWN	R. T.
AUTHOR	M FLIS	REPORT Nº	11268
DATE	June 1981	PLAN No	TASh 237

TUNNEL POSITION

5600 N

5400 N

5200 N

BASELINE 5000 N

5000 N

4800 N

4600 N

4400N

4200 N

5000 E

5100E

5200 E

5300E

5400E

5500 E

5600E

5700E

5800E

5900E

6000E

6100E

6200E

6300 E

6400 E

6500E

6600E

4500 N

DH 4573

Narrawa Reward Au Mine

Squib W mine

Higgs Au Mine

15% Pb,Zn

"191"

"20xR"

N.W.C.

MN

U.T.E.M Anomalies and Conductor Trace.

191 Approx. position of Dighem Anomalies.

20xR

5 cm

0 25 50 100 200 metres

SCALE 1·2500

788100

CRA EXPLORATION PTY LIMITED

DALCOATH GRID
Normalised V.L.F. - E.M. Dips
N.W. Cape Transmitter (295° MN)
Pheonix V.L.F. - 2

REF	SK 55 3		
SCALE	1:2500	drawn	R. T
AUTHOR	M.F.F.	REPORT	N°. 11268
DATE	OCT 1981	PLAN No	TASh 536

788101

425 000 mE

5 405 000mN

LEGEND

Contours in ohm-m
at eight intervals per decade

100
75
56
42
31
23
17
13
10

Note

The numbers face in the direction of increasing value.

** NOTE **

Approximate position of Dalcoath Granite Grid indicated.

5 cm

CRA EXPLORATION PTY. LIMITED

PORTION OF
DIGHEM II SURVEY, SHEFFIELD TAS.
RESISTIVITY

Ref: SK55 - 3	
Scale : 1 : 25 000	*Drawn: R. T.*
Author: M. F.	*Report N°. 11268*
Date: 29 - 4 - 1982	*Plan N°. TASh 730*

788102

425 000 mE

5 405 000 mN

1

ANOMALY GRADE	EM GRADE SYMBOL	MHO RANGE
6	●	≥ 100
5	✱	50 — 99
4	●	20 — 49
3	◉	10 — 19
2	○	5 — 9
1	○	≤ 4
	×	Possible conductor

DIGHEM anomalies are divided into six grades of conductivity - thickness product. This product in mhos is the reciprocal of resistance in ohms. The mho is a measure of conductance, and is a geologic parameter. Most swamps yield Grade 1 anomalies but highly conducting clays can give Grade 2 anomalies. The multi-coil anomaly shapes often allow surface conductors to be recognized, and these are indicated by the letter S on this map. The remaining Grade 1 and 2 anomalies could be weak bedrock conductors. The higher grades indicate increasingly higher conductances. Examples: The ore bodies of the Magusi River camp yield Grade 4 anomalies, while Matagobi and Whistle give Grade 5. Graphite and sulphides can span all grades but, in this survey area, field work may show that the different grades indicate different types of conductors.

identifier — e.g. 38 ← mho value

Depth is greater than: 50 feet; 100 feet; 150 feet; 200 feet

In-phase and Quadrature of Standard Coil is greater than: 5 ppm; 10 ppm; 15 ppm; 20 ppm

Refer to list of anomalies in survey report for the actual ppm values for all coils, and for conductor depths.

The actual mho value is plotted beside the EM grade symbol. The letter is the anomaly identifier. The horizontal rows of dots indicate anomaly amplitude on the flight record, and the vertical column gives the estimated depth. This depth may be unreliable because the stronger part of the conductor may be deeper or to one side of the flight line, or because of a shallow dip or conductive overburden effects.

	Conductor axis
S	Probable surface response
S?	Possible surface response
L	Probable line (power, telephone, pipe, or fence)
L?	Possible line
?	Questionable anomaly
	Apparent thickness > 10 m
V	Dip
100 g	Direct magnetic correlation of 100 gammas

DIGHEM maps are designed to provide a correct impression of conductor quality by means of the conductance grade symbols. The symbols can stand alone with geology when planning a follow-up program. The actual mho values are plotted for those who wish quantitative data. The anomaly ppm and depth are indicated by inconspicuous dots which should not distract from the conductor patterns, while being helpful to those who wish this information. The map provides an interpretation of all conductors in terms of length, strike direction, conductance and depth. The accuracy is comparable to an interpretation from a ground EM survey having the same line spacing.

** NOTE **

Approximate position of Dalcoath Granite Grid indicated.

5 cm

CRA EXPLORATION PTY. LIMITED

PORTION OF DIGHEM II SURVEY, SHEFFIELD TAS. ELECTROMAGNETICS

Ref: SK55 - 3	
Scale: 1 : 25 000	Drawn: R. T.
author: M. F.	Report N°. 11268
Date: 29 - 4 - 1982	Plan N°. TASh 731

788103

425 000 mE

5 405 000 mN

5 cm

ISOMAGNETIC LINES

(total field)

1000 ..... 1000 gammas

200 ..... 200 gammas

..... 50 gammas

..... 25 gammas

..... magnetic depression

Magnetic Inclination within the survey area : 72°

** NOTE **

Approximate position of Dalcoath Granite Grid indicated.

CRA EXPLORATION PTY. LIMITED

PORTION OF
DIGHEM II SURVEY, SHEFFIELD TAS.
MAGNETICS

Ref : SK55 - 3	
Scale: 1 : 25 000	Drawn: R. T.
Author : M. F.	Report N°. 11268
Date: 29 - 4 - 1982	Plan N°. TASh 732

788104

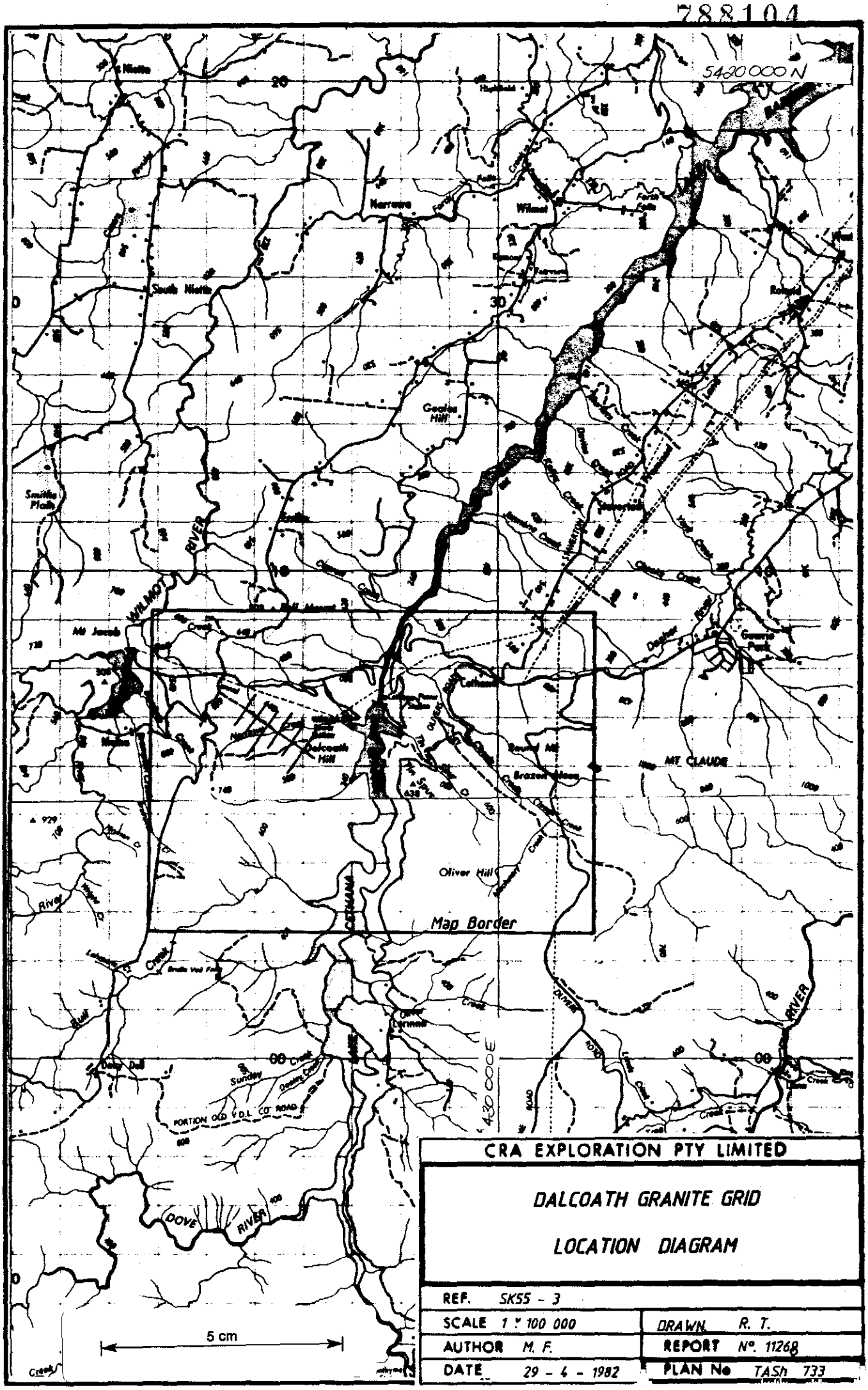

CRA EXPLORATION PTY LIMITED

DALCOATH GRANITE GRID

LOCATION DIAGRAM

REF. SK55 - 3	
SCALE 1 " 100 000	DRAWN R. T.
AUTHOR M. F.	REPORT N°. 11268
DATE 29 - 4 - 1982	PLAN No TASh 733

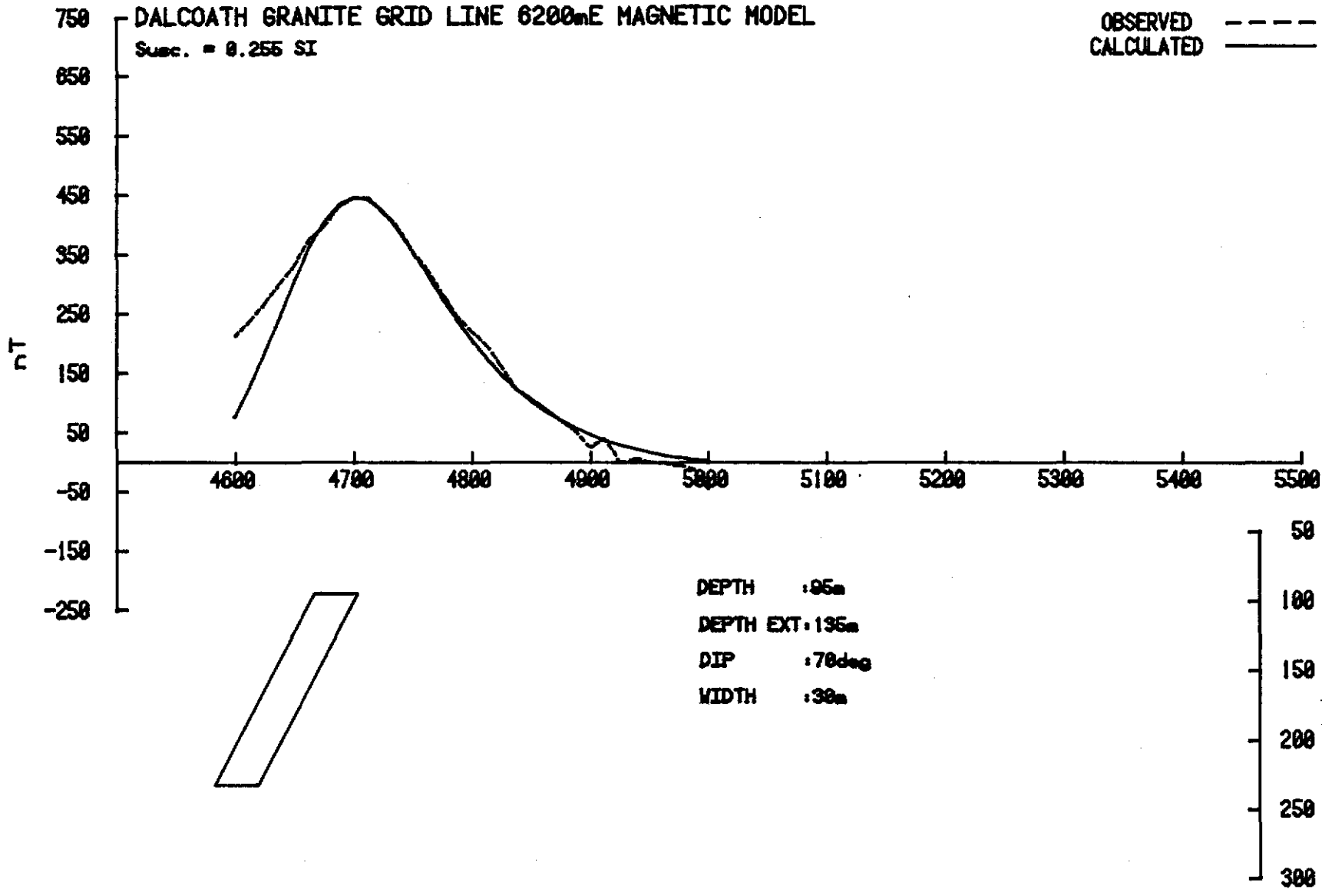

REPORT N°. 11268

PLAN N°. TASh 734

788105

DALCOATH GRANITE GRID LINE 5300mE MAGNETIC MODEL

Susc. = 0.105 SI

OBSERVED - - - -

CALCULATED ———

nT

750
650
550
450
350
250
150
50
-50
-150
-250

4600 4700 4800 4900 5000 5100 5200 5300 5400 5500

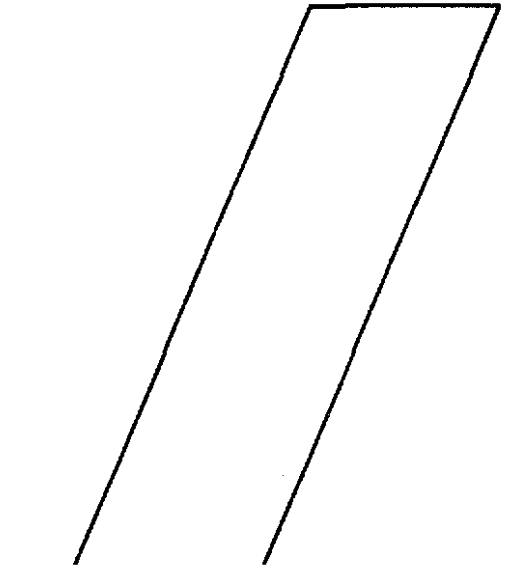

DEPTH : 105m

DEPTH EXT: 435m

DIP : 70deg

WIDTH : 100m

50
100
150
200
250
300

REPORT N°. 11268

PLAN N°. TASh 735

7881106